Evaluation On The Printability And Properties Of 3D-Printed Part Fabricated Using Plant Fibre Reinforced Polymer Composite Filament

AMIRUL ZAKWAN BIN MAZLI

B092010126

BACHELOR OF MANUFACTURING ENGINEERING TECHNOLOGY (PRODUCT DESIGN) WITH HONOURS

2023

Faculty of Industrial and Manufacturing Technology and Engineering

Evaluation On The Printability And Properties Of 3D-Printed Part Fabricated Using Plant Fibre Reinforced Polymer Composite Filament

AMIRUL ZAKWAN BIN MAZLI

Bachelor of Manufacturing Engineering Technology (Product Design) with Honours

2023

Evaluation On The Printability And Properties Of 3D-Printed Part Fabricated Using Plant Fibre Reinforced Polymer Composite Filament

AMIRUL ZAKWAN BIN MAZLI

A thesis submitted
in fulfillment of the requirements for the degree of
Bachelor of Manufacturing Engineering Technology (Product Design) with Honours

Faculty of Industrial and Manufacturing Technology and Engineering

UNIVERSITI TEKNIKAL MALAYSIA MELAKA

2

UNIVERSITI TEKNIKAL MALAYSIA MELAKA

BORANG PENGESAHAN STATUS LAPORAN PROJEK SARJANA MUDA

TAJUK: **Evaluation On The Printability And Properties Of 3d-Printed Part Fabricated Using Plant Fibre Reinforced Polymer Composite Filament**

SESI PENGAJIAN: **2023-2024 Semester 1**

Saya **AMIRUL ZAKWAN BIN MAZLI**

mengaku membenarkan tesis ini disimpan di Perpustakaan Universiti Teknikal Malaysia Melaka (UTeM) dengan syarat-syarat kegunaan seperti berikut:

1. Tesis adalah hak milik Universiti Teknikal Malaysia Melaka dan penulis.
2. Perpustakaan Universiti Teknikal Malaysia Melaka dibenarkan membuat salinan untuk tujuan pengajian sahaja dengan izin penulis.
3. Perpustakaan dibenarkan membuat salinan tesis ini sebagai bahan pertukaran antara institusi pengajian tinggi.
4. **Sila tandakan (✓)

☐ TERHAD (Mengandungi maklumat yang berdarjah keselamatan atau kepentingan Malaysia sebagaimana yang termaktub dalam AKTA RAHSIA RASMI 1972)

☐ SULIT (Mengandungi maklumat TERHAD yang telah ditentukan oleh organisasi/badan di mana penyelidikan dijalankan)

☑ TIDAK TERHAD

Disahkan oleh:

Alamat Tetap:

NO 5, LORONG SERI SEMENTA 8B,

TAMAN SERI SEMENTA,

42100, KLANG, SELANGOR.

Cop Rasmi:

TS. DR. SYAHIBUDIL IKHWAN BIN ABDUL KUDUS
Pensyarah Kanan
Fakulti Teknologi dan Kejuruteraan Industri dan Pembuatan
Universiti Teknikal Malaysia Melaka

Tarikh: 10/1/2024

Tarikh: 10/1/2024

** Jika tesis ini SULIT atau TERHAD, sila lampirkan surat daripada pihak berkuasa/organisasi berkenaan dengan menyatakan sekali sebab dan tempoh laporan PSM ini perlu dikelaskan sebagai SULIT atau TERHAD.

DECLARATION

I declare that this Choose an item. entitled " Evaluation On The Printability And Properties Of 3D-Printed Part Fabricated Using Plant Fibre Reinforced Polymer Composite Filament" is the result of my own research except as cited in the references. The Choose an item. has not been accepted for any degree and is not concurrently submitted in candidature of any other degree.

Signature :

Name : Amirul Zakwan Bin Mazli

Date : 10/1/2024

APPROVAL

I hereby declare that I have checked this thesis and in my opinion, this thesis is adequate in terms of scope and quality for the award of the Bachelor of Manufacturing Engineering Technology (Product Design) with Honours.

Signature :

Supervisor Name : *Ts. Dr. Syahibudil Ikhwan Bin Abdul Kudus*

Date : 10/1/2024

DEDICATION

To my supervisor, Ts.Dr. Syahibudil Ikhwan Abdul Kudus,

To my second supervisor, Dr Mastura Mohammad Taha,

To my seniors, Hazliza Aida, Nurul Nadia Mohamad,

My parents, Rahinah AB Rahim, Mazli Abdul Manap,

And my fellow friends.

ACKNOWLEDGEMENTS

In the Name of Allah, the Most Gracious, the Most Merciful

First and foremost, I would like to thank and praise Allah the Almighty, my Creator, my Sustainer, for everything I received since the beginning of my life. I would like to extend my appreciation to the Universiti Teknikal Malaysia Melaka (UTeM) for providing the research platform. Thank you also to the Malaysian Ministry of Higher Education (MOHE) for the financial assistance.

My utmost appreciation goes to my main supervisor, Ts.Dr. Syahibudil Ikhwan Abdul Kudus, all his support, advice and inspiration. His constant patience for guiding and providing priceless insights will forever be remembered. Also, to my co-supervisor, Dr Mastura Mohammad Taha, who constantly supported my journey. My special thanks go to Hazliza Aida, and Nurul Nadia Mohamad for all the help and support I received from them.

Last but not least, from the bottom of my heart I express gratitude to my beloved parents, Rahinah Ab Rahim and Mazli Abdul Manap, for their encouragements and who have been the pillar of strength in all my endeavors. My close friends, housemates, and classmates, for their patience and understanding. Finally, thank you to all the individual(s) who had provided me with the assistance, support and inspiration to embark on my study.

ABSTRACT

This study introduces the utilization of poly(lactic acid) (PLA), an environmentally friendly thermoplastic material, for fused deposition modeling (FDM) applications. Specifically, sugar palm fiber, commonly used in reinforcement for polymer composites, was incorporated into PLA to create a sugar palm PLA filament. The primary objectives were to assess the printability of this filament with 3D printers, examine its extrusion behavior, evaluate its impact on physical and mechanical properties, and compare it with commercially available PLA filament. The testing process aimed to address tensile strength, bending resistance, and impact resistance. Challenges encountered during testing included issues related to complex part production, filament adhesion to the build plate, filament sticking, clogging, and inconsistent flow, commonly associated with natural fiber bio-composite filaments. To optimize filament processing conditions and printing parameters, the study successfully generated complete and warpage-free samples. Characterization of the PLA and sugar palm fiber blend involved various analyses, including physical and mechanical tests. The printability of the sugar palm PLA filament was evaluated through dimensional accuracy, surface roughness, and mechanical performance tests (tensile, impact, and flexural). The ability to print high-quality, warpage-free samples from this blend suggests the potential for using this filament as a new feedstock material for FDM applications in both industrial and home settings. Findings indicated that bio-composite filaments can be successfully printed. However, further optimization of parameters is required to ensure smooth and consistent filament extrusion and printing. This optimization is crucial to minimize labor and produce end-products with improved strength and resolution, facilitating the creation of high-quality printed objects with minimal effort.

ABSTRAK

Kajian ini memperkenalkan penggunaan poli(asid laktik) (PLA), bahan termoplastik mesra alam, untuk aplikasi pemodelan penyusunan bersama (FDM). Secara khusus, serat kelapa sawit, yang biasanya digunakan sebagai penguat untuk komposit polimer, telah disatukan ke dalam PLA untuk membentuk filamen kelapa sawit PLA. Objektif utama adalah untuk menilai kebolehcapaian filamen ini dengan pencetak 3D, mengkaji perilaku ekstrusi, menilai kesannya terhadap sifat fizikal dan mekanikal, serta membandingkannya dengan filamen PLA komersial yang terdapat di pasaran. Proses ujian bertujuan untuk menangani kekuatan regangan, rintangan lenturan, dan rintangan impak. Cabaran yang dihadapi semasa ujian termasuk isu-isu berkaitan dengan pengeluaran bahagian yang kompleks, penempelan filamen pada plat pembinaan, pelekatan filamen, sumbatan, dan aliran yang tidak konsisten, yang biasanya dikaitkan dengan filamen bio-komposit serat semulajadi. Bagi mengoptimumkan keadaan pemprosesan filamen dan parameter pencetakan, kajian ini berjaya menghasilkan sampel yang lengkap dan bebas daripada kemekapan. Pencirian campuran PLA dan serat kelapa sawit melibatkan pelbagai analisis, termasuk ujian fizikal dan mekanikal. Kebolehcapaian filamen kelapa sawit PLA dinilai melalui ketepatan dimensi, kekasaran permukaan, dan ujian prestasi mekanikal (regangan, impak, dan lenturan). Keupayaan untuk mencetak sampel berkualiti tinggi dan bebas kemekapan daripada campuran ini mencadangkan potensi penggunaan filamen ini sebagai bahan bekalan baru untuk aplikasi FDM di kedua-dua persekitaran industri dan rumah. Penemuan menunjukkan filamen bio-komposit dapat dicetak dengan berkesan. Walau bagaimanapun, optimasi lanjut parameter diperlukan untuk memastikan ekstrusi dan pencetakan filamen yang lancar dan konsisten. Optimum ini penting untuk meminimumkan tenaga kerja dan menghasilkan produk akhir dengan kekuatan dan resolusi yang ditingkatkan, memudahkan penciptaan objek cetak berkualiti tinggi dengan usaha yang minima.

TABLE OF CONTENTS

LIST OF TABLES

LIST OF FIGURES

LIST OF SYMBOLS AND ABBREVIATIONS

AM	-	Additive Manufacturing
FDM	-	Fused Deposition Modeling
CAD	-	Computer Aided Design
STL	-	Standard Triangulation Language
3D	-	3-Dimensional
PLA	-	Polylactic Acid
SPF	-	Sugar Palm Fibre

LIST OF APPENDICES

CHAPTER 1

INTRODUCTION

1.1 Background

This project aims to investigate the printability and properties of 3D-printed parts fabricated using a plant fibre-reinforced polymer composite filament. The study utilizes an Additive Manufacturing (AM) printing system available at Fakulti Teknologi Kejuruteraan Mekanikal dan Pembuatan (FTKMP), Universiti Teknikal Melaka (UTeM). The project builds on recent advancements in AM, specifically in biobased thermoplastic polymers and natural fiber-reinforced bio composite filaments. These materials offer advantages over traditional oil-based materials, including lower carbon footprints, reusability, abundance, and comparable prices. The study incorporates cutting-edge manufacturing and material technologies to develop and analyze filaments of bio composite materials. An assessment of their suitability for Fused Deposition Modelling (FDM) is conducted, investigating dimensional accuracy, surface roughness, and mechanical properties. The results demonstrate the printability of the bio composite filaments, but further optimization is needed for improved strength and resolution. This optimization will enhance the quality of printed end-products while minimizing labor.

In the past few years, there has been an increasing focus on biobased and biodegradable composites, driven by their renewable nature, carbon neutrality, and cost-effectiveness (Rafiee et al., 2021). As the recognition of the scarcity of non-renewable resources grows, so does our awareness of the need to rely on renewable resources. This era could be referred to as the cellulosic century since an increasing number of renewable plant resources are being identified for various products. It is commonly assumed that natural fibres are renewable and sustainable, but this is not entirely accurate. While the living plants from which the natural fibres are derived are indeed renewable and sustainable, the fibres themselves are not (Faruk et al., 2012). Natural fibres have emerged as a promising alternative to synthetic fibres in terms of their potential to serve as reinforcement materials with comparable qualities.

1.2 Problem Statement

The growing interest in sustainable and environmentally friendly materials for 3D printing has spurred exploration into alternative filaments. The combination of Sugar Palm Fibre (SPF) with Polylactic Acid (PLA) has emerged as a potential substitute for traditional filaments. However, a comprehensive understanding of the printability of SPF/PLA filaments and their impact on physical properties and product appearance, in comparison to commercial PLA filaments, is crucial for their successful integration into Additive Manufacturing (AM) processes. The first problem statement addresses the need for a comparative printability analysis between SPF/PLA filament and commercial PLA filament. This involves evaluating alternative filament options based on their physical properties and final product appearance. The printability of SPF/PLA filaments presents challenges that necessitate careful examination, considering factors such as dimensional accuracy and surface roughness. These factors can influence the overall print quality and success rate of the filament. Additionally, variations in physical properties, including viscosity, melt flow rate, and interlayer adhesion, can significantly impact the dimensional accuracy, surface finish, and overall appearance of printed objects.

The second problem statement focuses on the mechanical property analysis between SPF/PLA filament and commercial PLA filament. This analysis includes evaluating tensile, flexural, and impact performance. Mechanical properties are critical in determining the functional reliability and performance of 3D printed objects. The adoption of SPF/PLA filaments as an alternative to commercial PLA filament underscores the need for a thorough analysis of their mechanical properties. Assessing dimensional accuracy, surface roughness, and conducting tensile, flexural, and impact tests will provide essential insights into the feasibility and suitability of these filaments for various applications. Understanding the mechanical properties between SPF/PLA filaments and commercial PLA filaments is crucial for assessing their performance in different applications. Variations in filament composition, fiber-matrix interaction, and processing parameters can significantly impact the dimensional accuracy, surface roughness, and mechanical strength of printed objects. Analyzing these properties is essential to determine the applicability of SPF/PLA filaments as a viable alternative.

1.3 Objective

The objective of this research work can be concluded as follows:

1. To assess the printability between the biocomposite filament made from sugar palm-derived polylactic acid (PLA) and commercial PLA filament in the 3D printing process utilizing the FDM system in terms of physical properties.

2. To assess the printability between the biocomposite filament made from sugar palm-derived polylactic acid (PLA) and commercial PLA filament in the 3D printing process utilizing the FDM system in terms of mechanical properties.

3. To compare the printability between SPF/PLA filament and the standard PLA filament.

1.4 Scope of Project

The scope of this research are as follows:

- To do a literature search reviews on topic AM, Sugar Palm Bio composite Filament, Natural Fibre
- To familiarize with AM, and FDM Machine.
- To extrude a biocomposite filament made from sugar palm-derived polylactic acid (PLA) by using an extruder machine.
- To print out the samples by using a FDM Machine.
- To measure and analyze the accuracy and surface roughness of the printed products.
- To peform tensile, impact and flexural test on the printed products.
- To carry out the differences between a biocomposite filament and a synthetic filament on accuracy, surface roughness and mechanical properties.

CHAPTER 2

LITERATURE REVIEW

2.1 Additive Manufacturing Technology

AM, is a technique that enables the creation of complex structures and geometries by building successive layers of materials based on three-dimensional (3D) model data. It originated with Charles Hull's development of stereolithography (SLA) in 1986 (Melchels, 2012) and has since seen advancements such as powder bed fusion, FDM, inkjet printing, and contour crafting (CC). With its diverse methods, materials, and equipment, 3D printing has undergone significant evolution and has the potential to revolutionize manufacturing and logistics processes. Various industries, including construction (Camacho et al., 2018), aerospace (Najmon et al., 2019), and biomechanics (Wang et al., 2020), have embraced AM.

AM refers to a method of combining materials through processes like fusion, binding, or solidification, which involves the use of liquid resin and powders. It constructs parts layer by layer, guided by 3D computer-aided design (CAD) modelling. Various terms, such as 3D printing (3DP), rapid prototyping (RP), direct digital manufacturing (DDM), rapid manufacturing (RM), and solid freeform fabrication (SFF), can be used to describe the different processes within AM (Abdulhameed et al., 2019). Printability characterizes a material's capacity to craft a 3D object through layered deposition while preserving its structural integrity post-printing. The literature underscores the significance of rheological properties, including the storage modulus, yield stress, consistency index, and flow behaviour index, as pivotal indicators of a material's printability (Pérez et al., 2019). In addition, other researchers have delved into the mechanical properties of the printed part as an integral facet of printability assessment (Kontárová et al., 2020). The intricate interplay of 3D printer parameters, encompassing nozzle speed, movement, and layer height, significantly shapes the ultimate quality of the printed structure. In processes like Fused Deposition Modelling (FDM), where a polymeric filament is extruded and deposited layer by layer, the composition of the filament distinctly influences the feeding mechanism. The movement of the filament through FDM machinery, propelled by rotating gears, generates the requisite pressure to initiate the deposition of high-viscosity melts. Hence, the scrupulous selection of the filament composition stands as a critical factor in achieving the desired final product performance (Govender et al., 2021). Within the scope of this project, printability is evaluated by categorizing it into two types which are physical and mechanical properties. Physical properties, encapsulating surface roughness and the precision of sugar palm fibres, contribute significantly to the overall quality of the printed product. Concurrently, mechanical properties, inclusive of tensile, flexural, and impact resistance, wield substantial influence in determining the final product's performance.

The growing preference for 3D manufacturing systems over traditional techniques is due to several advantages, including accurate fabrication of intricate geometries, efficient material usage, design flexibility, and customization options. A wide range of materials such as plastics, resins, rubbers, ceramics, glass, concretes, and metals are currently used in 3D printing. (Bogue, 2013). Polylactic acid (PLA) and acrylonitrile butadiene styrene (ABS) are commonly used polymers in composite 3D printing (Anderson, 2017). Advanced metals and alloys find application in the aerospace sector due to the limitations of traditional processes in terms of time, complexity, and cost. Ceramics are primarily utilized in 3D-printed scaffolds, while concrete is the main material for AM in construction. However, the mechanical properties and anisotropic behaviour of 3D printed parts still pose limitations, particularly for large-scale printing. Therefore, achieving an optimized printing pattern is crucial in controlling flaw sensitivity and anisotropic behaviour, aiming to enhance the potential and performance of 3D printed objects.

AM is the application of technology that played a significant role in accelerating time-to-market and fostering innovation. It involves the swift creation of a model or prototype of a part or finished product, which undergoes testing and analysis before mass production. Commercial 3D printers typically share similar functionalities in this process. The printer converts the design into a three-dimensional item using computer-aided design (CAD). The design is then split into various two-dimensional blueprints, which tell the 3D printer where to deposit each subsequent layer of material. (Attaran, 2017).

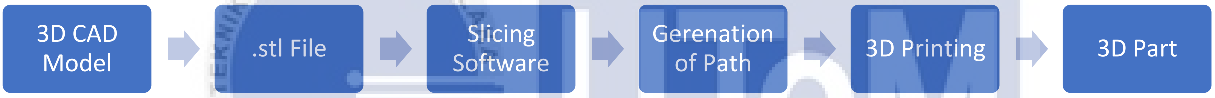

Figure 2.1: Systemic process of AM (Wang et al., 2020)

The various AM technologies employ specific mechanisms to construct objects layer by layer, each with their own advantages and disadvantages. The major patented AM technologies are briefly described below. In 2015, the ISO/ASTM 52900:2015 standard was established to standardize terminology, classify different process categories, and outline associated AM technologies (ISO/ASME International, 2015). ISO (2015) offers explanations regarding the fundamental processes of AM, including the types of materials that can be utilized in different process categories. These standards play a crucial role in highlighting the distinctions among characteristics, processes, and terminologies of different AM technologies, as well as their current limitations. Therefore, it is important to consider these standards when selecting technologies and identifying suitable spare parts for AM. The seven AM process categories (along with the corresponding AM technologies in parentheses) are as follows:

1. Material extrusion
2. Vat Polymerisation
3. Powder Bed Fusion
4. Material Jetting
5. Binder Jetting
6. Direct Energy Deposition
7. Sheet Lamination

Table 2.1 Classification of AM technology by ASTM International (Gao et al., 2015)

CATOGORIES	TECHNOLOGIES	PRINTED "INK"	POWER SOURCE	STRENGTH/DOWNSIDES
Material Extrusion	Fused Deposition Modelling (FDM)	Thermoplastics, Ceramic Slurries, Metal Pastes	Thermal Energy	Inexpensive extrusion machine and the capability of multi-material printing. However, it has limitations in terms of part resolution, which may be limited, and surface finish, which can be poor.
	Contour Crafting			
Powder Bed Fusion	Selective Laser Sintering (SLS)	Polyamide/ Polymer	High-Powered Laser Beam	High accuracy, detailed prints, and the ability to create high-density parts with specific strength and stiffness. These methods involve powder handling and recycling, as well as the need for support and anchor structures during the printing process. The resulting parts are fully dense and exhibit high specific strength and stiffness.
	Direct Metal Laser Sintering (DMLS)	Atomized metal powder (17-4 PH stainless steel, cobalt chromium, titanium Ti6AI-4V), ceramic powder,		
	Selective Laser Melting (SLM)			
	Electron Beam Melting (EBM)		Electron Beam	

Vat Photopolymerization	Stereolithography (SLA)	Photopolymer, Ceramics (Alumina, zirconia, PZT)	Ultraviolet Laser	Include fast building speed, high part resolution, although it may result in overcutting and scanned line shapes. However, the technology can be costly due to high expenses for supplies and materials.
Material Jetting	Polyjet / Inkjet Printing	Photopolymer, Wax	Thermal Energy / Photocuring	The capability of multi-material printing allows for the use of different materials in the same print, while achieving a high-quality surface finish. However, it should be noted that the materials used in this process may have lower strength compared to other options.
Binder Jetting	Indirect Inkjet Printing (Binder 3DP)	Polymer Powder (Plaster, Resin), Ceramic Powder, Metal Powder	Thermal Energy	Enables the production of objects with vibrant and diverse colors. However, it requires a post-processing step called infiltration. This step involves the filling of voids or gaps in the printed object to enhance its structural integrity. The method also offers a wide range of material options, allowing for greater versatility in material selection. However, one drawback is that finished parts may exhibit high levels of porosity, which can affect their strength and durability.
Sheet Lamination	Laminated Object Manufacturing (LOM)	Plastic Film, Metallic Sheet, Ceramic Tape	Laser Beam	This technology provides a superior surface quality, resulting in a smooth and polished appearance. It is also characterized by affordability, with low costs associated with materials, machines, and the overall printing process. However, there can be challenges related to decubing, which

				involves removing the printed object from the build platform.
Direct Energy Deposition	Laser Engineer Net Shaping (LENS) Electronic Beam Welding (EBW)	Melted Powder and Metal Wire	Laser Beam	Allows for the repair of damaged or worn-out parts, extending their lifespan and reducing the need for replacements. It also enables the printing of functionally graded materials, where different properties are incorporated into a single part. However, achieving these capabilities often requires the use of post-processing machines to achieve the desired results.

AM technologies can be categorized based on the materials used, as the implemented materials in AM vary significantly. This review examines AM technologies by dividing them into four categories: liquid-based, solid-based, and powder-based production methods (Bikas et al., 2016).

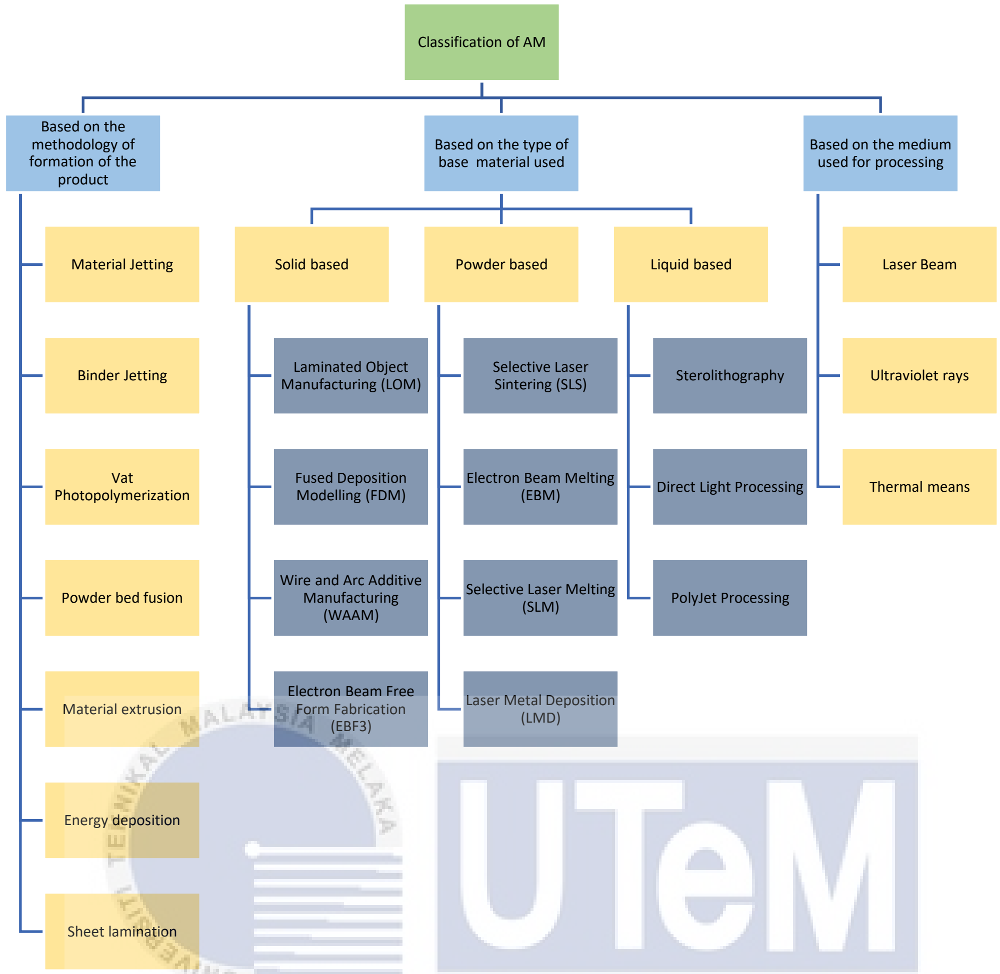

Figure 2.2: Classification of AM processes (Alghamdi et al., 2021)

2.1.1 Additive Manufacturing system

Various AM methods have been developed to meet the demand for printing intricate structures with high precision. Advancements in AM technologies have been driven by factors such as rapid prototyping, printing large structures, reducing defects, and improving mechanical properties. The widely used method, FDM utilizes polymer filaments. Other AM techniques include selective laser sintering (SLS), selective laser melting (SLM), liquid binding in 3D printing (3DP), inkjet printing, contour crafting, stereolithography, direct energy deposition (DED), and laminated object manufacturing (LOM) .(Ngo et al., 2018).

Table 2.2: Comparison of RP techniques (Boejang, 2021)

No.	Manufacturer	RP Techniques	Rp technologies	Materials	Application
1	3DSystems® (USA)	Solidify liquid polymer	Stereolithography (SL)	Acrylate and epoxy resins	1. Master pattern for Rapid Tooling investment casting/RTV 2. Design verification 3. Tests- form&fit, etc
2	1. 3Dsystems®-USA 2. EOS GmbH® Germany	Sintered powder material	Laser Sintering (LS)	Polyamide, Elastomer, Polystyrene, Metal, Stainless steel, and sand	1. Master pattern for RT (plastic & metal) 2. Functional prototype 3. Tooling inserts 4. Sand mold and cavity
3	Stratysis®-USA	Extrusion of material and heat	Fused Deposition Modelling (FDM)	Thermoplastic Elastomer Wax Polycarbonate, etc.	1. Master pattern for RT 2. Functional prototype 3. Tooling insert
4	Z Corporation®-USA	3D printing	Print head and binder	Starch and Plaster	1. Concept model 2. Master pattern for RT
5	Helysis/CubicTechnology®-USA	Lamination of materials	Laminated Object Manufacturing (LOM)	Adhesive paper, ceramics, plastic sheet	1. Concept model 2. Master patter for RT (sand casting)
6	EnvisionTecGmbH®Germany	Solidify liquid polymer	Digital Light Processing (DLP) and masking	Photocurable resin-acrylate	1. Concept modelling 2. Master pattern for RT (jewellery industry)

The application of AM spans across various industries, including aerospace, automotive, healthcare, consumer goods, architecture, and more. This technology offers numerous advantages, such as increased design flexibility, reduced production time and costs, improved product customization, and the ability to create intricate geometries that would be challenging or impossible with traditional manufacturing methods.

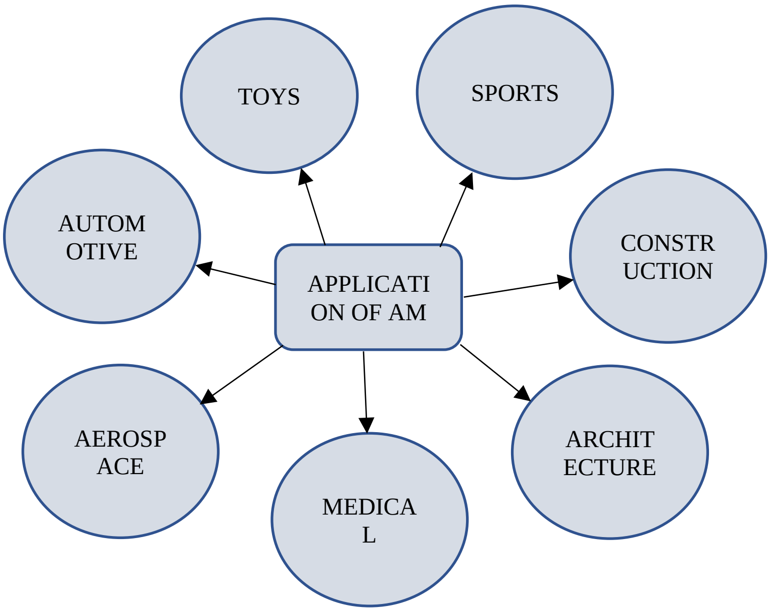

Figure 2.3: Application of AM (Ngo et al., 2018)

The capability to use 3D printing (AM) for medical purposes, such as implants and prostheses, has gained attention. AM allows for the creation of intricate structures in implants, promoting better bone integration and matching the surrounding bone's rigidity (Al-Makky & Mahmoud, 2016). In dentistry, AM is used for various applications like splints, orthodontic devices, and dental models. Researchers are also exploring the potential of AM for creating artificial tissues and organs. In the aerospace industry, AM is attractive for small-scale production (B. Lyons, 2012) due to its ability to produce complex components and spare parts, reducing weight and enhancing fuel efficiency. For example, General Electric reduced the number of components in their jet engines, resulting in significant fuel savings.

2.2 Fused Deposition Modelling (FDM) Technique

FDM (Fused Filament Fabrication), also known as FFF (Fused Filament Fabrication), is a 3D printing technique that builds objects layer by layer by extruding melted material through a nozzle onto a platform (Wong & Hernandez, 2012). It offers a wide range of material options, including plastics, composites, and metals. Multi-nozzle setups can enhance versatility. However, FDM faces challenges like poor interlayer bonding (anisotropy) (Kazmer, 2017)and limited surface quality due to filament parameters (Wong & Hernandez, 2012).

The FDM process is a rapid prototyping (RP) technology initially created by Stratasys. It involves the horizontal deposition of melted thermoplastic materials, such as ABS and PLA (the most commonly used materials in FDM), which are extruded from a nozzle head. This method allows for the fabrication of parts through a layer-by-layer approach (Grim, 2003; Too et al., 2002)

In FDM, supporting structures may be necessary for overhanging features, and these structures can be either break-away or water-soluble (Grim, 2003). Water-soluble structures are dissolved in a solution that does not impact the part's material, whereas break-away structures are manually removed from the part surface. Water-soluble supports can be used in recessed areas and on minor features to keep them in place. Various factors, such as filament feeding rate, extrusion width, linear plotting speed, and layer thickness, are controlled during the FDM process. These parameters are linked since the FDM system's speed is determined by the linear plotting speed and feeding rate, both of which are dependent on the material's melting and feeding capabilities via the nozzle.. (Carneiro et al., 2015).

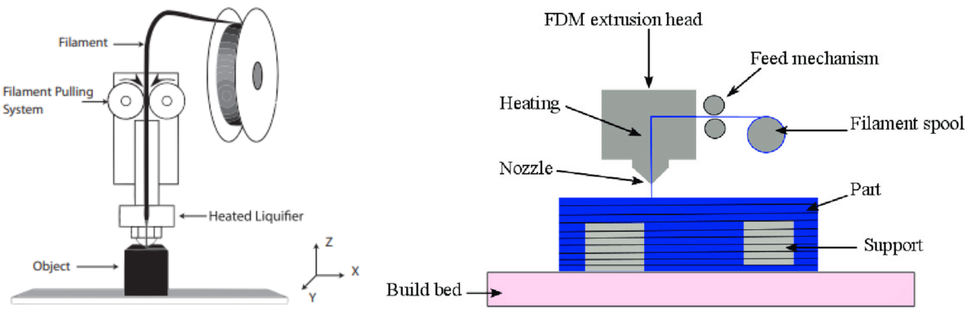

Figure 2.4: Illustration of the FDM technique (Alafaghani et al., 2017)

Similar to other AM systems, FDM starts with a CAD file, typically in .stl format, which is used to create the cross-sectional profiles for layer-by-layer printing. The CAD file provides the outline of the layers, while the software determines the infill pattern for each layer and sets the path of the nozzle (Carneiro et al., 2015). The final print file settings determine whether the focus is on geometric resolution (fine prints) or mechanical performance.

To illustrate the impact of feeding rate and linear movement speed on extrusion width for a given layer thickness, Figure 2.6 shows how increasing the feeding rate results in a wider extrusion, while decreasing the linear plotting speed leads to a similar outcome, given a fixed feed rate. Considering adjacent paths (Figure 2.7), here is a range between two extreme scenarios: paths that are very close together, causing overlap and excess filament deposition, and paths that are far apart, resulting in gaps and weak bonding between them. Optimizing the path width by adjusting the feed rate to the linear plotting speed ratio becomes necessary to achieve a balance. Thicker paths enhance bonding and mechanical performance but may compromise geometric resolution. On the other hand, thinner paths ensure shape accuracy at the expense of mechanical properties (Carneiro et al., 2015).

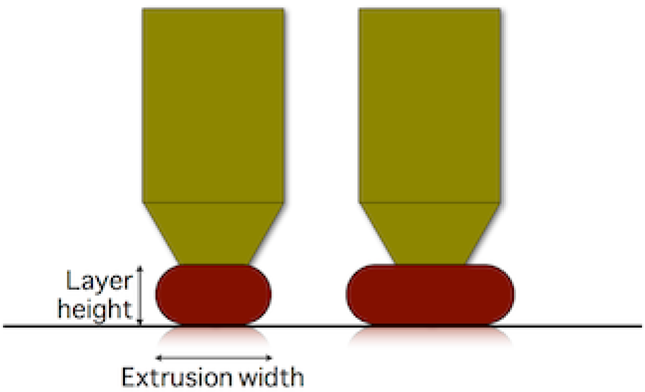

Figure 2.5: FDM extrusion width parameter illustration (Hodgson, 2011)

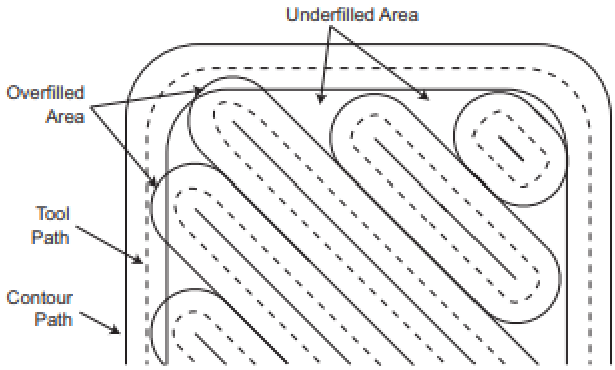

Figure 2.6: Illustration of the paths influence when seeking to obtain geometric precision or mechanical performance. (Carneiro et al., 2015)

FDM offers several advantages as a highly reliable process with a low initial investment and relatively inexpensive materials. It can be operated in office environments, has short build times for thin-walled parts, produces limited material waste (mostly in supporting structures), and allows for the use of different materials or colors within the same object or layer. However, there are drawbacks to consider. FDM requires materials with low melting temperatures, and if supports are needed for overhangs, the surface finish may be poor, requiring additional manual work to improve aesthetics (Carneiro et al., 2015).

2.3 Poly(lactic acid)

PLA is a thermoplastic and biodegradable material that has emerged as a highly innovative material with diverse applications. Its biocompatibility makes it suitable for medical applications, as it is not metabolically harmful (Antoniac et al., 2019; Belaid et al., 2020). Through the FDM method, PLA can be processed as a filament and transformed into various forms, commonly used as implants (Pitjamit et al., 2020). The recent development of a PLA/graphene oxide (GO) nanocomposite material using the 3D printing scaffolding technique of FDM has shown great potential in biological applications. Extensive analysis of scaffolding parameters such as morphology, chemistry, structural and mechanical properties, and biocompatibility revealed that the PLA/GO nanocomposite exhibits promising mechanical properties and cytocompatibility, making it suitable for bone formation applications (Kaynak & Varsavas, 2019).

The fabrication of high-quality filaments is crucial for the successful application of 3D printing, and it has garnered significant attention from both industry and academia. Among the polymers commonly used for filament preparation, acrylonitrile butadiene styrene (ABS) and polylactic acid (PLA) have emerged as the most popular choices. PLA offers several advantages over ABS due to its biodegradability, bio-absorbability, renewability, excellent mechanical strength, and processability. Numerous studies have demonstrated the promising potential of PLA filaments in various applications. For instance, Gaal et al. (Gaal et al., 2017) successfully fabricated integrated microfluidic devices using PLA filaments through FDM 3D printing. Wang et al. (Wang et al., 2016) utilized PLA filament to print bone tissue scaffolds in a cold atmospheric plasma environment. Melocchi et al. (Melocchi et al., 2018) investigated the feasibility of using FDM 3D printing with PLA filaments for manufacturing capsular model devices for oral pulsatile release. Li et al. (Li et al., 2016) employed the rapid prototyping approach of 3D printing to manufacture continuous carbon fibre reinforced PLA composites. Tiersch et al. (Tiersch & Monroe, 2016) explored the application of PLA filaments in cryobiology devices using 3D printing technology. These examples highlight the wide-ranging potential and versatility of PLA filaments in various fields. Table **2.3** shows the primary parameters for 3D printer.

Table 2.3: Primary parameters for the 3D printer (Liu et al., 2018)

Parameters	values
extruder temperature Te (°C)	220
build plate temperature Tb(°C	60
speed while extruding Ve (mm/s)	60
speed without extruding Vt(mm/s)	120
gap between nozzle tip & build layer d (mm)	0.1

filling ratio F (%)	100

Tables Table **2.4** and Table **2.5** shows the advantages and disadvantages of PLA

Table 2.4: Advantages of PLA (Xometry, 2022)

No.	Aspects	Descriptions
1	Biocompatibility	PLA is highly biocompatible and safe for human use, even during prolonged contact with the skin. It degrades into non-toxic lactic acid, making it suitable for medical applications like stents and sutures that gradually dissolve within the body over several months.
2	Low-Energy Production	PLA has a low melting point of 165 °C, requiring less energy for production compared to petroleum-based plastics. Its polymerization process consumes 25 to 55% less energy than traditional petroleum-based polymers, making it environmentally friendly.
3	Mechanical Properties	PLA exhibits favorable strength and stiffness at room temperature, although it may not withstand sudden impact loads as effectively.
4	Food Safety	PLA is FDA-recognized as safe and non-toxic, making it suitable for direct contact with food without health risks.
5	Composability	PLA is compostable in theory but requires specific conditions only found in specialized composting facilities.

Table 2.5: Disadvantages of PLA (Xometry, 2022)

No.	Aspects	Descriptions
1	Hydrophobic Nature	Although hydrophobicity can have advantages in certain scenarios, it can also lead to adverse effects such as localized swelling when used in vivo.
2	Limited Thermal Resistance	PLA has a relatively low glass transition temperature of 55 °C, restricting its suitability for applications that involve temperatures exceeding 50 °C. Despite its easy processability due to the low melting temperature, caution must be exercised in high-temperature environments.
3	Low Toughness	PLA exhibits brittleness and lacks flexibility, making it prone to fracturing rather than bending when subjected to impact loads.
4	High Permeability	PLA allows the passage of both gases and water, resulting in its permeability to these substances. This characteristic should be taken into account when considering applications where gas or water barriers are required.

2.4 Natural Fibre

Natural fibre reinforced thermoplastics are highly favoured by various industries due to their positive characteristics, including lightweight, high strength, and cost-effectiveness. These composites consist of two main components: the matrix and the reinforcement (Ali et al., 2018). Additionally, natural fibres possess biodegradable properties, aligning with the principles of eco-friendly materials. However, there are notable challenges associated with the use of such composites, primarily related to the adhesion bonding between the reinforcement and polymer matrix. This bonding issue can result in costly consequences such as poor wetting, swelling, and dimensional instability, ultimately impacting the mechanical and physical properties of the composite. From a physical standpoint, natural fibres tend to be hydrophilic, which can lead to water absorption and dimensional swelling. However, these issues can be mitigated through appropriate chemical treatments of the natural fibres (Obada et al., 2020).

As environmental concerns continue to grow, the development of polymer composites that can be decomposed or recycled has become increasingly important (Tholibon et al., 2019). The benefits of substituting synthetic and carbon fibres with natural fibres include reduced air toxicity, reduced respiratory difficulties, increased recyclability, and renewability, improved mechanical qualities, and improved waste management. (Tholibon et al., 2019). Governments are now mandating the use of green materials that can be recycled and reused. The decreasing availability of petroleum resources has highlighted the necessity of preserving renewable sources for future generations, prompting industries to embrace sustainable production practices.

As a first step towards manufacturing biodegradable and sustainable goods, researchers are now focusing on building base composites employing natural fibre reinforced biodegradable polymer matrices. Notably, Japan has achieved tremendous success in this field by using kenaf fibre reinforced polylactic acid (PLA) into the production of a variety of goods.(Netravali, 2005). Environmental concerns, such as air pollution and waste disposal, which have implications for the entire ecosystem, have motivated researchers to explore biodegradable composites as alternatives to petroleum-based materials.

Natural fibres can be derived from various sources such as plants, animals, or the environment (refers Table 2.6) . Figure 2.7 and Figure 2.8 provide an overview of the classification of bio composites and natural fibres (Ilyas, Sapuan, Atikah, et al., 2021; Sabaruddin et al., 2021). One of the notable benefits of natural fibres over commercial fibres is their recyclability and biodegradability. The natural fibre market and production have experienced significant advancements, with a particular focus on PLA composites. In industrial development, natural fibres are widely recognized as reinforcements in polymeric materials, including the use of glass fibres as matrix materials (Asyraf, Ishak, Sapuan, et al., 2021; Wambua et al., 2003). The polymer itself is obtained through the fermentation of agricultural sources such as corn, potatoes, sugar beets, and others. Natural fibers, although biodegradable, face challenges including consistency variations, moisture absorption sensitivity, and low thermal stability, hindering their progress. (Asyraf, Rafidah, et al., 2021; Suriani et al., 2021).

Table 2.6: Sources of natural fibres **(Gholampour & Ozbakkaloglu, 2020)**

Fibre	Source
Hair	Hairy mammals and animals like sheep, goats, alpacas, horses.
Avian	Feathers of birds.
Silk	Dried saliva of bugs or insects
Bast	Jute, Flax, Hemp, Ramie, Kenaf, Roselle, Mesta
Leaf	Sisal, Banana, Abaca, Pina,
Seed	Kapok, Cotton, Luffa, Milk weed
Fruit	Coir, Oil palm
Wood	Softwood, Hardwood
Stalk	Rice, Wheat, Barley, Maize, Oat, Rye
Grass	Bamboo, Bagasse, Corn, Sabai, Rape, Esparto, Cancry
Asbestos cloth	Asbestos
Glass	Mixed silicates

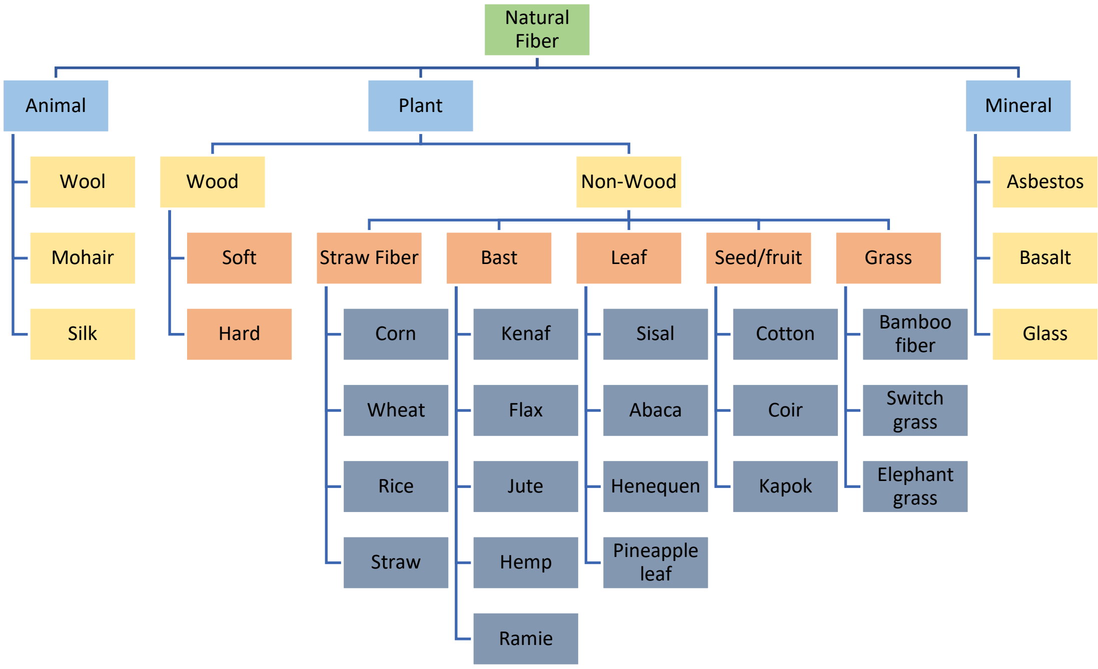

Figure 2.7 Classification of natural fibres (Ilyas, Sapuan, Harussani, et al., 2021)

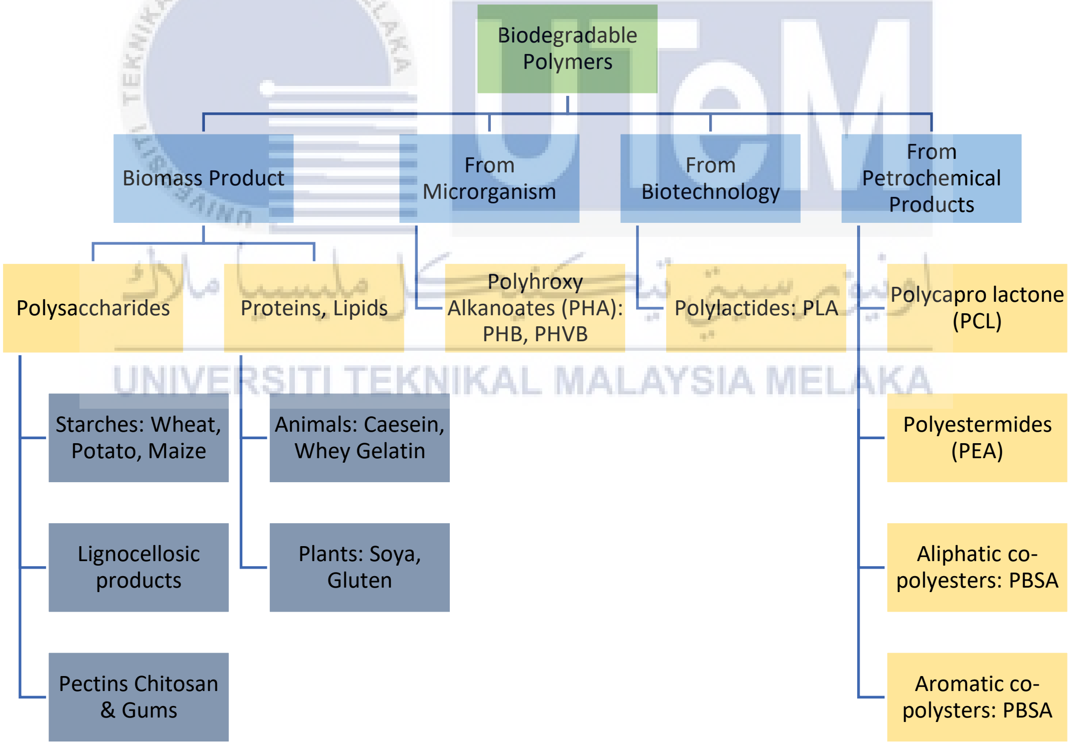

Figure 2.8: Classification of biodegradable polymers **(John & Thomas, 2008)**

Extensive studies on the processing effects and properties of natural fibres have shown improvements in mechanical properties, aligning with the National Policy on Industry 4.0

(Industry 4WRD). Researchers and industry players have shown great interest in the applications of natural fibres in diverse fields, including the military, automotive, industrial, furniture, civil, and biomedical sectors (Alam et al., 2014; Asyraf et al., 2019; Asyraf, Ishak, Sapuan, & Yidris, 2020; Asyraf, Ishak, Sapuan, Yidris, et al., 2020a, 2020b; Asyraf, Rafidah, et al., 2020; Mazani et al., 2019; Nurazzi et al., 2020, 2021). Studies on wood-plastic composites, which combine wood flour with recycled plastic, have demonstrated enhanced mechanical properties with increasing fibre content (Migneault et al., 2008). Non-wood fibres, such as plant straw, leaves, bast, fruit, seed, or grass, are also utilized in composite materials. Straw fibres from sources like maize, wheat, and rice hulls are known for their solid, rigid, low-density, and sustainable characteristics. These natural fibre reinforced composites are commonly used as deck boards in housing construction materials (Mukherjee & Kao, 2011).

The biopolymer PLA has garnered significant attention in various industries due to its impact on the adhesion between fibres or matrix, which greatly influences the mechanical performance of bio composites. Recent research conducted by (Mukherjee & Kao, 2011) has uncovered that the mechanical properties of natural fibres are governed by two key factors: cellulose content and microfibril angle. Higher mechanical properties in fibres lead to improved mechanical properties in the resulting bio composites. The cellulose content directly affects the mechanical properties of natural fibres. Table **2.7** provides an overview of the intricate chemical composition and cellular structures of natural fibres, which vary depending on the plant parts and origins. Lignocellulosic fibres exhibit distinct physical, chemical, and mechanical behaviours attributed to differences in cellulose crystallinity (Cosgrove, 2005). The chemical composition of a fibre is determined by its type, with cellulose, hemicellulose, and lignin being the primary components (Ferreira et al., 2018) (Martins et al., 2004). Each fibre exists as a composite material, with rigid cellulose microfibrils surrounded by an amorphous matrix containing hemicellulose and lignin (Abral et al., 2020; Ilyas et al., 2018).

Table 2.7: Chemical composition of selected common natural fibres (Ilyas, Sapuan, Harussani, et al., 2021)

Fibres	Holocellulose (Wt%)					
	Cellulose (wt%)	Hemicelullose (wt%)	Lignin (wt%)	Ash (wt%)	Extractives (wt%)	Crystallinity (wt%)
Sugar palm fibre	43.88%	7.24	33.24	1.01	2.73	55.8
Wheat straw fibre	43.2 ± 0.15	34.1 ± 1.2	22.0 ± 3.1	-	-	57.5
Soy hull fibre	56.4 ± 0.92	12.5 ± 0.72	18.0 ± 2.5	-	-	59.8
A recanut husk fibre	34.18	20.83	31.6	2.34	-	37
Helicateres isora plant	71 ± 2.6	3.1 ± 0.5	21 ± 0.9	-	-	38
Pineapple leaf fibre	81.27 ± 2.45	12.31 ± 1.35	3.46 ± 0.58		-	35.97
Ramie fibre	69.83	9.63	3.98	-	-	55.48
Oil palm mesocarp fibre (OPMF)	28.2 ± 0.8	32.7 ± 4.8	32.4 ± 4.0	-	6.5 ± 0.1	34.3
Oil palm empty fruit bunch (OPEFB)	37.1 ± 4.4	39.9 ± 0.75	18.6 ± 1.3	-	3.1 ± 3.4	45
Oil palm frond (OPF)	45.0 ± 0.6	32.0 ± 1.4	16.9 ± 0.4	-	2.3 ± 1.0	54.5
Oil palm empty fruit bunch (OPEFB) fibre	40 ± 2	23 ± 2	21 ± 1	-	2.0 ± 0.2	40
Rubber wood	45 ± 3	20 ± 2	29 ± 2	-	2.5 ± 0.5	46
Curauna fibre	70.2 ± 0.7	18.3 ± 0.8	9.3 ± 0.9	-	-	64
Banana fibre	7.5	74.9	7.9	0.01	9.6	15
Sugarcane bagasse	43.6	27.7	27.7	-	-	76
Kenaf bast	63.5 ± 0.5	17.6 ± 1.4	12.7 ± 1.5	2.2 ± 0.8	4.0 ± 1.0	48.2
Phoenix dactylifera palm leaflet	33.5	26	27	-	6.5	50
Pheonix dactylifera palm rachis	44	28	14	2.5	-	55
Kenaf core powder	80.26	80.26	23.58	-	-	48.1
Water hyacinth fibre	42.8	20.6	4.1	-	-	59.56
Wheat fibre	43.2 ± 0.15	34.1 ± 1.2	22.0 ± 3.1	-	-	57.5
Sugar beet fibre	44.95 ± 0.09	25.40 ± 2.06	11.23 ± 1.66	17.67 ±	-	35.67
Mengkuang leaves	37.3 ± 0.6	34.4 ± 0.2	24 ± 0.8	24 ± 0.8	2.5 ± 0.02	55.1

2.5 Bio composite

Bio composites are composites that are considered compatible with living organisms and/ or environmentally friendly. They consist of a diverse range of organic and/or inorganic components, including natural and synthetic polymers, polysaccharides, proteins, sugars, ceramics, metals, and nanocarbons. Bio composites can take various forms, such as films, membranes, mouldings, coatings, particles, fibres, and foams. In addition to research focused on enhancing the fundamental mechanical properties and functionalities of these materials, there have been numerous studies dedicated to the development of eco-friendly composites and biomedical materials for applications in fields such as sensors, tissue engineering, implants, and scaffolds (Haraguchi, 2014). **Error! Reference source not found.** shows classification of biocomposites.

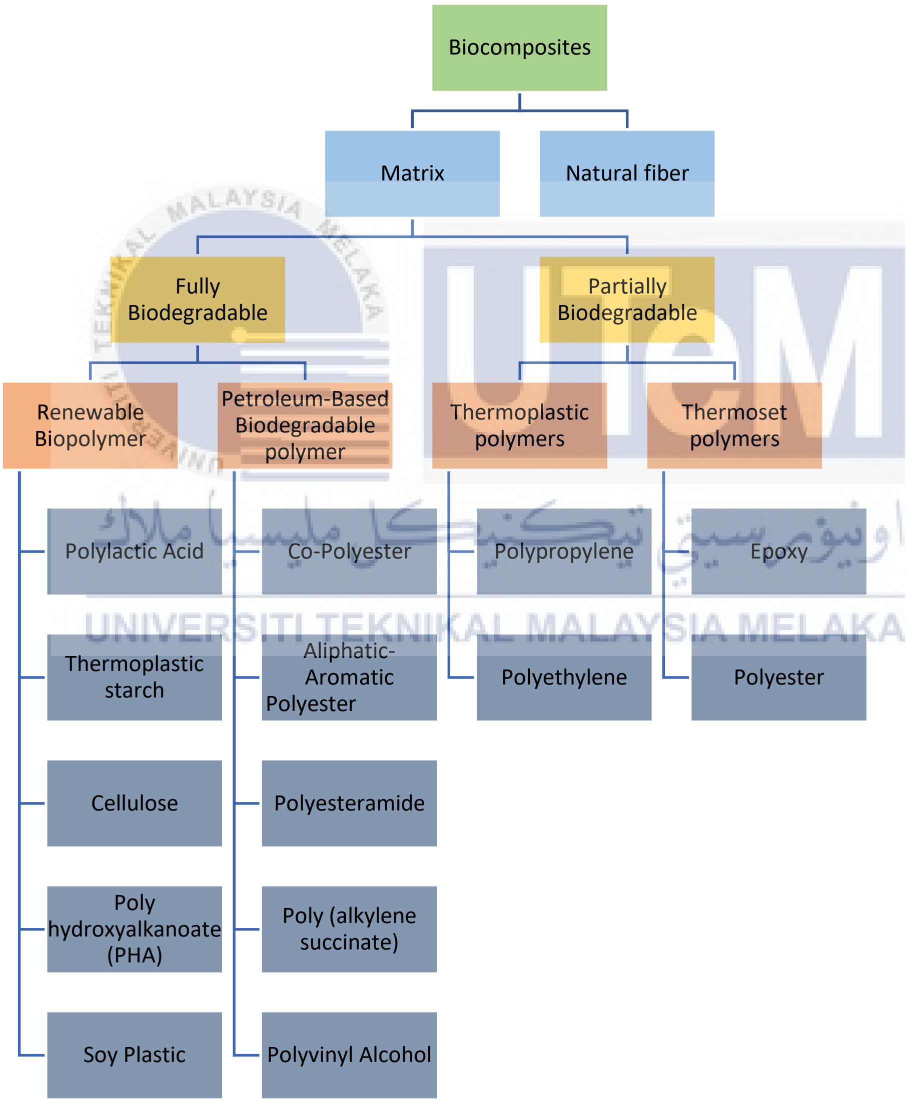

Figure 2.9: Classification of biocomposites (Ilyas, Sapuan, Harussani, et al., 2021).

Bio composites combine organic and inorganic components, including natural polymers like starch, cellulose, and chitosan, as well as synthetic polymers such as PVA and polypropylene. (Faruk et al., 2012; John & Thomas, 2008). Bio composites offer a wide range of combinations for different applications, including organic/inorganic, organic/organic, and inorganic/inorganic combinations. Examples include chitosan/HAp, alginate/HAp, glucose oxidase/CNT/graphene oxide, sodium alginate/silk fibroin, starch/lignin, and HAp/titania rods, among others. (Tjong, 2009). Bio composites can be prepared and processed using methods like electro-spinning, layer-by-layer deposition, thermo-moulding, and compression-moulding. They can be obtained in forms like films, membranes, fibres, coatings, foams, and hydrogels.

Several studies have explored the use of biomaterials as fillers in PLA polymer matrices for various purposes (Wasti & Adhikari, 2020). One such investigation focused on lignin as a filler material in thermoplastic polymer matrices derived from bio-sources. In a study by Tanase et al, a bio composite filament made of PLA and soda lignin was evaluated for FDM 3D printing. The findings showed that reducing the lignin concentration enhanced the flexibility of PLA bio composites. However, using acetylated or unmodified lignin resulted in decreased flexibility when the lignin loading exceeded 10 wt%. (Opedal et al., 2019).

Polylactic acid (PLA) is a flexible polymer derived from sustainable agricultural waste through fermentation into a carboxylic acid. It undergoes polymerization via a cyclic dilactone, lactide, to modify its structure (Ilyas, Sapuan, Harussani, et al., 2021). Growing environmental concerns, as well as the enforcement of new regulations and rules, have prompted businesses to develop eco-friendly products. (Ali et al., 2020).

Several studies have focused on the development of fully biodegradable composite structures by combining PLA and natural fibre. These composites, composed of renewable and biodegradable materials, have gained attention as recyclable and environmentally friendly materials. They offer notable benefits, including reduced manufacturing costs and simplified waste disposal through landfill, incineration, or green treatment methods like (Sapuan & Abdan, 2020). Biopolymers are suitable for various composite fabrication techniques such as injection moulding, extrusion, and compression moulding. However, research on composites derived from recycled raw materials as matrices has been limited.

Biopolymers are not meant for single use; they meet the longer-term requirements of sustainable materials. Studies have shown that natural fibre composites exhibit higher stiffness than glass fibre composites, indicating their strength (Oksman et al., 2003). The adhesion between the fibre and matrix is a dynamic process influenced by multiple variables. Lignin, as identified by Graupner (Graupner, 2008), has been found to enhance the bond between the fibre and matrix, leading to the development of advanced natural fibre reinforced PLA composites. Reinforcing PLA composites with natural fibres plays a crucial role in expanding the applications of bio composites in the mechanical field. PLA stands out due to its high-volume applications in various industrial demands between biodegradable polymers. Its effective life cycle assessment demonstrates advantages such as reduced transportation requirements and lower greenhouse gas emissions. The exceptional properties of PLA-based bio composites, including biodegradability, renewability, and lower CO_2 emissions, contribute to their market performance.

2.6 Sugar Palm

The sugar palm tree is widely distributed in Malaysia, particularly in rural areas such as Bruas-Parit in Perak, Raub in Pahang, Jasin in Melaka, and Kuala Pilah in Negeri Sembilan. It grows naturally in various locations throughout the country (Razak & Ferdiansyah, 2005). Some specific plantations of sugar palm trees can be found in Tawau (Sabah, West Malaysia), where Kebun Rimau Sdn.Bhd. has planted around 809 hectares, and in Benta and Pahang, where there are 50 hectares of sugar palm tree plantations (Sahari et al., 2012). However, the cultivated area of sugar palm trees is smaller compared to other palm species like oil palm and coconut.

The sugar palm tree has approximately 150 local names, indicating its diverse uses among villagers. In Malaysia, it is known as either "enau" or "kabung." This tree is highly valued for its various parts, including the root, stem, fibres, leaves, sap from flowers, and fruits, which are utilized to make a wide range of useful products (Adawiyah et al., 2013). Almost every part of the sugar palm tree has value, and it is considered a versatile multipurpose tree. A single sugar palm tree can yield at least 60 different products, making it truly multifunctional (Lavelle, 2011).

Despite being abundant in Malaysia, sugar palm fibre (locally known as "ijuk fibre") has not been widely used as reinforcement in polymer composites (Sahari et al., 2012). Traditionally, local communities utilize this fibre to make brooms, brushes, septic tank base filters, door mats, carpets, chair/sofa cushions, and ropes. Although the fibre is known for its strength and stiffness, limited research has been conducted to fully explore the potential of sugar palm fibres and their composites (Lavelle, 2011; Sastra et al., 2006a).

Another notable aspect of sugar palms is their ability to produce biopolymers, specifically starch. The starch obtained from the trunks of sugar palm trees can be used to create biodegradable polymers. These polymers can then be reinforced with natural fibres to form green composites. The use of sugar palm-based composites offers advantages such as renewability, biodegradability, affordability, and abundant availability, particularly in tropical countries like Malaysia, Indonesia, Cambodia, and the Philippines. As a result, sugar palm composites hold great promise in the field of bio composite materials. Figure 2.8 shows the chemical composition of fibers from different parts of the sugar palm tree.

Table 2.8: Chemical composition of fibers from different parts of the sugar palm tree **(Sahari & Sapuan, 2012)**

composition	sugar palm frond	sugar palm bunch	ijuk	sugar palm trunk
cellulose (%)	66.49	61.76	52.29	40.56
helocellulose (%)	81.22	71.78	65.62	61.1
lignin (%)	18.89	23.48	31.52	46.44
Ash (%)	3.05	3.38	4.03	2.38
Moisture (%)	2.74	2.7	7.4	1.45
Extraction (%)	2.46	2.24	4.39	6.3

Figure 2.10: Naturally woven sugar palm fiber from sugar palm trunk (Sanyang et al., 2016)

Figure 2.11: (a) Sugar palm tree, (b) sugar palm fibre bundle, (c) combed sugar palm fibres, (d) sugar palm fibres soaked in 1% NaOH solution, (e) yarning process, and (f) sugar palm fibre yarn (Norizan et al., 2018)

2.6.1 Chemical Treatments

The purpose of these chemical treatments was to enhance the bonding between the fibre and matrix of the SPF/PLA composite. By immersing the SPF particles in alkaline and silane solutions, the surface properties of the particles were modified, leading to improved adhesion between the fibres and the matrix. The combination treatment aimed to capitalize on the benefits of both the alkaline and silane treatments. Chemical treatments in polymers are intricate, and the choice of appropriate solvents is crucial. When the polymer interacts on a molecular level with solvents, it undergoes a viscosity change. This alteration, similar to most physical changes, is reversible, resulting in the treated parts returning to a solid state after a certain period of exposure. The occurrence of such a reaction is particularly intriguing because any AM process exhibits a "staircase effect" in the direction of layering. The flow of the viscous material enables surface smoothing. Alternatively, since polymer surfaces are easily permeable, coatings can be applied to enhance surface roughness and confer additional attributes to it (Casado, 2021). In this project, the bio composite filament was treated with NaOH + Silane treatment. The thermal and rheological properties of bio-composite filament materials play a vital role in the advancement of bio-composite FDM filaments. This is because the printing process of FDM heavily relies on the heating and extrusion process.(Nasir et al., 2022).

Table 2.9: Mechnical properties of sugar palm fiber and saturated polyester composite (Nurazzi et al., 2020)

properties	material		
	untreated sugar palm fibre	treated sugar palm fibre	unsaturated polyester
density (g/cm3)	1.292	1.193	1.212
tensile strength (Mpa)	156.96	332.28	44.4
Tensile modulus (Gpa)	4.96	17027	3.54
Elongation at break (%)	7.98	5.3	2.15

2.6.2 Physical and Mechanical Properties

Bachtiar et al. (Bachtiar et al., 2010) described that the age and altitude of the fibre obtained from the sugar palm tree influence its strength. (Ishak et al., 2013). SPF exhibits heat resistance up to 150 °C, with a flash point of 200 °C (Sastra et al., 2006). The harvested SPF from the tree trunk is categorized into grades A to E based on its dimensions, including thickness and length (Rashid et al., 2017)

In terms of mechanical properties, Bachtiar et al. (Chandrasekar et al., 2017) reported that SPF has a tensile strength of 190.29 MPa, a tensile modulus of 3.69 GPa, and an elongation at break of 19.6%. Nurazzi et al. (My et al., 2017) mentioned that SPF is made up of black fibres with great tensile strength, similar to coir, bamboo, and kenaf fibres. Table 2.10 compares the mechanical properties of SPF to those of other lignocellulosic fibres. SPF has a huge benefit in terms of durability and longevity since, unlike coir fibres, it is unaffected by heat and moisture.

Additionally, SPF exhibits resilience to seawater, making it suitable for marine applications (Misri et al., 2010). Table **2.11** shows the mechanical properties of fibers from different parts of sugar palm tree while Table **2.12** shows the mechanical properties of fibers from different parts of sugar palm tree.

Table 2.10: Comparison of the mechanical performance of SPF with other lignocellulosic fibres (Asyraf et al., 2022)

Fibre	Density (g/cm3)	Tensile Modulus (Gpa)	Tensile Strength (Mpa)	Elongation At Brek (%)
Sugar Palm	1.292	4.96	156.96	7.98
Bagasse	1.5	17	290	
Bamboo	1.25	11 To 17	140 To 230	
Flax	0.6 To 1.1	27.6	354 To 1035	2.7 To 3.2
Hemp	1.48	70	690	1.6 To 4
Jute	1.3	26.5	393 To 773	1.5 To 1.8
Kenaf	1.45	53	215.4	1.6
Sisal	1.5	9.4 To 22	511 To 535	2.0 To 2.5
Pineapple	0.8 To 1.6	1.44	400 To 627	14.5
Coir	1.2	4 To 6	138.7	30

Table 2.11: Mechanical properties of fibers from different parts of sugar palm tree **(Sahari & Sapuan, 2012)**

Fibres	Sugar Palm Frond	Sugar Palm Bunch	Sugar Palm Trunk	Ijuk
Tensile Strength (Mpa)	421.4	365.1	198.3	276.6
Tensile Modulus (Gpa)	10.4	8.6	3.1	5.9
Elongation At Break (%)	9.8	12.5	29.7	22.3

Table 2.12: Mechanical and physical properties of unsaturated polyester composites reinforced sugar palm fibre obtained from different parts (Ishak et al., 2013)

Composites	SPF/PE	SPB/PE	SPT/PE	Ijuk/PE
Tensile Strength (Mpa)	15.18	12.81	9.82	11.47
Tensile Modulus (Gpa)	0.39	0.43	0.56	0.47
Elongation At Break (%)	8.07	5.04	3.19	4.45
Flexural Strngth (Mpa)	38.91	35.17	41.9	33.74
Flexural Modulus (Gpa)	3	2.75	3.36	2.42
Impact Strength	8.09	6.58	3.92	4.57
Water Absorption	1.57	1.35	0.39	0.65
Thickness Swelling	1.56	1.11	0.5	0.76

2.6.3 Thermal Properties

Thermal characterization is a crucial laboratory method used to assess the composite material's ability to withstand heat. This evaluation holds significant importance in various fields, such as food, pharmaceuticals, organic and inorganic chemicals, engineering, automobile, aerospace, and defence industries (Asyraf, Ishak, Norrrahim, et al., 2021).

Tests like dynamic mechanical analysis (DMA) and thermogravimetric analysis (TGA) are used for thermal characterization. They measure parameters such as weight loss, stiffness, strength, dimensional changes, and heat flow with respect to temperature. (Saba et al., 2016). Thermal analysis provides valuable insights into composite properties, such as molecular structure, decomposition behavior, crystallization, oxidation, stability, viscoelasticity, mobility, glass transition temperature (Tg), volatilization, and crosslinking. Table **2.13** shows the optimal thermal properties of SPF mentioned by previous published works.

Table 2.13: Optimal thermal properties of SPF mentioned by previous published works (Asyraf, Ishak, Norrrahim, et al., 2021)

natural fibre	temperature of initial decomposition (T onset) (°C)	Maximum decomposition temperature (T max) (°C)

sugar palm	228	312
flax	220	39
okra	220	359
kenaf	219	284
jute	205	283
hemp	250	390
caraua	230	335
roselle	210	366

2.7 Summary

This chapter serves as a comprehensive exploration of the research topics relevant to this project. Extensive information and resources were gathered from reputable and officially published sources, particularly academic journals. The content presented in this chapter is intended to provide a foundation of knowledge and guidance for the subsequent chapter, Chapter 3 Methodology. The aim is to establish a clear and effective working procedure that will facilitate the achievement of the study's objectives. By meticulously compiling information from trusted sources, this chapter ensures that the project is built upon a strong and reliable knowledge base. The topics covered in this chapter are carefully selected to align with the objectives of the study. The information serves as a roadmap, outlining the necessary processes and technologies that will be employed in the upcoming methodology chapter. The research conducted for this chapter involves a critical review and synthesis of existing literature, enabling a comprehensive understanding of the subject matter. The chosen sources are reputable and recognized in the academic community, ensuring the reliability and validity of the information presented.

CHAPTER 3

METHODOLOGY

3.1 Introduction

In this chapter, a comprehensive methodology is presented to ensure the successful implementation of the project. The experiment involves utilizing an AM system, and FDM with Sugar Palm Filament. The primary focus of this project is to investigate the dimensional accuracy, surface roughness, and mechanical properties of the printed parts. To evaluate the project, the methodology encompasses three key steps: planning, implementation, and analysis. Several stages are followed to achieve the desired results. In summary, the project begins with an experimental study that involves producing Sugar Palm Filament. CAD designs are then transferred into the STL file format and verified using Ultimaker Cura Software. The prototypes are fabricated using FDM, and an investigation is conducted to assess the dimensional accuracy, surface roughness, and mechanical properties of the printed parts from the FDM machine. Additionally, a comparison between new and commercial filaments for the printed parts will be carried out. To provide a visual representation of the project methodology, Figure 3.1 presents a flowchart illustrating the methods employed in this study.

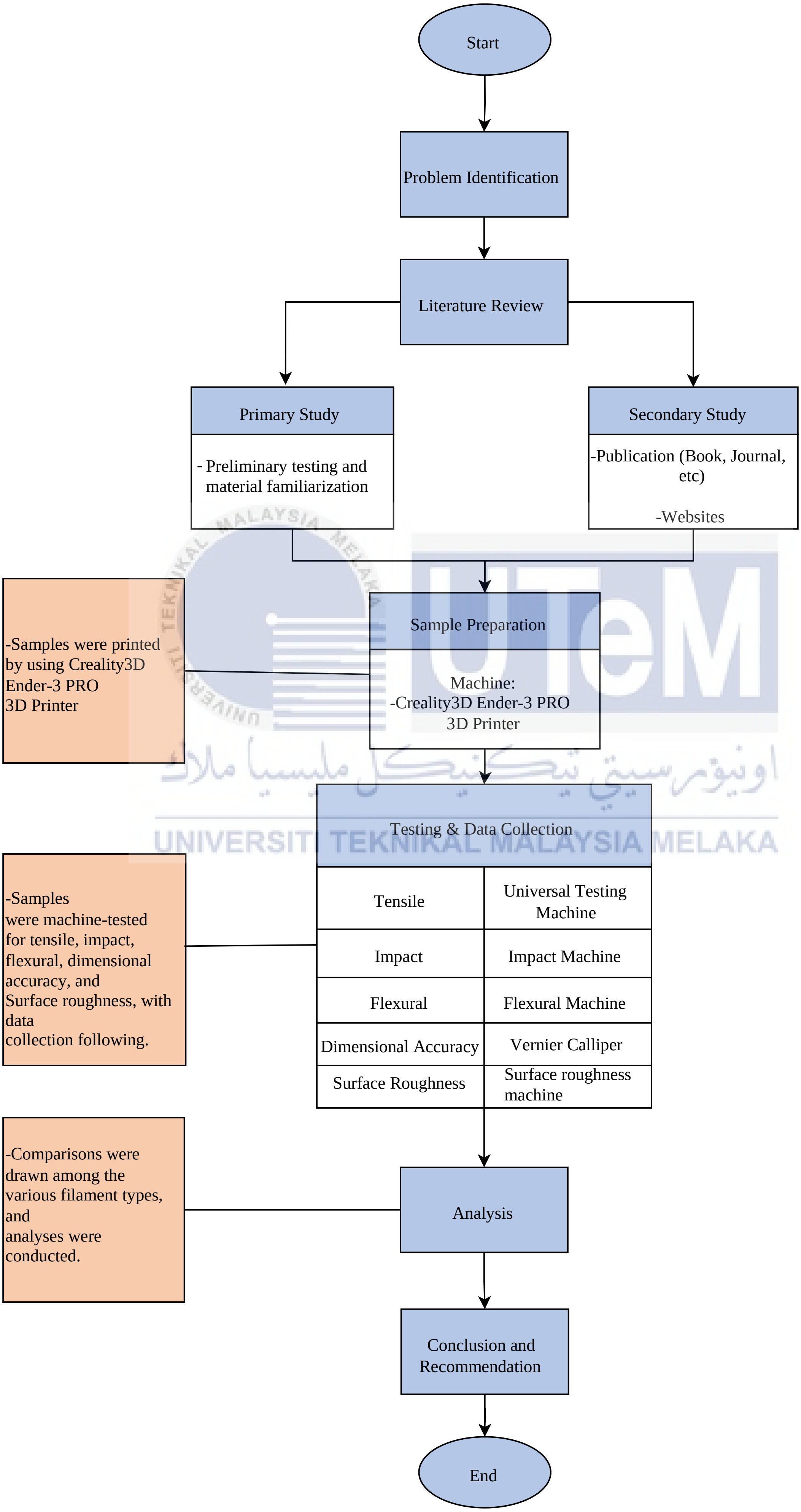
Start
Problem Identification
Literature Review
Primary Study
- Preliminary testing and material familiarization
Secondary Study
-Publication (Book, Journal, etc)
-Websites
Sample Preparation
Machine:
-Creality3D Ender-3 PRO 3D Printer
-Samples were printed by using Creality3D Ender-3 PRO 3D Printer
Testing & Data Collection
Tensile
Universal Testing Machine
Impact
Impact Machine
Flexural
Flexural Machine
Dimensional Accuracy
Vernier Calliper
Surface Roughness
Surface roughness machine
-Samples were machine-tested for tensile, impact, flexural, dimensional accuracy, and Surface roughness, with data collection following.
Analysis
-Comparisons were drawn among the various filament types, and analyses were conducted.
Conclusion and Recommendation
End

Figure 3.1: Flowchart of project

3.2 Primary study

In the primary study, the research methodology centers on experimental testing, focusing on critical parameters such as surface roughness, dimensional accuracy, and mechanical testing encompassing tensile, flexural, and impact assessments. This empirical approach involves a meticulous examination of firsthand data, providing a nuanced understanding of the subject matter. Surface roughness measurements offer insights into the quality of surfaces, dimensional accuracy provides a gauge of precision, and mechanical testing assesses the material's structural integrity. By conducting experiments, the primary study aims to contribute new and valuable information to the existing body of knowledge, enhancing the empirical foundation of the literature review.

3.3 Secondary study

Secondary study revolves around an extensive exploration of published works, drawing from a variety of sources, including books, journals, articles, and reputable websites. Books, as comprehensive repositories of knowledge, provide in-depth discussions and theoretical frameworks, while scholarly journals present peer-reviewed research articles offering detailed analyses and interpretations. Articles from reputable sources contribute additional perspectives and findings, enhancing the breadth of the review. Additionally, websites from established organizations and academic institutions offer supplementary information, ensuring a holistic overview of the subject matter. By synthesizing insights from both primary experimental studies and secondary literature sources, this literature review aims to provide a comprehensive analysis, enriching the understanding of the chosen topic and contributing to the broader knowledge base in the field.

3.4 3D Printing Fabrication

3D printing fabrication, also referred to as AM is a groundbreaking technique that involves the creation of physical objects using a 3D printer. This technology enables the conversion of digital designs into tangible products by building them layer by layer. The process commences by generating a 3D model using specialized software or obtaining an existing model from a digital repository. This digital representation serves as the blueprint for the object that will be printed.

Subsequently, the 3D model undergoes slicing, where it is divided into thin horizontal layers using slicing software. These layers are then transformed into instructions that the 3D printer can interpret. The printer follows these instructions precisely to construct the object layer by layer. During the printing process, the 3D printer deposits or solidifies material in a precise manner based on the sliced model. The choice of material depends on the type of printer and the desired characteristics of the final object. Common materials utilized include plastic filaments, resins, metals, ceramics, and even edible substances.

3.4.1 3D Printing Machine

During the fabrication process, the Creality3D Ender-3 PRO 3D Printer is utilized. This particular machine utilizes material extrusion, also known as the FDM process. The primary material used in this machine is PLA filament material.

Figure 3.2: FDM Machine (Creality3D Ender-3 PRO 3D Printer)

3D printing specifications

- Machine size: 440 x 420 x 465 mm
- Weight: 6.98 kg
- Printing size: 220 x 220 x 250 mm
- Printing precision: ± 0.1 mm
- Packaging size: 600 x 505 x 465 mm
- Nozzle size: standard 0.4 mm, can be in 0.3 mm or 0.2 mm.
- Maximum heated bed temperature: ≤110°C
- Printing Speed: ≤180 mm/s, normal 30-60 mm/s
- Connectivity: SD card, Online

Materials:

- Filament diameter: 1.75 mm
- Third-party filament: Yes
- Filament materials: PLA, ABS, wood, copper, gradient, etc.

Software requirements:

- Operating system: Window, Linux, Mac
- Recommend slicer: Cura/ Repeater-Host/ Simplify3D
- File types: STL, OBJ, AMF

3.4.2 3D Printing Process

The Creality3D Ender-3 PRO 3D Printer, equipped with a 0.4 mm nozzle diameter and a heating plate, offers a maximum printing area of 220 x 220 x 250 mm. With a precision of ± 0.1 mm, this printer ensures accurate manufacturing of the designed parts. The Ultimaker Cura program controls the 3D printer during the process, and the parameter settings for this particular print job were as follows:

3.5 Dimensional Accuracy Measurement and Analysis

Dimensional accuracy in 3D printing is the degree to which the printed object aligns with the intended dimensions outlined in the digital design. It plays a crucial role in ensuring the functionality and fit of the final product. To evaluate dimensional accuracy, precise measurements are taken using tools like vernier calliper. These measurements are then compared to the specified dimensions in the digital design, highlighting any variations and determining the level of accuracy achieved. In this project, the SPF+PLA printed parts will be compared to the PLA printed part to assess their dimensional accuracy.

3.6 Surface Roughness Measurement and Analysis

Surface roughness measurement is a crucial aspect of industries like manufacturing, engineering, and quality control as it involves the assessment and quantification of surface irregularities and variations. By measuring surface roughness, important information regarding texture, appearance, and overall surface quality can be obtained. This data is valuable in determining the suitability of a surface for specific applications, evaluating the performance of manufacturing processes, and ensuring compliance with desired standards and specifications.

In the evaluation process, a reference surface's finish is used as a basis for determining the surface roughness. Both the prototype and the original object are subjected to surface roughness calculations. To accomplish this, the Mitutoyo SJ-410 Surface Roughness Tester is employed, allowing for the measurement of the prototype's surface finish and the original object's surface roughness. To record the measurements obtained, a mini printer connected to the portable surface roughness tester is utilized.

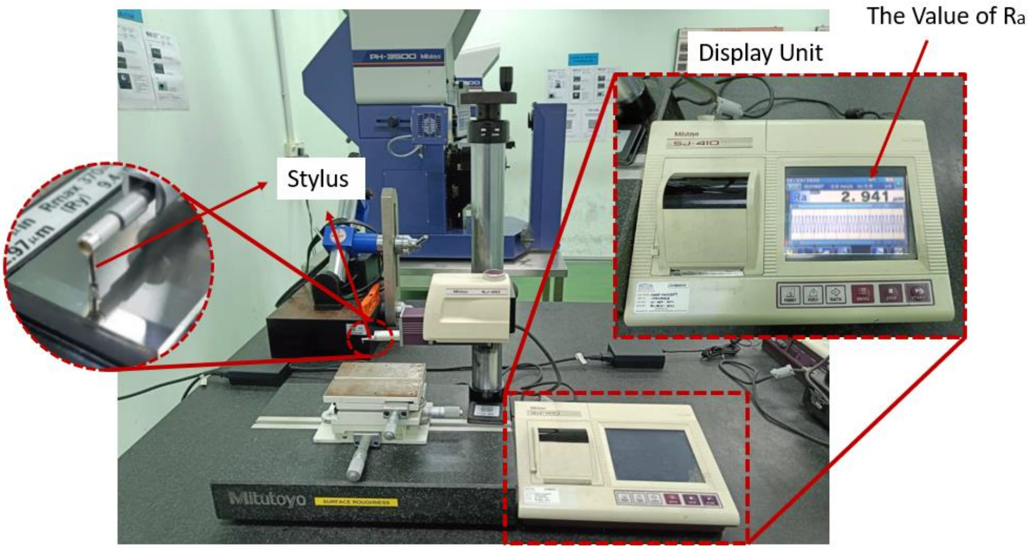

Figure 3.3 Mitutoyo SJ-410 Surface Roughness Tester

3.7 Mechanical Properties Testing and Analysis

Mechanical testing is a set of procedures used to evaluate the mechanical properties and behaviour of materials. These tests are conducted to understand how materials respond to different mechanical forces and stresses, providing valuable insights for design, manufacturing, and quality control purposes. Common mechanical tests include tensile testing, compression testing, flexural testing, hardness testing, impact testing, and fatigue testing. Each test focuses on specific aspects of a material's mechanical performance.

In this project, the specimens will undergo mechanical testing using three specific tests: tensile testing, flexural testing, and impact testing. Tensile testing will assess the material's response to pulling forces, while flexural testing will evaluate its resistance to bending. Impact testing will measure the material's ability to absorb energy under sudden, high-stress loading conditions. These tests will provide essential data on the mechanical properties of the specimens, aiding in the evaluation of their suitability for the intended application.

3.7.1 Tensile

A tensile test is a mechanical test conducted to evaluate the mechanical properties of a material under tension. It is one of the most common and fundamental tests used to determine how a material behaves under stretching or pulling forces. During a tensile test, a standardized test specimen of the material is subjected to an increasing axial load or force. The specimen is typically in the form of 'dog bone' shape. The test specimen is placed in a testing machine called a tensile testing machine or universal testing machine (UTM). The UTM applies a pulling force on the specimen in a controlled manner. As the force is gradually increased, the specimen undergoes deformation and elongation.

Figure 3.4: Universal testing machine

3.7.2 Flexural

A flexural test, also known as a bending test, is a mechanical test used to evaluate the strength and stiffness of a material when subjected to bending forces. It assesses the material's ability to resist deformation and fracture under bending conditions, simulating real-world scenarios where materials are subjected to bending or flexing loads. In a flexural test, a standardized test specimen is placed on supports at its ends, creating a span between the supports. The specimen is loaded with a force applied perpendicular to its longitudinal axis, causing it to bend. The force is gradually increased until the specimen reaches its maximum load or fractures.

Figure 3.5: Universal testing machine

3.7.3 Impact

An impact test is a mechanical test performed to evaluate a material's ability to withstand sudden, high-stress loading conditions. It assesses the material's toughness, resistance to fracture, and ability to absorb energy under impact or shock loads. During an impact test, a standardized test specimen is subjected to a sudden and intense force. This force is typically applied by striking the specimen with a pendulum or a falling weight. The impact generates a rapid and significant deformation in the material, simulating real-world scenarios where materials are exposed to sudden impacts or collisions.

Figure 3.6: IZOD Impact Tester

3.8 Analysis and Result

The objective of this analysis is to compare the Sugar Palm Filament, and PLA filament based on their dimensional accuracy, surface finish, and mechanical properties. To begin the comparison, the accuracy, surface finish, and mechanical properties of printed parts using these two filament types will be measured using its specific machine.

The collected data, including dimensional accuracy, surface finish, and mechanical properties, will be used to create a scatter graph. This scatter graph will provide a visual representation of the distribution and variation of the measured parameters among the different filament types. The analysis of dimensional accuracy, surface finish, and mechanical properties will be conducted by referring to this graph.

By comparing the physical properties, and mechanical properties of the printed parts from the two filaments, we can draw conclusions about their performance and suitability for specific applications. The results of this analysis will contribute to understanding the capabilities and limitations of each filament type, aiding in the selection of the most appropriate filament for future printing projects.

3.9 Summary

To summarize, this chapter presents and investigates the methodology employed in this project. Prior to conducting the experiment, experimental analysis was conducted to gain a clear understanding of the project requirements and develop a comprehensive plan. The chapter outlines the equipment and apparatus utilized in the study, as well as the measurement and analysis procedures that were established. The subsequent chapter, Chapter 4, will delve into more detailed analysis and present the results obtained from the experiment.

CHAPTER 4

RESULTS AND DISCUSSIONS

4.1 Introduction

This chapter presents a comprehensive exploration of the experimental approach undertaken in the project, focusing on the results and analysis of 3D printing fabrication, surface roughness and subsequent testing phases. The Slicing process involved careful parameter adjustments, influencing the precision of the subsequent 3D printing. The printing phase considered variables such as materials and printing parameters, affecting the physical and structural characteristics of the printed objects. Rigorous testing assessed mechanical strength, dimensional accuracy, and surface finish. The results provided valuable insights into the effectiveness of the methodologies, contributing to a holistic evaluation of the 3D printing processes employed. This synthesis forms the basis for further discussions and recommendations, enhancing the overall understanding of the project's experimental outcomes.

4.2 3D Printing Fabrication

The models are meticulously crafted using two distinct types of filament sugar palm fiber filament and PLA filament. The intricacies of the 3D printing process are delineated through the following steps in Table 4.1, with the Creality3D Ender-3 PRO serving as the designated printing machine.

Table 4.1 3D Printing Fabrication

No	Description	Image
1	• The Ultimaker Cura Software was opened. • The stl file was loaded.	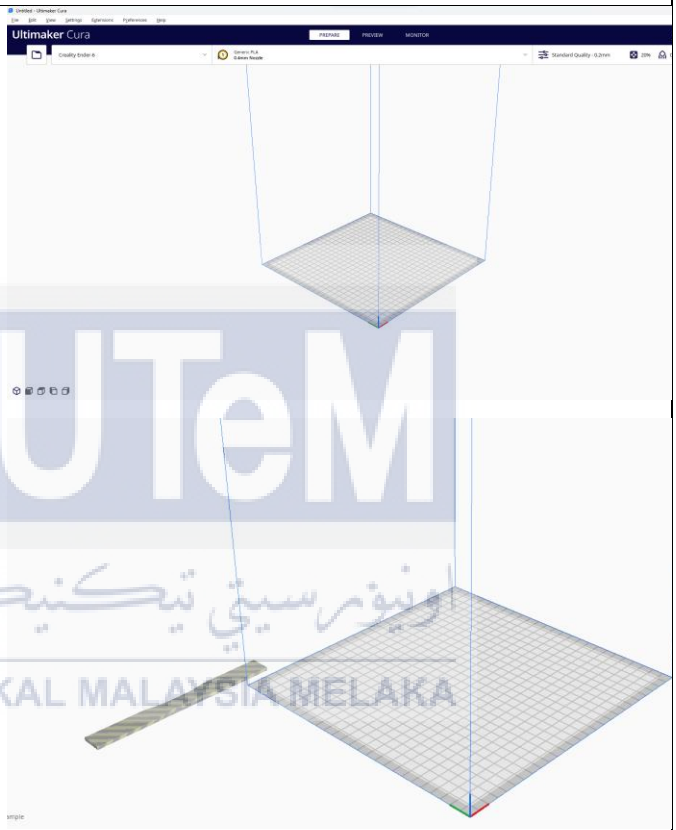

<table>
<tr>
<td>2</td>
<td>

- The design was placed on top of the bed.

</td>
<td>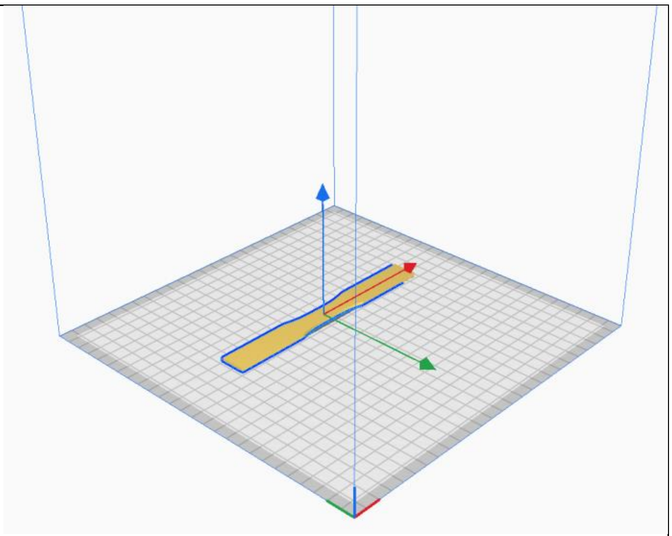</td>
</tr>
<tr>
<td>3</td>
<td>

- The printing parameters were set.

<table>
<tr><th>Parameter</th><th>Description</th></tr>
<tr><td>Layer height</td><td>0.18 mm</td></tr>
<tr><td>Infill density</td><td>100 %</td></tr>
<tr><td>Infill pattern</td><td>lines</td></tr>
<tr><td>Printing temperature</td><td>190 °C</td></tr>
<tr><td>Build plate temperature</td><td>80 °C</td></tr>
<tr><td>Printing speed</td><td>100 mm/s</td></tr>
</table>

</td>
<td>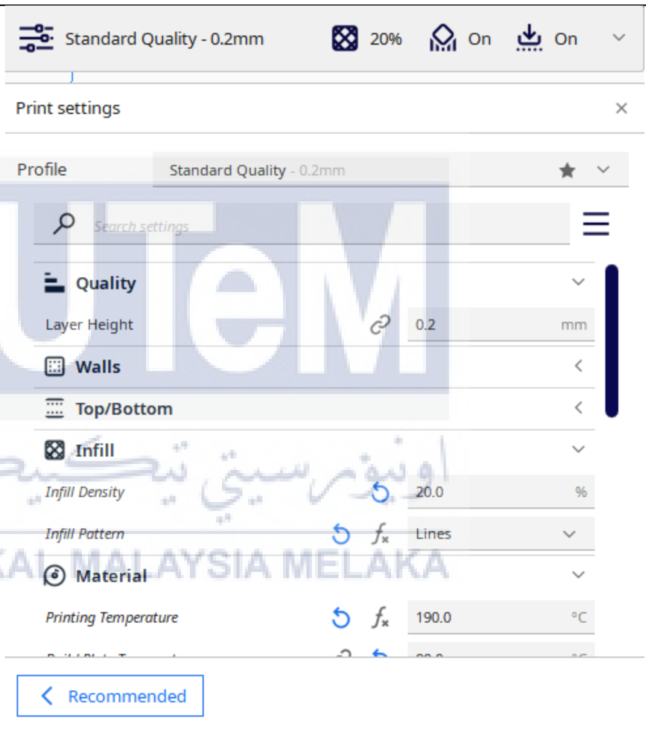
</td>
</tr>
</table>

<table>
<tr>
<td></td>
<td>
<table>
<tr><td>Build plate adhesion type</td><td>brim</td></tr>
</table>
</td>
<td>
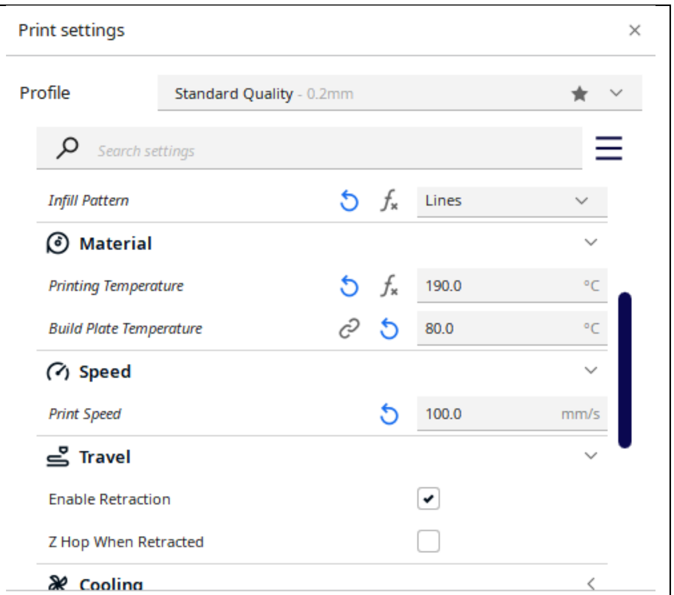

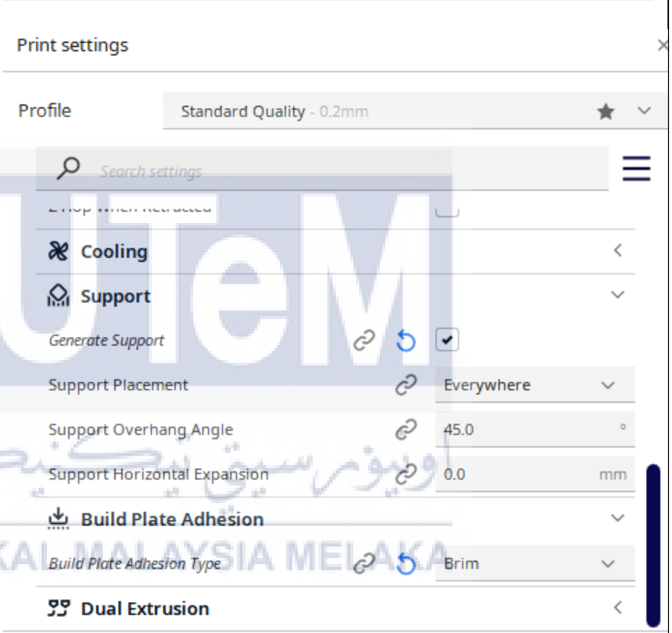

</td>
</tr>
<tr>
<td>4</td>
<td>

- The slicing process was started.

</td>
<td>
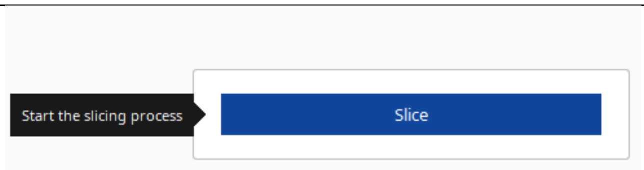

</td>
</tr>
</table>

5	• The preview button was clicked. • A pendrive was inserted into the computer . • The file was saved into the pendrive.	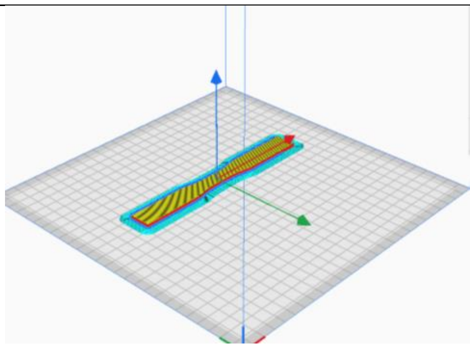 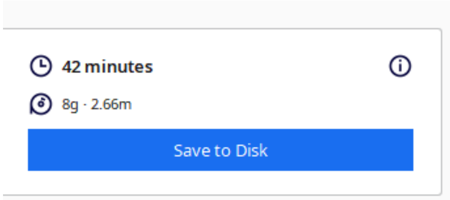
6	• The 3d printing machine was plugged in and switched on.	
	• The sim card was inserted into the 3d printing machine.	

7	• The filament was loaded into the 3d printing machine.	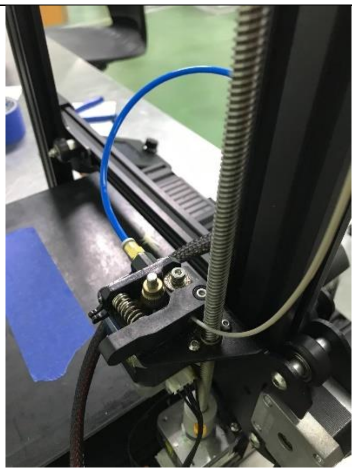
8	• A piece of 3d printing sellotape was cut and placed on top of the build plate.	
9	• The “ disable stopper “ was clicked.	

10	• The nozzle was move to the place where the sellotape was placed	
	• A piece of paper was placed right under the nozzle. • The paper was moved around and the bed was adjusted until theres a feel of friction between the nozzle and the paper. • The bed was adjusted if the gap between the nozzle and the paper is too small or too large • Levelling was completed.	 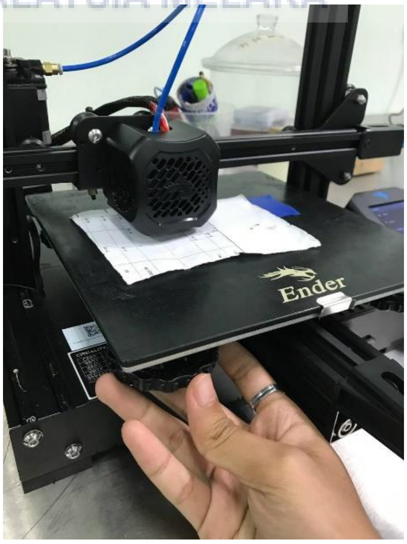

11	• The “ auto home “ was clicked. • The nozzle was back at its original position.	
12	• The “ Preheat PLA” was clicked.	
13	• The file of the product was clicked. • The 3d printing process was begun.	

14	• After the printing process was completed, the product was carefully removed from the build plate.	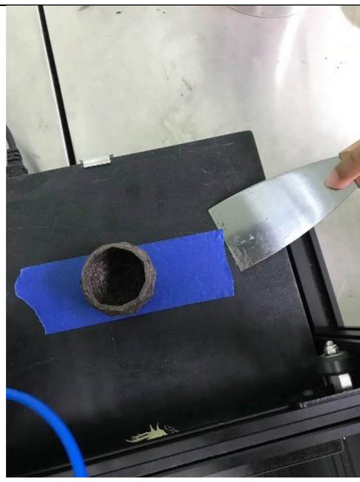
15	• The excess brim and sellotape was removed by using a cutter.	
16	• Final result of the 3d printing product	

17	• The process was repeated for the other type of filament.	

4.3 Surface Roughness

4.3.1 Aim of Surface Roughness Test

The Results and Discussion section of this report undertakes a comprehensive analysis of surface roughness outcomes in 3D printed products incorporating sugar palm fibers. A total of 18 specimens, divided equally into 9 for sugar palm fiber filament and 9 for PLA filament, are subjected to three assessments each sample 1, sample 2, and sample 3. This study meticulously examines how the integration of sugar palm fibers influences the surface finish of the printed objects, with a specific focus on comparing the results between the sugar palm fiber and PLA filament specimens. The surface roughness data serves as a crucial metric in understanding the textural qualities induced by the different filaments. This section aims to provide a nuanced discussion on the comparative implications and potential applications of sugar palm fibers and PLA filament in 3D printing, particularly in relation to their impact on surface characteristics.

4.3.2 Procedure of Surface Roughness Test

The following method describes the specifics of the surface roughness test procedur efor 3D printed specimens of sugar palm fiber and 3D printed specimens of PLA.

i. Mitutoyo SJ-410 Surface Roughness Tester as shown on Figure 3.3 was used as the tool to measure the surface roughness of both 3D printed specimens. The apparatus and objects have been set up as shown on Figure 4.1.

Figure 4.1 surface roughness setup

ii. The calibration was set before using the machine. The calibration must set to 0.00µm before taking any reading so that there will be no zero-error issue.

Figure 4.2 calibration process

iii. The Figure 4.3 shown the setup of surface roughness test of the 3D printed specimens. The clay was used to prevent the specimen from move during taking the reading.

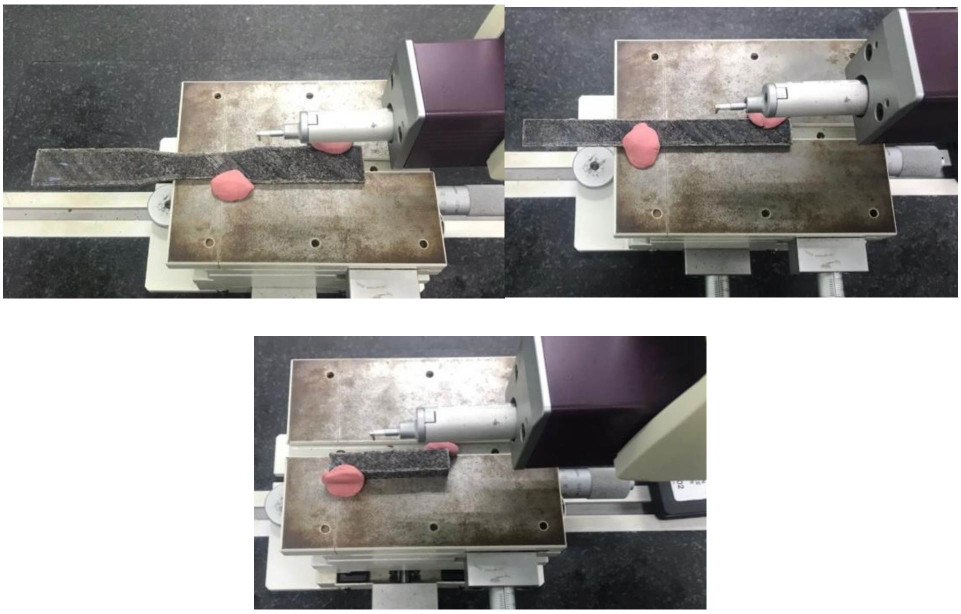

Figure 4.3 setup of specimens

iv. Measurement of surface roughness was carried out on the selected three (3) areas of the sugar palm fiber specimens and PLA bicycle specimens, as shown in Table 4.2 along with the view areas pointed of both prototype model.

Table 4.2 selected areas of 6 specimens

Type	Specimen 1	Specimen 2	Specimen 3
SPF/PLA	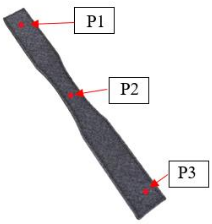	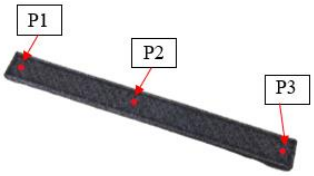	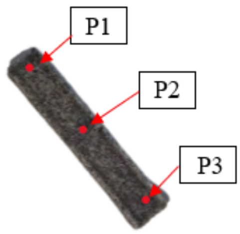

PLA	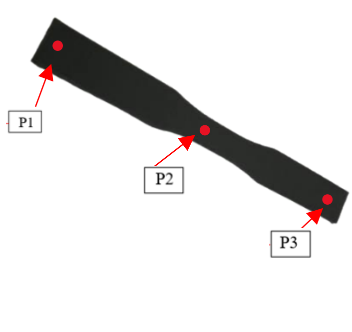	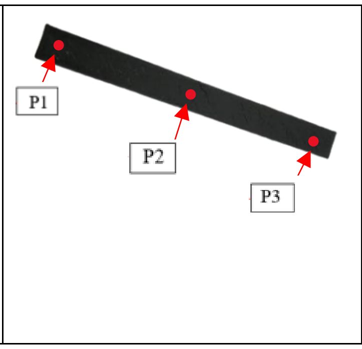	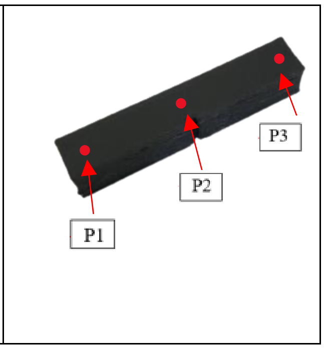

v. The tester's probe has been positioned in the selected region of the object and the knob was turned in a clockwise direction, in order to move down the stylus until the indicator on the screen was placed into the green box in order to move down the stylus as shown in Figure 4.4

Figure 4.4 stylus indicator region

vi. The start button was pressed and the reading was measured.

vii. This experiment was carried out until all readings of the surface roughness of the selected areas were determined. Three measurements reading were made for each region of the specimens.

4.3.3 Data of Surface Roughness Test

3 specific points 1, 2, and 3 (refer to the figure) on the 3D printed product has been designated for analysis. For each region, the surface roughness was calculated three times to derive an average experimental reading. The following shows the surface roughness readings from the three tests for the 3D printed product of SPF/PLA and PLA

4.3.3.1 Surface Roughness SPF/PLA

Table 4.3 surface roughness reading for SPF/PLA

	SPF+PLA				
	Pointed Area	**Experimental Reading, Ra (µm)**			**Average Experimental Reading, Ra (µm)**
		1	2	3	
S1	1	5.71	5.68	5.62	5.67
	2	4.46	4.38	4.42	4.42
	3	7.29	7.27	7.31	7.29
S2	1	14.67	14.74	14.79	14.73
	2	17.64	17.62	17.58	17.61
	3	22.73	22.76	22.80	22.76
S3	1	15.04	14.96	15.13	15.04
	2	18.88	18.66	18.62	18.72
	3	19.18	19.45	19.39	19.34

4.3.3.2 Surface Roughness of PLA

Table 4.4 surface roughness reading for PLA

PLA		
	Experimental Reading, Ra (µm)	**Average Experimental Reading, Ra (µm)**

	Pointed Area	1	2	3	
S1	1	1.09	1.03	1.11	1.08
	2	2.42	2.44	2.46	2.44
	3	1.16	1.14	1.19	1.16
S2	1	2.49	2.51	2.45	2.48
	2	2.11	2.08	2.15	2.11
	3	1.11	1.16	1.13	1.13
S3	1	1.05	1.02	1.07	1.05
	2	0.91	0.93	0.90	0.91
	3	1.97	2.01	1.98	1.99

4.3.3.3 Comparison of SPF/PLA and PLA

Table 4.5 lists the average of the experimental reading of each item. Based on the average surface roughness reading of the sugar palm fibre 3d printed and PLA 3d printed, the surface roughness comparison was performed.

Table 4.5 average surface roughness reading

		Average Surface Roughness Reading (µm)			
	Pointed areas	SPF+PLA	PLA	Different value	Percentage (%)
S1	1	5.67	1.08	4.59	80.95
	2	4.42	2.44	1.98	44.80
	3	7.29	1.16	6.13	84.09
S2	1	14.73	2.48	12.25	83.16
	2	17.61	2.11	15.50	88.02
	3	22.76	1.13	21.63	95.04
S3	1	15.04	1.05	13.99	93.02
	2	18.72	0.91	17.81	95.14
	3	19.34	1.99	17.35	89.71

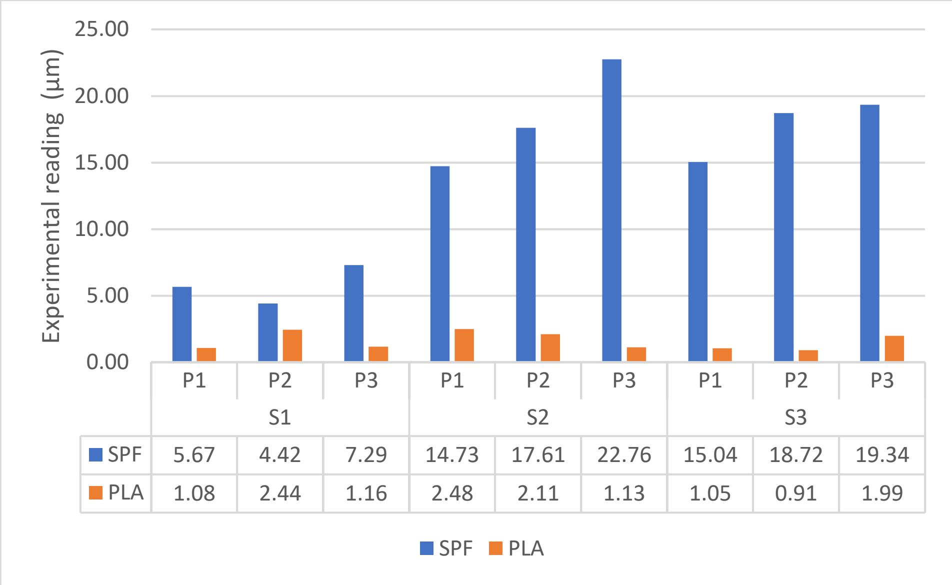

Figure 4.5 comparison of average reading of surface roughness

The bar chart in Figure 4.5 was used to graphically summarize the percentage difference in the mean measurement of surface roughness. Based on Table 4.5, the percentage difference of specimen 1 for both pointed areas 1 (sugar palm fiber and PLA) is 80.95%, while at pointed areas 2, the difference is 44.80%. Pointed areas 3 show a percentage difference of 84.09%. For specimen 2, the percentage difference for area 1 is 83.16%, for area 2 it is 88.02%, and for area 3 it is 95.04%. Lastly, for specimen 3, pointed area 1 has a difference of 93.02%, area 2 is 95.14%, and area 3 is 89.71%. The overall percentage difference in sugar palm fiber is higher than PLA specimens in the selected areas.

The factor of higher surface roughness (Ra) of specimens fabricated from sugar palm fiber involves multiple factors. One of these factors is the brittleness of the material, which significantly contributes to increased surface roughness. Brittle materials are prone to fractures and irregularities during the printing process, leading to a less smooth surface finish. Furthermore, the indifferent sizing of the material filament diameter also plays a crucial role. Inconsistent filament diameter can result in uneven material deposition, causing variations in layer thickness and ultimately contributing to higher surface roughness. Lastly, the presence of porosity on the surface is another pertinent factor influencing surface roughness. Porosity is characterized by small voids or air pockets within the printed material, negatively impacts structural integrity and surface quality. Factors such as improper filament extrusion, inadequate layer bonding, or insufficient control of printing parameters can lead to the development of porosity on the surface, exacerbating the overall roughness of the specimens.

Moreover, variables such as STL file preparation, material properties, and printing parameters (including layer height, printing time, and component orientation) (Buj-Corral et al., 2021) influence surface consistency. For both prototypes, the printing parameters and part orientation parameters are the same. All the setup parameters are identical for both prototypes, as shown in the slicer process procedure in Table 4.1. Therefore, the difference that causes surface roughness for both materials is the material properties. This is because the sugar palm is handmade from the previous student, and from observation, the mixture ingredients of sugar palm fiber were not mixed well. During the printing process, the sugar palm fiber and PLA are visible on top of the surface of the product, indicating that the mixture was not properly blended. The quality of PLA is better than sugar palm fiber and based on the comparison of surface finish, the PLA specimens are better than the sugar palm fiber material. Therefore, the result of this project was as aspected, which is that the surface finish of the sugar palm fiber specimen is rougher than PLA at all points.

4.4 Dimesional Accuracy

4.4.1 Aim of Dimensional Accuracy

The following section of this report embarks on a thorough exploration of results and analysis concerning the dimensional accuracy of 3D printed products manufactured from two distinct filaments: sugar palm fiber and PLA. A total of 3 designs (based on Table 4.6) consists 6 specimens, thoughtfully distributed with 2 specimens for each design (SPF+PLA and PLA), underwent detailed evaluation to assess their dimensional precision. This comprehensive examination delves into the intricate details of the printing process, unveiling the influence of each filament on the final product's dimensional accuracy. Through a careful discussion of the obtained results, this section endeavors to unravel and compare the performance of sugar palm fiber and PLA filaments in achieving dimensional precision in the realm of 3D printing.

Table 4.6 Design for dimensional accuracy

Type	Design 1	Design 2	Design 3
SPF/PLA			
PLA			

4.4.2 Procedure of Dimensional Accuracy

i. A vernier calliper was utilized to measure the dimensional accuracy of 6 specimens.

Figure 4.6 vernier calliper

ii. The specimens were placed on a flat and level surface.

iii. The vernier calliper was set to zero.

Figure 4.7 setting the vernier calliper to zero

iv. The jaws of the vernier caliper were closed around one end of each specimen.

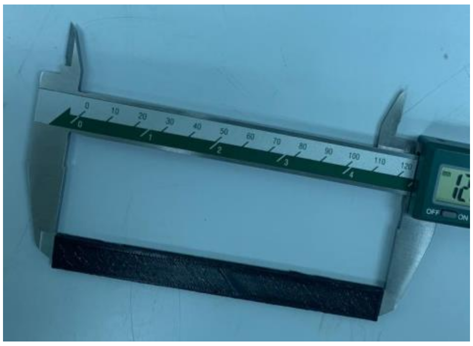

Figure 4.8 way to measure by using vernier calliper

v. The caliper was gently slid along the length, width, and height of each specimen until the opposite end was enclosed.

vi. Measurements were read and recorded from the vernier scale.

vii. This process was repeated for all the remaining specimens

4.4.3 Data of Dimensional Accuracy

Table 4.7 dimensional accuracy reading

Design	Type	Value	Image
Design 1	SPF+PLA	Length = 56.89 mm	
		Width = 13.00 mm	
		Height = 3.05 mm	

	PLA	Length = 56.96 mm	
		Width = 13.01 mm	
		Height = 3.04 mm	
Design 2	SPF+PLA	Length = 126.91 mm	

		Width = 13.02 mm	
		Height = 3.11 mm	
	PLA	Lenght = 126.74 mm	

		Width = 12.99 mm	
		Height = 3.30 mm	
Design 3	SPF+PLA	Length = 5.55 mm	

		Width = 10.09 mm	
		Height = 9.96 mm	

	PLA	Length = 5.5 mm	
		Width = 10.01 mm	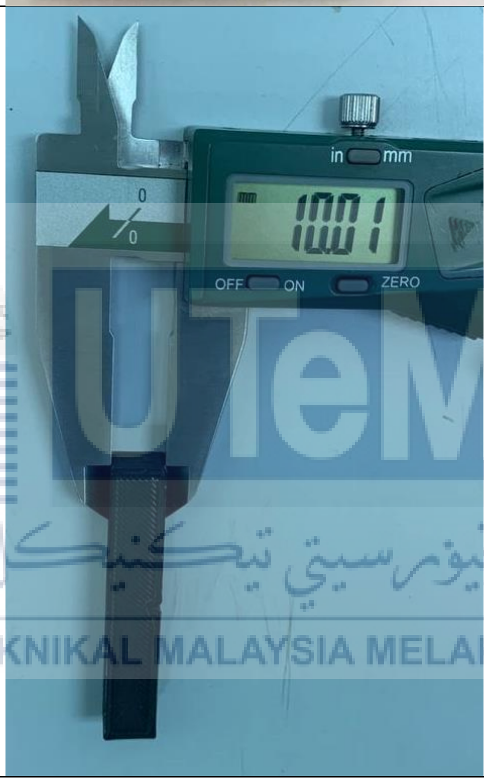

		Height = 10.00 mm	

Table 4.8 comparison reading of dimensional accuracy between designs

Design 1		SPF+PLA	PLA	value difference (mm)	percentage different (%)
	length	56.89	56.96	0.07	0.12
	width	13.00	13.01	0.01	0.08
	height	3.05	3.04	0.01	0.33

Design 2		SPF+PLA	PLA	value difference (mm)	percentage different (%)
	length	126.91	126.74	0.17	0.13
	width	13.02	12.99	0.03	0.23
	height	3.11	3.30	0.19	6.11

Design 3		SPF+PLA	PLA	value difference (mm)	percentage different (%)
	length	5.55	5.50	0.05	0.90
	width	10.09	10.01	0.08	0.79
	height	9.96	10.00	0.04	0.40

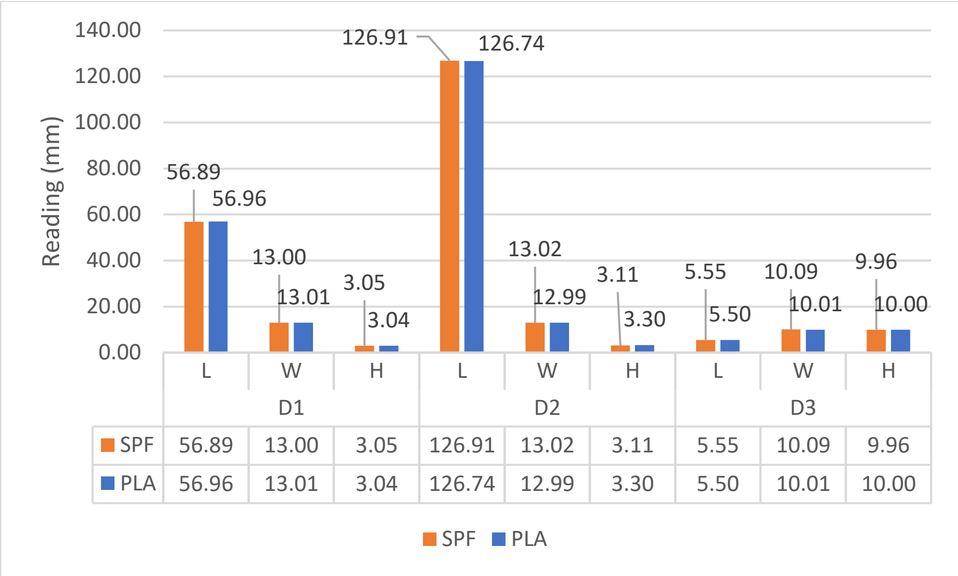

Figure 4.9 dimensional accuracy graph

In the analysis based on the Table 4.8, for Design 1, the length of SPF+PLA measures 56.89 mm, slightly differing from PLA, which has a length of 56.96 mm, resulting in a minimal difference of 0.07 mm, equivalent to 0.12%. The width of SPF+PLA is recorded as 13.00 mm, while PLA measures 13.01 mm, indicating a slight difference of 0.01 mm, or 0.08%. The height of SPF+PLA at 3.05 mm is nearly identical to PLA at 3.04 mm, with a minimal difference of 0.01 mm, or 0.33%.

For Design 2, SPF+PLA has a length of 126.91 mm, slightly surpassing PLA at 126.74 mm, with a difference of 0.17 mm, equivalent to 0.13%. The width of SPF+PLA is 13.02 mm, while PLA measures 12.99 mm, resulting in a difference of 0.03 mm, or 0.23%. The height of SPF+PLA at 3.11 mm contrasts with PLA at 3.30 mm, showing a noticeable difference of 0.19 mm, equivalent to 6.11%.

In the case of Design 3, the length of SPF+PLA is 5.55 mm, slightly different from PLA at 5.50 mm, with a difference of 0.05 mm, or 0.9%. The width of SPF+PLA is 10.09 mm, while PLA measures 10.01 mm, indicating a difference of 0.08 mm, or 0.8%. The height of SPF+PLA at 9.96 mm is closely aligned with PLA at 10.00 mm, showing a minimal difference of 0.04 mm, equivalent to 0.4%.

In summary, the graph of the dimensional accuracy data can be seen in Figure 4.9. The percentage differences in dimensional measurements for the three designs are relatively small. For Design 1, the variations ranged from 0.08% to 0.33%. Design 2 exhibited slightly larger differences, with percentages ranging from 0.13% to 6.11%. Design 3 displayed percentage differences ranging from 0.4% to 0.9%. Overall, while there are variations among the designs, the percentage differences indicate generally close alignment in the dimensional accuracy of the specimens for each design as by another researcher which said there is no significant differences when comparing PLA printed part to CAD design (M. Ali, 2016). Thus, the result of this dimensional accuracy test was as aspected, which is the accuracy of the SPF printed part is close to PLA printed part is achieved.

4.5 Mechanical Properties Testing

The examination of test outcomes extends to specimens fabricated from both SPF combined with PLA and PLA alone. These specimens underwent thorough assessments across multiple mechanical parameters, including tensile, flexural, and impact tests. This comprehensive testing protocol aims to unveil the nuanced impact of incorporating Sugar Palm Fiber on the overall mechanical performance in comparison to the baseline PLA material.

4.5.1 Tensile Test

4.5.1.1 Aim of Tensile Test

The primary goal of a tensile test is to analyze the mechanical properties of a material when subjected to axial loading. This test specifically evaluates how a material reacts to forces applied in tension, emphasizing the assessment of key properties such as tensile strength, yield strength, elongation, and other pertinent characteristics. Through tensile testing, engineers and researchers gain a comprehensive understanding of a material's response to stretching forces, uncovering valuable insights into its strength, ductility, and deformation traits. Such information holds critical importance in processes such as material selection, quality control, and the design of structures and components where substantial tensile forces come into play.

4.5.1.2 Procedure of Tensile Test

The following method describes the specifics of the tensile test procedure for 3D printed specimens of sugar palm fiber and 3D printed specimens of PLA.

i. The Shimadzu precision universal tester, Autograph AG-X plus, as shown in Figure 3.4, was used to measure the tensile strength of both 3D printed specimens. The apparatus and objects were set up as depicted in Figure 4.10.

Figure 4.10 tensile specimen setup

ii. The specimen was marked 25 mm from both ends to indicate the clamping area.

iii. The specimen was then loaded into the machine and securely tightened.

iv. The tensile test was conducted following ASTM D638-14 standards at a speed of 5 mm/min.

v. This experiment was carried out until all readings of the tensile test were determined. Three measurements were taken for this test for both filaments.

4.5.1.3 Data of Tensile Test

Figure 4.11 illustrates the tensile properties of SPF/PLA and PLA materials, showcasing load-displacement curves. These curves reflect a proportionate increase in load corresponding to displacement, until reaching the proportional limit. Figure 4.13 illustrates the tensile properties of SPF/PLA and PLA materials, showcasing tensile stress-strain curves. These curves reflect a proportionate increase in tensile stress corresponding to strain, consistent with Hooke's law, until reaching the proportional limit. It's noteworthy that the proportional limitations differ between materials. Given PLA's inherently brittle nature, PLA composite experienced failure after the initiation of the first crack. The result of this tensile test was as aspected, which is that the total ultimate tensile strength of the sugar palm fiber specimen is lower than PLA.

Force-Displacement graph of SPF/PLA tensile

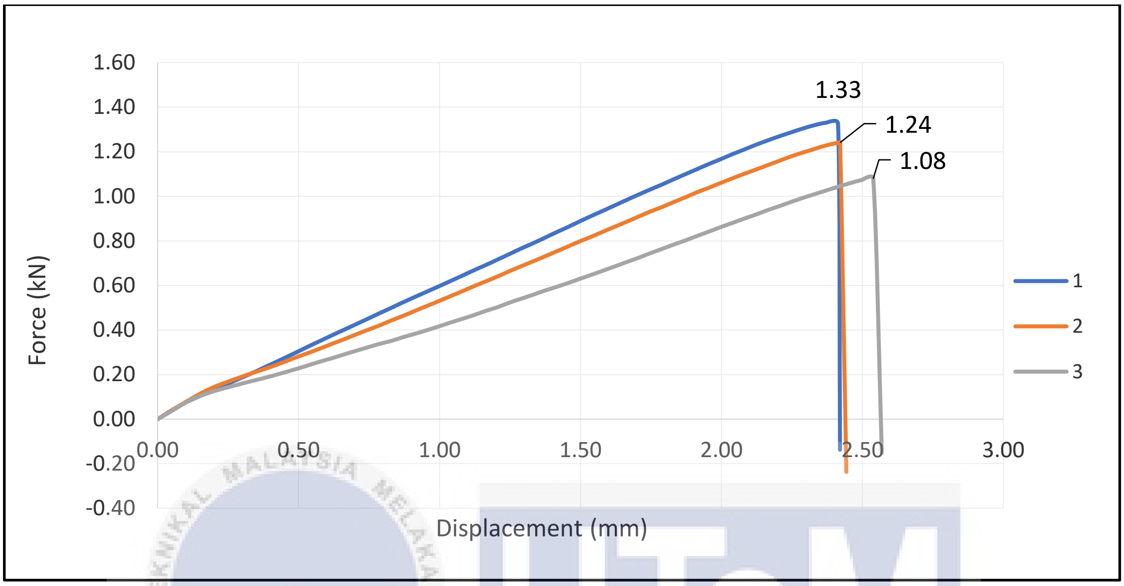

Force-Displacement graph of PLA tensile

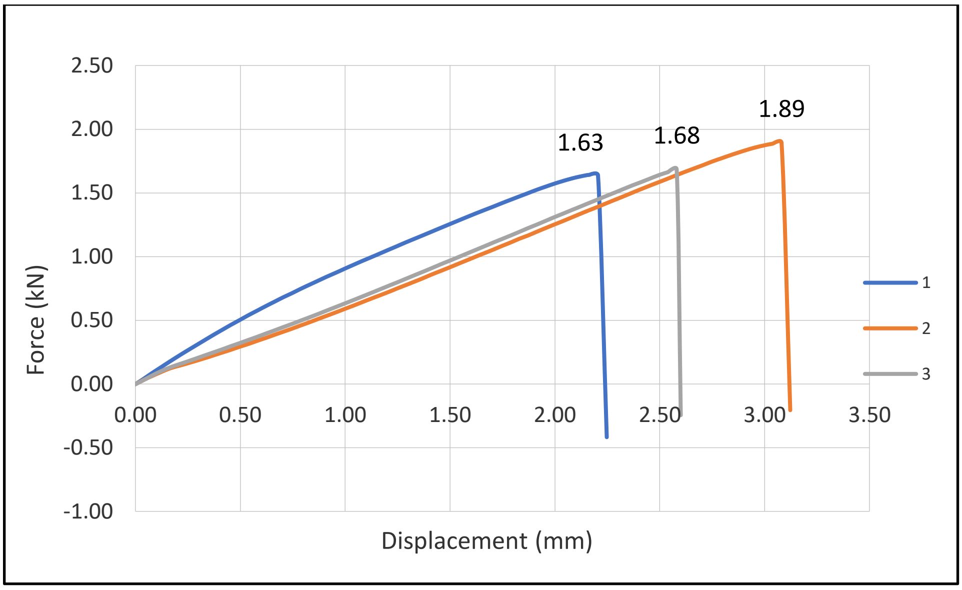

Figure 4.11 force-displacement graph of SPF/PLA and PLA

Table 4.9 comparison reading of time, force and dispacement between SPF/PLA and PLA

	SPF			PLA		
	Time	Force	Displacement	Time	Force	Displacement
	sec	kN	mm	sec	kN	mm
S1	29.00	1.33	2.41	26.50	1.64	2.21
S2	29.09	1.24	2.42	37.00	1.89	3.08
S3	30.50	1.08	2.54	31.00	1.68	2.58

The tensile test results for SPF/PLA and PLA filament samples reveal distinctive mechanical behaviors based on Table 4.9.

In the context of sugar palm fiber, sample 1 of sugar palm fiber demonstrated the highest force value at 1.33 kN with 2.41 mm displacement at 29 seconds, indicating superior load-bearing capacity and the ability to withstand the highest force among the tested samples. Sample 2, with a value of 1.24 kN with 2.42 mm displacement at 29.09 seconds, also exhibited considerable strength but was surpassed by Sample 1. The observed differences in values among the samples may be attributed to variations in material mixture and printing issues, such as incomplete layers. Sample 3, registering a value of 1.08 kN with 2.54 mm displacement at 30.50 seconds, experienced the lowest force before failure, indicating it can only bear the lowest force compared to Samples 1 and 2.

In the case of PLA, Sample 2 exhibited the highest force value at 1.89 kN with 2.21 mm displacement at 37 seconds, indicating superior load-bearing capacity within the PLA samples. Sample 3, with a value of 1.68 kN with 3.08 mm displacement at 31 seconds, also showed significant strength but was surpassed by Sample 1. The observed differences in values among the PLA samples may be attributed to variations in material mixture and printing issues, such as incomplete layers. Sample 1, with a value of 1.64 kN with 2.58 mm displacement at 26.5 seconds, experienced the lowest force before failure, suggesting a potentially less robust material compared to Samples 2 and 3.

In summary, for sugar palm fiber, Sample 1 demonstrated the highest force values with lowest displacement, while for PLA, Sample 2 exhibited the highest force values with lowest displacement among the rest, indicating the strongest material in terms of load-bearing capacity. Variations among these three samples may be attributed to various factors.

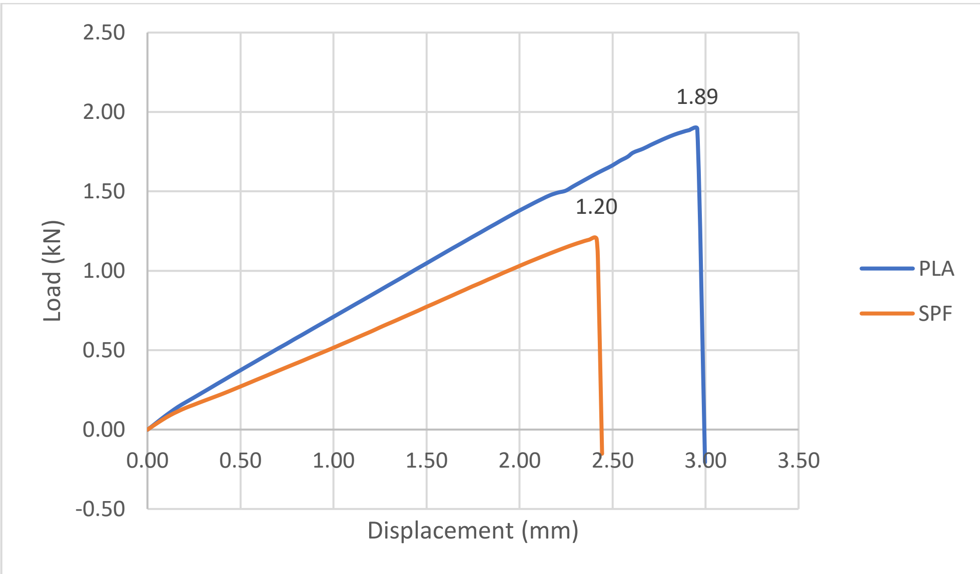

Figure 4.12 comparison average load-displacement graph of SPF/PLA

Table 4.10 comparison average reading load-displacement of SPF/PLA and PLA

SPF+PLA		PLA			
Force	Displacement	Force	Displacement	Displacement different	FORCE PERCENTAGE DIFFERENT (%)
kN	mm	kN	mm	mm	
1.20	2.41	1.89	3.08	0.67	36.45

The observed difference in average tensile strength values between 3D printed components using PLA filament and SPF+PLA filament can be sen in Table 4.10, where PLA exhibited a higher value of 1.89 kN at a displacement of 2.41 mm compared to SPF's 1.20 kN at a displacement of 3.08 mm, can be explained by various material-specific factors. Despite a difference of 0.67 mm in displacement, PLA shows a higher elongation capability. The percentage difference in forces between the two filaments is small at 36.45%, but PLA still outperforms in both applied force and displacement. This is attributed to PLA's synthetic nature, boasting remarkable tensile strength due to its crystalline structure, molecular weight, and robust intermolecular bonding (Ave et al., 2011). The manufacturing process ensures meticulous and controlled material composition, making PLA suitable for applications demanding structural integrity and robust load-bearing capabilities.

In contrast, sugar palm fiber, while environmentally friendly, may not match PLA's tensile strength. Natural fibers like sugar palm introduce variations in composition, and the interfacial bonding between these fibers and the printing matrix may not be as robust as in synthetic polymers. These inherent distinctions result in an overall lower tensile strength for SPF. The discussion highlights the material-specific characteristics influencing tensile strength and emphasizes the superior performance of PLA in structural and load-bearing applications.

In general, a higher displacement indicates greater elongation or ductility of the material before failure. This can be advantageous in applications where flexibility and deformation tolerance are critical. For example, in applications where a material needs to absorb energy or undergo deformation without fracturing, a higher displacement may be preferable. This characteristic is often desirable in situations where impact resistance or the ability to withstand dynamic loads is essential. On the other hand, in applications where rigidity and minimal deformation are crucial, a lower displacement may be preferred. Materials with lower displacements tend to be more rigid and less prone to elongation, making them suitable for scenarios where structural stability and minimal deformation under load are priorities.

Stress-Strain graph of SPF/PLA

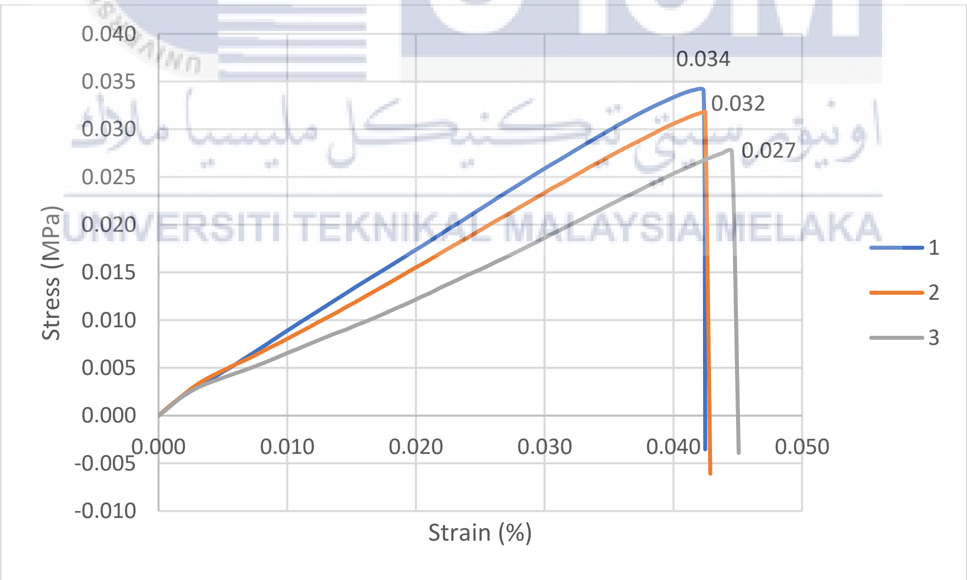

Stress-Strain graph of PLA

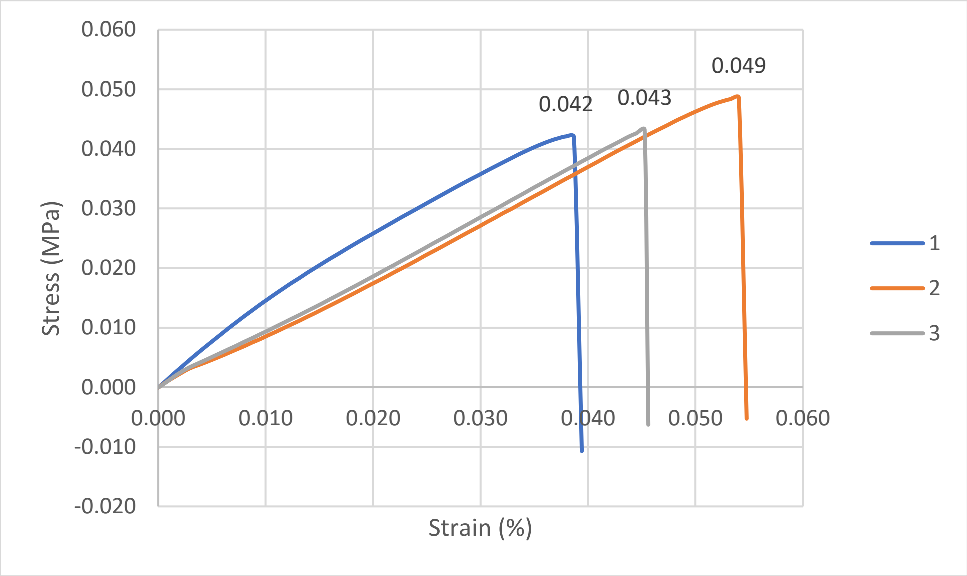

Figure 4.13 stress-strain graph of SPF/PLA and PLA

The tensile test results (shown in Figure **4.13**) for sugar palm fiber (SPF) and PLA (Polylactic Acid) filament samples highlight distinct mechanical behaviors.

For sugar palm fiber:

Starting with Sample 1 (0.034 MPa), this sample exhibited the highest stress value, indicating superior ability to withstand loads before failure. Sample 1 likely possesses the highest ultimate tensile strength (UTS) among the three, suggesting resilience under tension for applications demanding superior strength and load-bearing capabilities. Moving on to Sample 2 (0.032 MPa), although displaying the second-highest stress value, it falls short of Sample 1. However, Sample 2 still suggests substantial strength and a commendable UTS, making it suitable for applications requiring robust mechanical performance. Conversely, Sample 3 (0.028 MPa) demonstrated the lowest stress value, implying a comparatively lower UTS.

For PLA:

Starting with Sample 2 (0.049 MPa), this sample exhibited the highest stress value, indicating superior ability to withstand loads before failure. Similar to the sugar palm fiber scenario, Sample 1 likely possesses the highest UTS among the three, making it well-suited for applications demanding superior strength. Moving on to Sample 3 (0.043 MPa), although displaying the second-highest stress value, it falls short of Sample 1. However, Sample 3 still suggests substantial strength and commendable UTS, suitable for applications requiring robust mechanical performance. Conversely, Sample 1 (0.042 MPa) demonstrated the lowest stress value, suggesting a comparatively lower UTS.

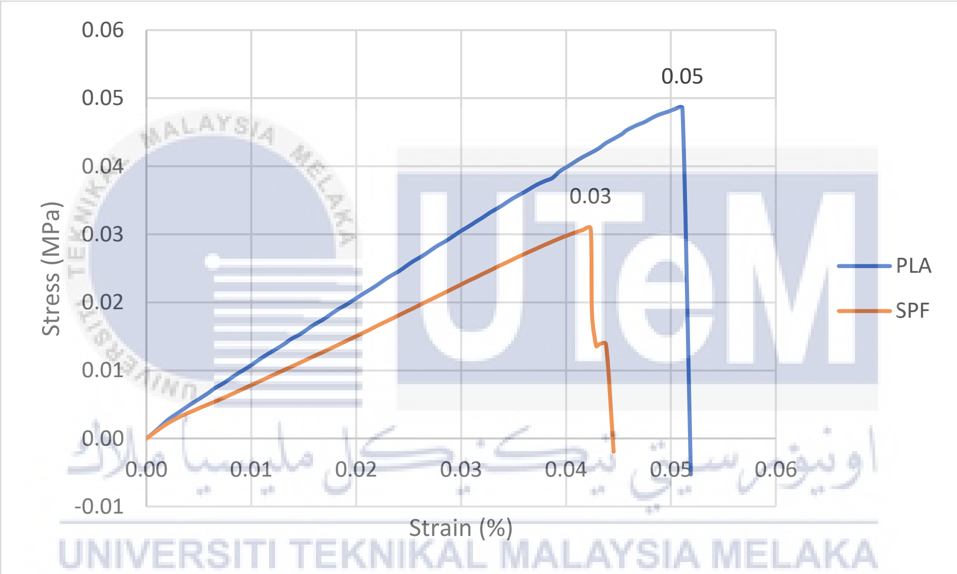

Figure 4.14 comparison average stress-strain graph of SPF/PLA

Table 4.11 comparison average reading of stress-strain SPF/PLA and PLA

SPF+PLA	PLA	Percentage Different (%)
0.03	0.05	36.49

Based on the Table 4.11 the comparison of tensile test results between 3D printed parts made from PLA filament and SPF+PLA filament, with average stress values of PLA at 0.05 MPa and SPF at 0.03 Mpa with a percentage different of 36.49 %, provides insights into the mechanical behavior of these materials under tension.

For PLA, the stress value of 0.05 MPa indicates the material's remarkable ability to withstand a substantial load before reaching failure. Known for its high tensile strength and stiffness, PLA finds extensive use in various applications, particularly in the field of 3D printing.

Conversely, SPF+PLA exhibited a stress value of 0.03 MPa, suggesting a comparatively lower load-bearing capacity compared to PLA. Being a natural and sustainable material, SPF may showcase variations in mechanical properties influenced by factors such as fiber orientation and processing methods.

In conclusion, the tensile test results unequivocally highlight the superior performance of PLA (Polylactic Acid) over Sugar Palm Fiber (SPF) in terms of stress resistance, with average values of 0.05 MPa and 0.03 MPa, respectively. PLA's remarkable ability to withstand higher loads by 36.49 % more than SPF before failure, coupled with its well-established high tensile strength and stiffness, positions it as a formidable material, especially in the context of 3D printing applications.

However, the determination of which material is "better" hinges on a nuanced consideration of specific application requirements and sustainability concerns. While PLA excels in mechanical strength, SPF offers a natural and sustainable alternative, albeit with a lower load-bearing capacity. The decision-making process should extend beyond mere tensile strength comparisons and consider factors such as environmental impact, resource renewability, and the intended purpose of the 3D printed parts.

4.5.2 Flexural Test

4.5.2.1 Aim of Flexural Test

The flexural test aims to evaluate a material's mechanical properties under bending loads, specifically focusing on flexural strength, modulus of elasticity, and deformation behavior. This test provides essential insights into the material's ability to withstand bending stress, aiding in material selection, quality control, and the design of structures and components where bending forces are significant.

4.5.2.2 Procedure of Flexural Test

i. The Shimadzu precision universal tester, Autograph AG-X plus, as shown in Figure 3.5, was used to measure the tensile strength of both 3D printed specimens. The apparatus and objects were set up as depicted in Figure 4.15.

Figure 4.15 setting up flexural machine

ii. Figure 4.16 shows that the specimen was marked at the center.

Figure 4.16 marking at the center

iii. The specimen (ASTM D790-10) was then placed into the machine, ensuring the centre is alligned to the machine

iv. The tensile test was conducted following ASTM-D638 standards at a speed of 5 mm/min.

v. This experiment was carried out until all readings of the flexural test were determined. Three measurements were taken for this test for both filaments.

4.5.2.3 Data of Flexural Test

Figure 5 presents the flexural properties of SPF/PLA, displaying load-displacement curves, while Figure 6 specifically illustrates PLA materials. These curves depict a proportional increase in load corresponding to displacement until reaching the proportional limit, providing insights into the bending behavior of the materials. Furthermore, Figure 7 showcases the flexural properties of SPF/PLA, and Figure 8 details PLA materials, exhibiting tensile stress-strain curves. These curves demonstrate a proportional increase in tensile stress corresponding to strain. As expected, the results indicate that the total ultimate tensile strength of the sugar palm fiber specimen is lower than that of PLA in this flexural testing scenario.

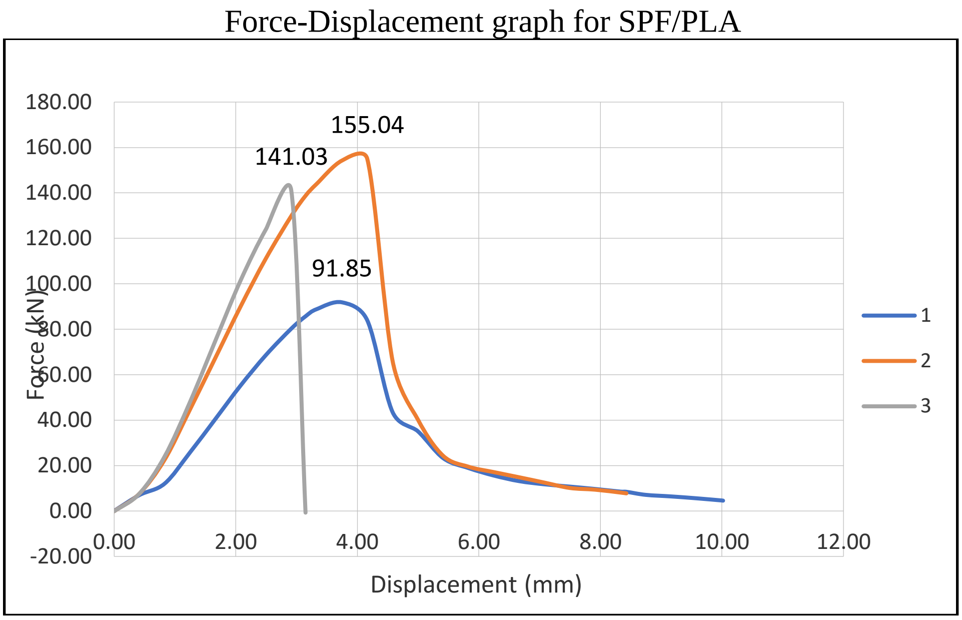

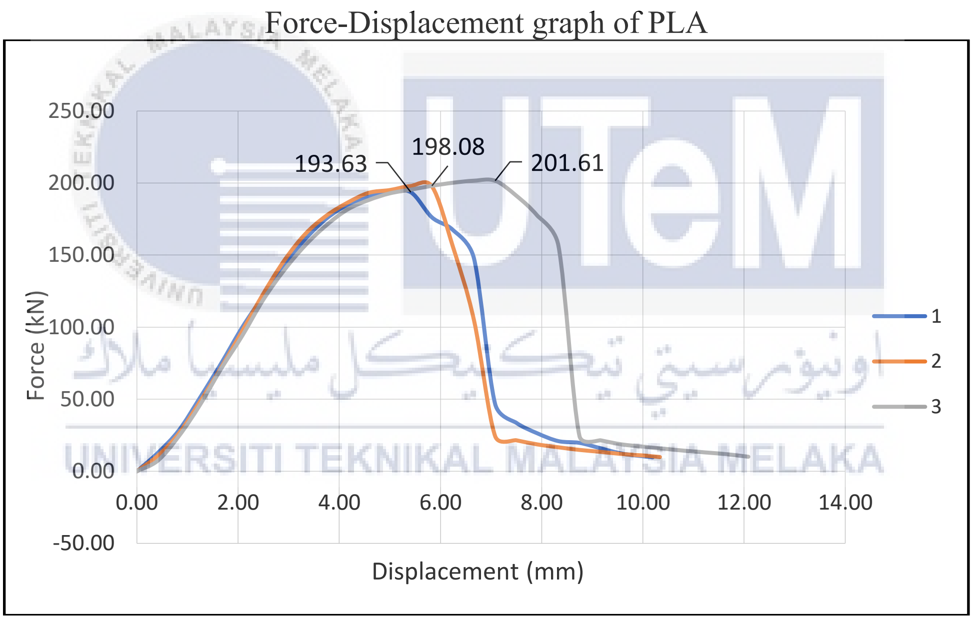

Figure 4.17 force-displacement graph of SPF/PLA and PLA

Table 4.12 comparison reading of time, force and displacement of SPF/PLA and PLA

	SPF+PLA			PLA		
	Time	Force	Displacement	Time	Force	Displacement
	sec	kN	mm	sec	kN	mm
S1	45.00	91.85	3.75	65.00	193.63	5.41
S2	50.00	155.04	4.16	70.00	197.76	5.83
S3	35.00	141.03	2.91	85.00	201.61	7.08

The flexural test results for SPF+PLA and PLA (Polylactic Acid) filament samples in Table 4.12 provide a comprehensive understanding of their bending behavior.

Sugar Palm Fiber (SPF):

The highest load value for SPF Sample 1 is 91.85 kN, observed at 45 seconds, with a 3.75 mm displacement, signifying the point just before considerable bending occurred. This suggests a certain degree of flexibility but potentially lower resistance to bending compared to Samples 2 and 3. SPF Sample 2, achieving a load value of 155.04 kN with 4.16 mm displacement at 50 seconds, demonstrates superior resistance to bending, making it suitable for applications requiring robust structural integrity. Sample 3, despite having a load value of 141.03 kN, experienced rupture with only 2.91 mm displacement at 141.03 seconds, resulting in a lower displacement compared to Sample 1. This indicates that Sample 3 ruptured quickly despite applying less force.

PLA (Polylactic Acid):

For PLA, Sample 1 now exhibits a significantly increased load value of 193.63 kN with 5.41 mm displacement at 65 seconds, showcasing its ability to withstand a higher force before substantial bending. This implies a higher level of strength and rigidity, making it potentially suitable for applications requiring robust structural integrity. PLA Sample 2, with a load value of 198.08 kN and 5.83 mm displacement at 70 seconds, maintains superior resistance to bending, reinforcing its suitability for applications demanding high strength and rigidity. Sample 3, reaching the highest load value at 201.61 kN with 7.08 mm displacement at 85 seconds, exhibits the greatest resistance to bending among the three samples, making it potentially suitable for applications requiring robust structural integrity and high bending resistance.

In summary, the flexural test results, emphasizing the highest load values, provide a comprehensive view of the bending characteristics of SPF and PLA samples. While SPF demonstrates Sample 2 as having the highest resistance to bending, PLA's Sample 3 stands out for its superior resistance to bending, indicating its potential suitability for applications demanding both structural integrity and high bending resistance.

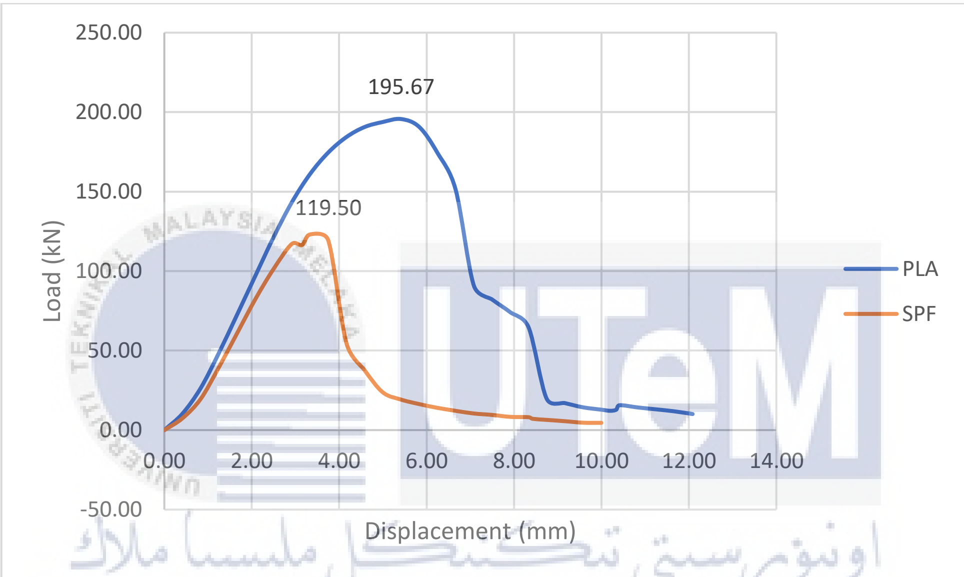

Figure 4.18 comparison of average force-displacement graph of SPF/PLA and PLA

Table 4.13 Comparison average reading of SPF/PLA and PLA

SPF+PLA		PLA			
Force	Displacement	Force	Displacement	Displacement different	FORCE PERCENTAGE DIFFERENT (%)
kN	mm	kN	mm	mm	
119.50	4.16	195.67	5.41	1.25	38.93

In summary, the comparison of flexural test results (Table 4.13), with PLA registering the highest load-displacement value at 195.67 kN and SPF at 119.50 kN, provides valuable insights into the bending characteristics of these 3D printed materials.

1. PLA:

PLA showcases a superior resistance to bending, indicated by its high load value of 195.67 kN and a displacement of 4.16 mm. This robust performance suggests that PLA can endure significant forces before experiencing substantial deformation, highlighting its exceptional strength and rigidity. Known for its well-established mechanical properties, including excellent flexural strength, PLA emerges as a preferred choice for applications demanding structural integrity and robust load-bearing capabilities. The minimal displacement difference of 38.93% underlines PLA's consistent and reliable bending behavior, reinforcing its suitability for diverse applications.

2. SPF:

In contrast, SPF+PLA records a lower highest load value in the graph at 119.50 kN, coupled with a displacement of 5.41 mm. This signifies a comparatively lower resistance to bending when compared to PLA. Despite SPF+PLA's recognition for sustainability and environmental friendliness, the lower load value hints at potential limitations in flexural strength and rigidity. The inherent variations in material properties associated with natural fibers like sugar palm, along with potential challenges in interfacial bonding between the fibers and the matrix, may contribute to SPF+PLA's reduced bending resistance.

The force percentage difference of 38.93% accentuates the nuanced advantage of PLA over SPF in bending characteristics. PLA's superior resistance to bending, minimal displacement difference, and established mechanical properties make it a compelling choice for applications requiring both structural integrity and reliable load-bearing capabilities

Stress-Strain Graph of SPF/PLA

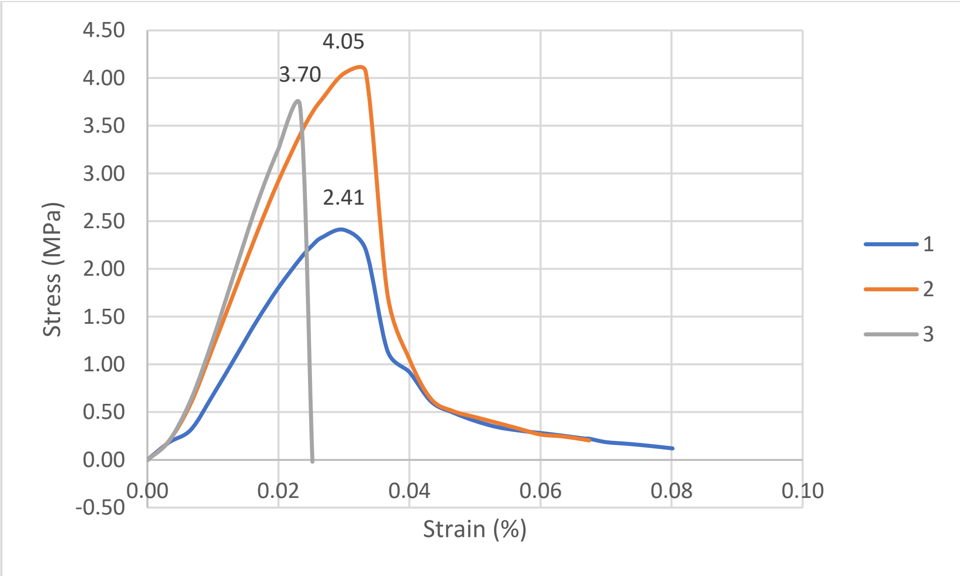

Stress-Strain Graph of PLA

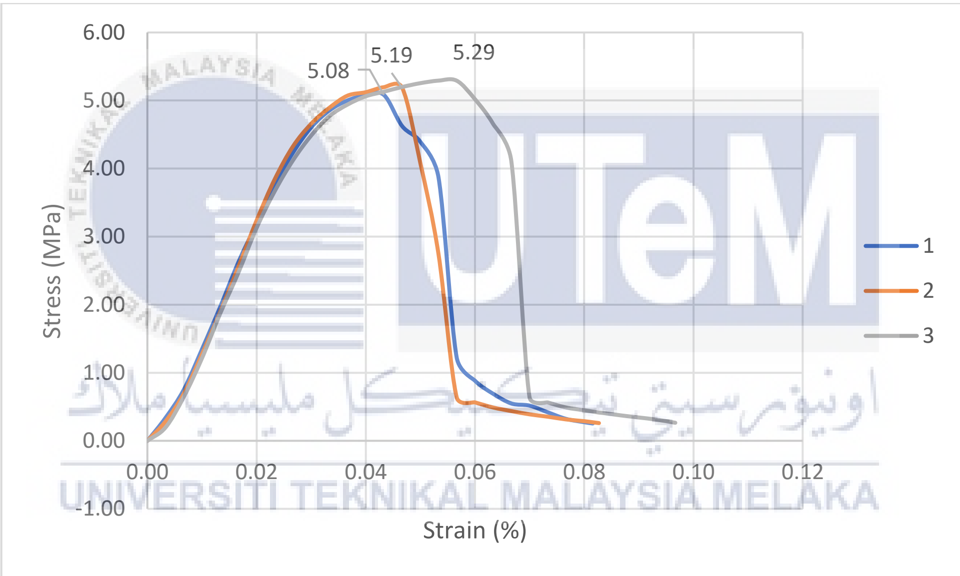

Figure 4.19 stress-strain graph of SPF/PLA and PLA

The results of the flexural test, as depicted by the stress-strain graph in Figure 4.19, offer valuable insights into the mechanical behavior of 3D printed samples made from sugar palm fiber (SPF) and PLA (Polylactic Acid) filament.

1. SPF:

In examining the stress-strain graph, Sample 1 recorded a stress value of 2.41 MPa, indicating a moderate ability to withstand bending forces. This suggests a balance between flexibility and strength, making it suitable for applications that require a combination of these characteristics. Moving to Sample 2, which exhibited a higher stress value of 4.05 MPa, the material demonstrates superior resistance to bending, implying increased strength and rigidity. This makes it potentially suitable for applications demanding robust structural integrity. Sample 3, with a stress value of 3.70 MPa, falls between the other samples, indicating a moderate level of bending resistance and a balance between flexibility and strength.

2. PLA:

Turning to PLA, Sample 1 showcased a stress value of 5.08 MPa, indicating a substantial ability to withstand bending forces. This implies high strength and rigidity, making it suitable for applications where structural integrity is paramount. Sample 2 maintained a slightly higher stress value at 5.19 MPa, suggesting superior resistance to bending compared to Sample 1 and reinforcing its suitability for applications demanding high strength and rigidity. Sample 3 exhibited the highest stress value at 5.29 MPa, showcasing the greatest resistance to bending among the PLA samples and making it potentially suitable for applications requiring robust structural integrity and high bending resistance.

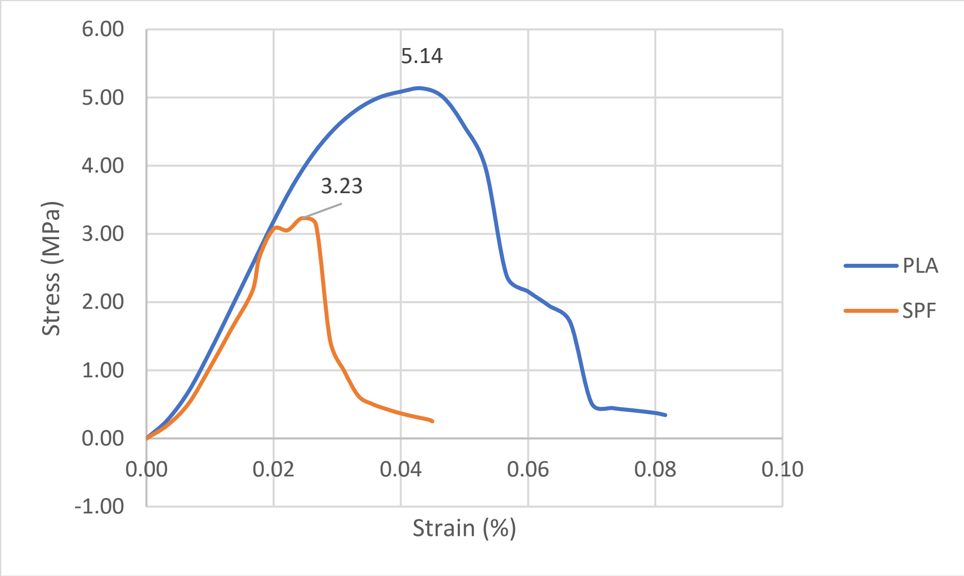

Figure 4.20 comparison average stress-strain graph of SPF/PLA and PLA

Table 4.14 comparison average reading of SPF/PLA and PLA

SPF+PLA	PLA	Percentage Different (%)
3.23	5.14	37.16

The comparison of SPF+PLA and PLA can be seen in Table 4.14 with the highest stress value in the graph at 5.14 MPa, PLA demonstrates remarkable strength and rigidity in response to bending forces. This implies that PLA can endure substantial loads before experiencing significant deformation. The elevated stress value positions PLA as a robust material, particularly in applications where structural integrity and load-bearing capabilities are critical. The molecular structure and manufacturing process of PLA contribute to its outstanding tensile and flexural strength, making it a reliable choice for various engineering applications(Team Xometry, 2022). The stress value for PLA is 37.16% higher than that of SPF, underscoring its superior performance.

In contrast, SPF+PLA registers a lower highest stress value in the graph at 3.23 MPa. While SPF offers sustainable and environmentally friendly aspects, the lower stress value suggests a moderate ability to resist bending forces. Natural fibers like sugar palm may introduce variations in material properties, and the interfacial bonding between the fibers and the printing matrix may not be as robust as in synthetic polymers like PLA. This results in a lower overall stress value for SPF in the flexural test. The stress value for SPF+PLA is 37.16% lower than that of PLA, indicating a significant difference in bending resistance.

In summary, the stress-strain graph findings underscore the superior bending resistance of PLA over SPF+PLA, as evidenced by the higher stress value. PLA's higher strength and rigidity make it exceptionally suitable for applications prioritizing structural integrity and load-bearing capabilities. On the other hand, while SPF+PLA offers sustainability benefits, its lower stress value indicates limitations in flexural strength, emphasizing the need for thoughtful material selection based on specific application requirements. The percentage difference of 37.16% accentuates the nuanced distinction in bending performance between PLA and SPF+PLA.

4.5.3 Impact Test

4.5.3.1 Aim of Impact Test

The impact test aims to evaluate a material's resistance to sudden, high-force impacts, focusing on its ability to absorb energy and withstand fracture. This test provides insights into material toughness, notch sensitivity, and resistance to brittle fracture, offering essential information for material selection, quality control, and design considerations in applications where resistance to sudden impacts is critical.

4.5.3.2 Procedure of Impact Test

i. The Shimadzu precision universal tester, CHARPY-IZOD, as shown in Figure 3.6, was used to measure the twst of both 3D printed specimens. The apparatus and objects were set up as depicted in Figure 4.21.

Figure 4.21 impact test setup

ii. Figure 4.22 shows that the specimen (V notched Charpy type) was placed on the machine

Figure 4.22 placement of the impact specimen

iii. The load of 4.4 kg was pushed to side to set as the initial point

iv. The needle was pushed to zero scale to avoid zero error

v. The the cage of the machine was closed to prevent any unwanted incident from happen.

vi. The load was let down by pulling the lever behind the machine

vii. This experiment was carried out until all readings of the impact test were determined. Three measurements were taken for this test for both filaments.

4.5.3.3 Data of Impact Test

In this context, the impact strength values are typically represented on a graph, showcasing the relationship between applied force and material response. The result of this impact test was as aspected, which is that the impact strength of the sugar palm fiber specimen is lower than PLA.

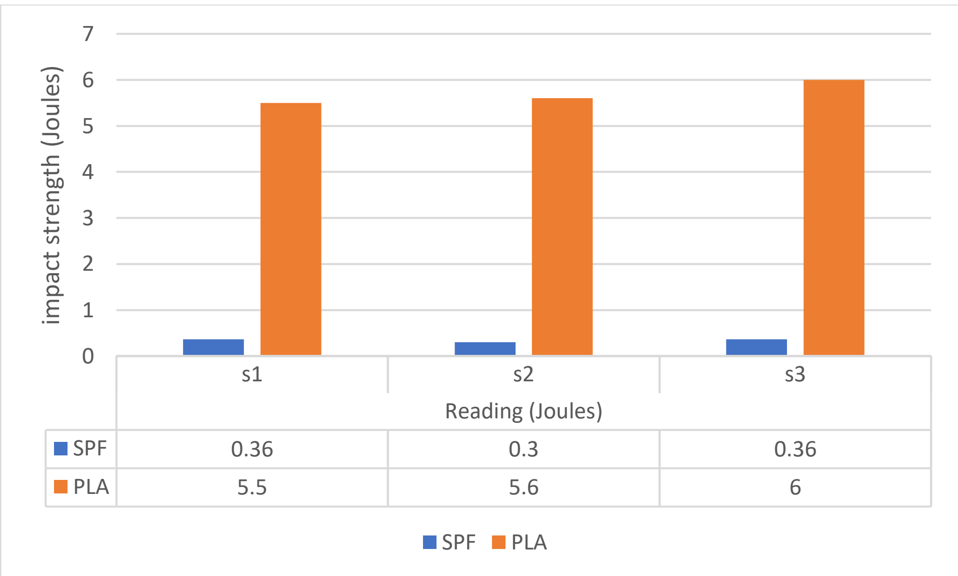

Figure 4.23 impact strength graph of SPF/PLA and PLA

Table 4.15 reading for each impact test sample

	Reading (Joules)		percentage different (%)
	SPF+PLA	PLA	
S1	0.36	5.50	93.45
S2	0.30	5.60	94.64
S3	0.36	6.00	94.00

Based on the Table 4.15 where in the case of PLA, the impact resistance remains consistently high across all three specimens, with recorded energy absorption of 5.5 joules for Specimen 1, 5.6 joules for Specimen 2, and 6 joules for Specimen 3. This consistent performance underscores PLA's reliability and robustness, demonstrating its ability to uniformly absorb substantial energy under impact conditions. These results position PLA as a dependable material for applications that prioritize resilience to sudden forces or impacts.

In contrast, the impact resistance of SPF+PLA exhibits significant variation among its three specimens. Specimen 1 shows 0.36 joules of energy absorption, Specimen 2 records 0.3 joules, and Specimen 3 demonstrates 0.36 joules during impact. The range in these readings suggests inconsistent performance in energy absorption, indicating that the natural and fibrous characteristics of SPF+PLA may lead to variations in impact resistance. Despite offering sustainability benefits, the less effective energy dissipation observed in the impact test results may limit the suitability of SPF+PLA for applications where robust impact resistance is crucial. The percentage difference for Samples 1, 2, and 3 is 93.45%, 94.64%, and 94.00%, respectively.

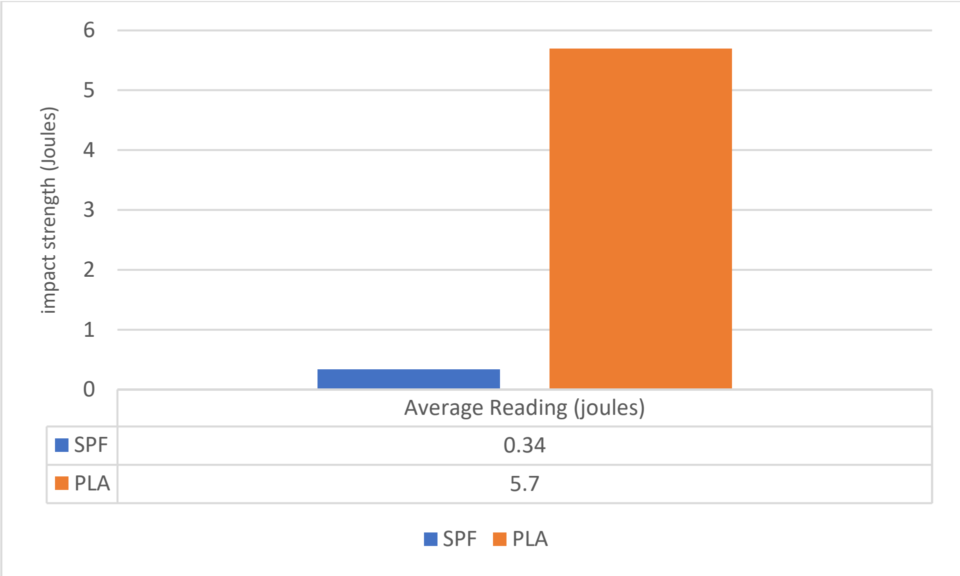

Figure 4.24 comparison average graph of impact strength of SPF/PLA and PLA

Table 4.16 comparison average reading of impact strength of SPF/PLA and PLA

	SPF+PLA	PLA	percentage different (%)
average reading (Joules)	0.34	5.7	94.04

Impact testing provides crucial insights into a material's resistance to sudden, high stress loading conditions, such as those encountered in real-world applications where the material may experience impact or shock. When analyzing impact test data for specimens made from SPF+PLA and PLA, with values of 0.34 for SPF and 5.7 for PLA, there are several aspects to elaborate on (refers Table 4.16).

The impact test results directly reflect the impact strength of each material. In this context, PLA demonstrates a significantly higher impact strength at 5.7 J compared to SPF at 0.34 J. Impact strength is a critical property, especially in applications where materials need to withstand sudden loading or potential impact forces. The higher impact strength of PLA suggests its superior ability to absorb energy during impact, making it more suitable for applications where impact resistance is a crucial factor.

Impact testing is often used to assess a material's toughness, which is the ability to absorb energy and deform plastically before fracture. The higher impact strength of PLA indicates greater toughness compared to SPF. Material toughness is essential for applications where the material may experience dynamic loading or impact forces, as it helps prevent catastrophic failure and enhances the material's durability.

PLA is a synthetic polymer sourced from renewable materials, offering a homogenous and controlled molecular structure during manufacturing. This ensures consistent composition and predictable mechanical properties, including excellent impact strength (L. Wang et al., 2017). PLA's orderly polymer chain arrangement, inherent stiffness, and rigidity contribute to its ability to resist impact forces, preventing catastrophic failure under sudden loading conditions. Higher molecular weight in PLA correlates with improved impact resistance. In contrast, SPF, a natural fiber material, may exhibit variations in composition and introduces heterogeneities due to its composite structure. The weaker interfacial bonding between SPF fibers and the matrix material, compared to synthetic polymers like PLA, contributes to lower overall impact strength in SPF. PLA's superior impact resistance is attributed to its controlled molecular structure, optimized processing, inherent properties, and challenges posed by SPF's composite nature. This makes PLA a preferred choice in applications requiring robust impact resistance.

The percentage difference of 94.04 % between the impact strength values of SPF and PLA further accentuates the significant performance gap, reinforcing PLA's superiority in absorbing energy and withstanding impact forces by 94.04 % more than SPF.

4.6 Summary

The chapter provides a comprehensive overview of the experimental approach in the project, focusing on 3D printing fabrication, surface roughness, and subsequent testing phases. The slicing process involved careful parameter adjustments, influencing precision in 3D printing. Variables such as materials and printing parameters affected the physical and structural characteristics of the printed objects. Rigorous testing assessed mechanical strength, dimensional accuracy, and surface finish, offering valuable insights into the methodologies' effectiveness. The meticulous crafting of models using sugar palm fiber and PLA filaments was detailed, with the Creality3D Ender-3 PRO as the designated printing machine. The Table 4.5 graphically summarizes the percentage differences in mean surface roughness measurements. Notably, the percentage differences varied across pointed areas for specimens 1, 2, and 3, with sugar palm fiber exhibiting higher differences than PLA in the selected areas. The factors contributing to higher surface roughness in sugar palm fiber specimens include material brittleness, inconsistent filament diameter, and the presence of porosity. These factors collectively lead to increased irregularities and decreased smoothness in the printed surface. In summary, the percentage differences in dimensional measurements across three designs are relatively small, showcasing generally close alignment in the dimensional accuracy of specimens. The tensile test results highlight PLA's superior performance over sugar palm fiber in terms of stress resistance by 36.49 % more. Similarly, the stress-strain graph underscores PLA's superior bending resistance by 37.16% more, making it suitable for applications prioritizing structural integrity. The impact strength comparison between SPF and PLA further emphasizes PLA's significant superiority in absorbing energy and withstanding impact forces. PLA's controlled molecular structure, inherent stiffness, and homogeneity contribute to its consistent composition and predictable mechanical properties. This ensures excellent impact strength, making PLA a preferred choice in applications requiring robust resistance to sudden loading conditions. The percentage difference of 94.04% in impact strength values reinforces PLA's substantial advantage over SPF in absorbing energy and withstanding impact forces.

CHAPTER 5

CONCLUSION AND RECOMMENDATIONS

5.1 Conclusion

This study explores the viability of Sugar Palm Fibre (SPF) combined with Polylactic Acid (PLA) as an alternative filament for 3D printing, aiming to understand its printability challenges and mechanical properties in comparison to commercial PLA filaments. The first aspect delves into a comparative analysis, focusing on printability, dimensional accuracy, and surface roughness. Challenges such as viscosity, melt flow rate, and interlayer adhesion are identified as critical factors influencing print quality. The second aspect involves a thorough examination of mechanical properties, including tensile, flexural, and impact performance, to assess the feasibility of SPF/PLA filaments for various applications. The findings underscore the potential of SPF/PLA filaments as sustainable alternatives, emphasizing the need for careful consideration of printability challenges and a detailed understanding of their mechanical characteristics. With further refinement, this innovative filament holds promise for efficiently producing high-quality printed objects, suitable for both industrial and home settings.

Objective 1 – The overall findings align with the project's objective, which aimed to assess the printability of a biocomposite filament derived from sugar palm-based polylactic acid (PLA) in comparison to a commercial PLA filament in the context of 3D printing using the Fused Deposition Modeling (FDM) system. The evaluation focused primarily on the physical properties of the printed objects. Chapter 4 provides a detailed analysis of factors such as dimensional accuracy, surface finish, and overall print quality. The results reveal that the surface roughness of the SPF/PLA is notably rougher compared to PLA. However, it is noteworthy that the dimensional accuracy remains precise, with differences only amounting to an insignificant percentage. This suggests that while surface roughness may be a consideration, the biocomposite filament maintains satisfactory accuracy in its printed objects, contributing valuable insights to the understanding of its performance in FDM-based 3D printing.

Objective 2 - The objective of evaluating the printability of a biocomposite filament, derived from SPF/PLA, and comparing it with a commercial PLA filament in the 3D printing process using the FDM system, has been addressed with a specific focus on mechanical properties. The conducted mechanical property tests included assessments of strength, stiffness, and durability. Diverse tests, such as tensile strength, flexural strength, and impact resistance, were performed to gain insights into the ability of the printed products to withstand applied forces and stresses. The results presented in Chapter 4 indicate that, across the three tests, PLA outperforms SPF/PLA. In both tensile and flexural tests, the percentage difference is approximately 30% to 40%, while in the impact test, the difference ranges from 90% to 100%. These findings underscore the superior mechanical performance of PLA in comparison to the sugar palm-derived PLA biocomposite.

Objective 3 – The objective of comparing the printability between SPF/PLA filament and the standard PLA filament has been successfully addressed, considering both physical and mechanical properties. The evaluation encompassed factors such as dimensional accuracy, surface finish, tensile strength, flexural strength, and impact resistance. As detailed in the analysis, the findings provide a comprehensive understanding of how SPF/PLA filament performs in relation to the standard PLA filament in the context of 3D printing. This comparison aids in assessing the material's suitability for diverse applications, highlighting its strengths and potential areas for improvement in both physical and mechanical aspects within the FDM system.

5.2 Limitation

1. Limited Resources: The availability of an insufficient quantity of filament posed constraints on fabricating an adequate number of samples for testing. A greater quantity of samples would have enhanced the accuracy of the testing outcomes.
2. Improper Material Mixture: The SPF/PLA filament, produced by a previous student, exhibited issues related to improper mixing. This was evident in the visible separation of the fiber and PLA components at the surface of the printed products, impacting the overall quality of the filament.
3. Improper Filament Diameter: Challenges arose due to the filament's diameter not meeting the minimum requirement during the extrusion process. This limitation rendered the filament unusable for printing, resulting in material wastage.
4. Machine Unavailability: The unavailability of certain machines necessitated the use of third-party equipment. Utilizing different types of machines introduced the risk of data inconsistency, as variations in machine capabilities could impact the quality and accuracy of the measured data. For instance, employing a manual testing machine in activities like impact testing posed the potential for technical errors, further compromising the reliability of the collected data during testing.

5.3 Recommendation

1. Increased Filament Availability: To overcome the limitation of limited resources, it is recommended to secure a sufficient quantity of filament to enable the fabrication of a more extensive set of samples. This will enhance the reliability and precision of the testing results by allowing for a broader representation of the material's performance.
2. Improved Material Mixing Process: Considering the issue of improper material mixture observed in the SPF/PLA filament, it is recommended to review and enhance the filament production process. Proper mixing techniques should be implemented to ensure a homogenous blend of fiber and PLA, addressing the visible separation issues and improving the overall quality of the printed products.
3. Filament Diameter Control: To avoid challenges related to improper filament diameter, meticulous control measures should be implemented during the filament extrusion process. Regular monitoring and adjustment of the extrusion parameters can help ensure that the filament consistently meets the minimum diameter requirements, minimizing material wastage and improving efficiency.
4. Upgrade Testing Facilities: Given the impact of facility limitations on the final quality of 3D printed products, it is advisable to consider upgrading to advanced 3D printers with enhanced capabilities. Additionally, investing in automated testing equipment can help reduce technical errors in manual testing processes, leading to more accurate and reliable data collection during various tests, such as the impact test.

REFERENCE

Abdul Razak, H., & Ferdiansyah, T. (2005). Toughness characteristics of Arenga pinnata fibre concrete. *Journal of Natural Fibers*, *2*(2), 89–103. https://doi.org/10.1300/J395v02n02_06

Abdulhameed, O., Al-Ahmari, A., Ameen, W., & Mian, S. H. (2019). Additive manufacturing: Challenges, trends, and applications. *Advances in Mechanical Engineering*, *11*(2). https://doi.org/10.1177/1687814018822880

Abral, H., Ariksa, J., Mahardika, M., Handayani, D., Aminah, I., Sandrawati, N., Pratama, A. B., Fajri, N., Sapuan, S. M., & Ilyas, R. A. (2020). Transparent and antimicrobial cellulose film from ginger nanofiber. *Food Hydrocolloids*, *98*. https://doi.org/10.1016/j.foodhyd.2019.105266

Adawiyah, D. R., Sasaki, T., & Kohyama, K. (2013). Characterization of arenga starch in comparison with sago starch. *Carbohydrate Polymers*, *92*(2), 2306–2313. https://doi.org/10.1016/j.carbpol.2012.12.014

Alafaghani, A., Qattawi, A., Alrawi, B., & Guzman, A. (2017). Experimental Optimization of Fused Deposition Modelling Processing Parameters: A Design-for-Manufacturing Approach. *Procedia Manufacturing*, *10*, 791–803. https://doi.org/10.1016/j.promfg.2017.07.079

Alam, M. M., Maniruzzaman, M., & Morshed, M. M. (2014). Application and Advances in Microprocessing of Natural Fiber (Jute)-Based Composites. In *Comprehensive Materials Processing* (Vol. 7, pp. 243–260). Elsevier Ltd. https://doi.org/10.1016/B978-0-08-096532-1.00714-7

Ali, A., Shaker, K., Nawab, Y., Jabbar, M., Hussain, T., Militky, J., & Baheti, V. (2018). Hydrophobic treatment of natural fibers and their composites—A review. In *Journal of Industrial Textiles* (Vol. 47, Issue 8, pp. 2153–2183). SAGE Publications Ltd. https://doi.org/10.1177/1528083716654468

Ali, M. (2016). *Measuring Accuracy of Two 3D Printing Materials*. https://scholarworks.bgsu.edu/ms_tech_mngmt/20

Ali, S. S. S., Razman, M. R., & Awang, A. (2020). The nexus of population, gross domestic product growth, electricity generation, electricity consumption and carbon emissions output in Malaysia. *International Journal of Energy Economics and Policy*, *10*(3), 84–89. https://doi.org/10.32479/ijeep.8987

Al-Makky, M., & Mahmoud, D. (2016). *THE IMPORTANCE OF ADDITIVE MANUFACTURING PROCESSES IN INDUSTRIAL APPLICATIONS*.

Anderson, I. (2017). Mechanical Properties of Specimens 3D Printed with Virgin and Recycled Polylactic Acid. *3D Printing and Additive Manufacturing*, *4*(2), 110–115. https://doi.org/10.1089/3dp.2016.0054

Antoniac, I., Popescu, D., Zapciu, A., Antoniac, A., Miculescu, F., & Moldovan, H. (2019). Magnesium filled polylactic acid (PLA) material for filament based 3D printing. *Materials*, *12*(5). https://doi.org/10.3390/ma12050719

Asyraf, M. R. M., Ishak, M. R., Norrrahim, M. N. F., Nurazzi, N. M., Shazleen, S. S., Ilyas, R. A., Rafidah, M., & Razman, M. R. (2021). Recent advances of thermal properties of sugar palm lignocellulosic fibre reinforced polymer composites. In *International Journal of Biological Macromolecules* (Vol. 193, pp. 1587–1599). Elsevier B.V. https://doi.org/10.1016/j.ijbiomac.2021.10.221

Asyraf, M. R. M., Ishak, M. R., Sapuan, S. M., & Yidris, N. (2019). Conceptual design of creep testing rig for full-scale cross arm using TRIZ-Morphological chart-analytic network process technique. *Journal of Materials Research and Technology*, *8*(6), 5647–5658. https://doi.org/10.1016/j.jmrt.2019.09.033

Asyraf, M. R. M., Ishak, M. R., Sapuan, S. M., & Yidris, N. (2020). Conceptual design of multi-operation outdoor flexural creep test rig using hybrid concurrent engineering approach. *Journal of Materials Research and Technology*, *9*(2), 2357–2368. https://doi.org/10.1016/j.jmrt.2019.12.067

Asyraf, M. R. M., Ishak, M. R., Sapuan, S. M., & Yidris, N. (2021). Comparison of Static and Long-term Creep Behaviors between Balau Wood and Glass Fiber Reinforced Polymer Composite for Cross-arm Application. *Fibers and Polymers*, *22*(3), 793–803. https://doi.org/10.1007/s12221-021-0512-1

Asyraf, M. R. M., Ishak, M. R., Sapuan, S. M., Yidris, N., Ilyas, R. A., Rafidah, M., & Razman, M. R. (2020a). Evaluation of Design and Simulation of Creep Test Rig for Full-Scale Crossarm Structure. *Advances in Civil Engineering*, *2020*. https://doi.org/10.1155/2020/6980918

Asyraf, M. R. M., Ishak, M. R., Sapuan, S. M., Yidris, N., Ilyas, R. A., Rafidah, M., & Razman, M. R. (2020b). Potential application of green composites for cross arm component in transmission tower: A brief review. In *International Journal of Polymer Science* (Vol. 2020). Hindawi Limited. https://doi.org/10.1155/2020/8878300

Asyraf, M. R. M., Rafidah, M., Azrina, A., & Razman, M. R. (2021). Dynamic mechanical behaviour of kenaf cellulosic fibre biocomposites: a comprehensive review on chemical treatments. In *Cellulose* (Vol. 28, Issue 5, pp. 2675–2695). Springer Science and Business Media B.V. https://doi.org/10.1007/s10570-021-03710-3

Asyraf, M. R. M., Rafidah, M., Ishak, M. R., Sapuan, S. M., Yidris, N., Ilyas, R. A., & Razman, M. R. (2020). Integration of TRIZ, morphological chart and ANP method for development of FRP composite portable fire extinguisher. *Polymer Composites*, *41*(7), 2917–2932. https://doi.org/10.1002/pc.25587

Asyraf, M. R. M., Syamsir, A., Supian, A. B. M., Usman, F., Ilyas, R. A., Nurazzi, N. M., Norrrahim, M. N. F., Razman, M. R., Zakaria, S. Z. S., Sharma, S., Itam, Z., & Rashid, M. Z. A. (2022). Sugar Palm Fibre-Reinforced Polymer Composites: Influence of Chemical Treatments on Its Mechanical Properties. In *Materials* (Vol. 15, Issue 11). MDPI. https://doi.org/10.3390/ma15113852

Attaran, M. (2017). The rise of 3-D printing: The advantages of additive manufacturing over traditional manufacturing. *Business Horizons*, *60*(5), 677–688. https://doi.org/10.1016/j.bushor.2017.05.011

Ave, rous, Luc, Kalia, & Susheel. (2011). *Biopolymers: Biomedical and Environmental Application*.

B. Lyons. (2012). *Additive Manufacturing in Aerospace Examples and Research Outlook*.

Bachtiar, D., Sapuan, S. M., & Hamdan, M. M. (2010). FLEXURAL PROPERTIES OF ALKALINE TREATED SUGAR PALM FIBRE REINFORCED EPOXY COMPOSITES. *International Journal of Automotive and Mechanical Engineering (IJAME)*, *ISSN*, 79–90. https://doi.org/10.15282/ijame.1.2010.7

Belaid, H., Nagarajan, S., Teyssier, C., Barou, C., Barés, J., Balme, S., Garay, H., Huon, V., Cornu, D., Cavaillès, V., & Bechelany, M. (2020). Development of new biocompatible 3D printed graphene oxide-based scaffolds. *Materials Science and Engineering C*, *110*. https://doi.org/10.1016/j.msec.2019.110595

Bikas, H., Stavropoulos, P., & Chryssolouris, G. (2016). Additive manufacturing methods and modeling approaches: A critical review. *International Journal of Advanced Manufacturing Technology*, *83*(1–4), 389–405. https://doi.org/10.1007/s00170-015-7576-2

Bogue, R. (2013). 3D printing: The dawn of a new era in manufacturing? *Assembly Automation*, *33*(4), 307–311. https://doi.org/10.1108/AA-06-2013-055

Buj-Corral, I., Sánchez-Casas, X., & Luis-Pérez, C. J. (2021). Analysis of am parameters on surface roughness obtained in pla parts printed with fff technology. *Polymers*, *13*(14). https://doi.org/10.3390/polym13142384

Carneiro, O. S., Silva, A. F., & Gomes, R. (2015). Fused deposition modeling with polypropylene. *Materials and Design*, *83*, 768–776. https://doi.org/10.1016/j.matdes.2015.06.053

Castro-Casado, D. (2021). Chemical treatments to enhance surface quality of FFF manufactured parts: a systematic review. In *Progress in Additive Manufacturing* (Vol. 6, Issue 2, pp. 307–319). Springer Science and Business Media Deutschland GmbH. https://doi.org/10.1007/s40964-020-00163-1

Chandrasekar, M., Ishak, M. R., Sapuan, S. M., Leman, Z., & Jawaid, M. (2017). A review on the characterisation of natural fibres and their composites after alkali treatment and water absorption. *Plastics, Rubber and Composites*, *46*(3), 119–136. https://doi.org/10.1080/14658011.2017.1298550

Cosgrove, D. J. (2005). Growth of the plant cell wall. In *Nature Reviews Molecular Cell Biology* (Vol. 6, Issue 11, pp. 850–861). https://doi.org/10.1038/nrm1746

Delgado Camacho, D., Clayton, P., O'Brien, W. J., Seepersad, C., Juenger, M., Ferron, R., & Salamone, S. (2018). Applications of additive manufacturing in the construction industry – A forward-looking review. *Automation in Construction*, *89*, 110–119. https://doi.org/10.1016/j.autcon.2017.12.031

Faruk, O., Bledzki, A. K., Fink, H. P., & Sain, M. (2012). Biocomposites reinforced with natural fibers: 2000-2010. In *Progress in Polymer Science* (Vol. 37, Issue 11, pp. 1552–1596). https://doi.org/10.1016/j.progpolymsci.2012.04.003

Ferreira, F. V., Mariano, M., Rabelo, S. C., Gouveia, R. F., & Lona, L. M. F. (2018). Isolation and surface modification of cellulose nanocrystals from sugarcane bagasse waste: From a micro- to a nano-scale view. *Applied Surface Science*, *436*, 1113–1122. https://doi.org/10.1016/j.apsusc.2017.12.137

Gaal, G., Mendes, M., de Almeida, T. P., Piazzetta, M. H. O., Gobbi, Â. L., Riul, A., & Rodrigues, V. (2017). Simplified fabrication of integrated microfluidic devices using fused deposition modeling 3D printing. *Sensors and Actuators, B: Chemical*, *242*, 35–40. https://doi.org/10.1016/j.snb.2016.10.110

Gao, W., Zhang, Y., Ramanujan, D., Ramani, K., Chen, Y., Williams, C. B., Wang, C. C. L., Shin, Y. C., Zhang, S., & Zavattieri, P. D. (2015). The status, challenges, and future of additive manufacturing in engineering. *CAD Computer Aided Design*, *69*, 65–89. https://doi.org/10.1016/j.cad.2015.04.001

Gary Hodgson. (2011). *Slic3er Manual*. Creative Commons BY- SA 3.0 License.

Gholampour, A., & Ozbakkaloglu, T. (2020). A review of natural fiber composites: properties, modification and processing techniques, characterization, applications. In *Journal of Materials Science* (Vol. 55, Issue 3, pp. 829–892). Springer New York LLC. https://doi.org/10.1007/s10853-019-03990-y

Govender, R., Kissi, E. O., Larsson, A., & Tho, I. (2021). Polymers in pharmaceutical additive manufacturing: A balancing act between printability and product performance. In *Advanced Drug Delivery Reviews* (Vol. 177). Elsevier B.V. https://doi.org/10.1016/j.addr.2021.113923

Graupner, N. (2008). Application of lignin as natural adhesion promoter in cotton fibre-reinforced poly(lactic acid) (PLA) composites. *Journal of Materials Science*, *43*(15), 5222–5229. https://doi.org/10.1007/s10853-008-2762-3

Hambali Boejang. (2021). *TOOLS AND TECHNOLOGIES FOR CONCURRENT PRODUCT DEVELOPMENT*. Penerbit Utem Press.
Haraguchi, K. (2014). Biocomposites. In *Encyclopedia of Polymeric Nanomaterials* (pp. 1–8). Springer Berlin Heidelberg. https://doi.org/10.1007/978-3-642-36199-9_316-1
Ilyas, R. A., Sapuan, S. M., Atikah, M. S. N., Asyraf, M. R. M., Rafiqah, S. A., Aisyah, H. A., Nurazzi, N. M., & Norrrahim, M. N. F. (2021). Effect of hydrolysis time on the morphological, physical, chemical, and thermal behavior of sugar palm nanocrystalline cellulose (Arenga pinnata (Wurmb.) Merr). *Textile Research Journal*, *91*(1–2), 152–167. https://doi.org/10.1177/0040517520932393
Ilyas, R. A., Sapuan, S. M., Harussani, M. M., Hakimi, M. Y. A. Y., Haziq, M. Z. M., Atikah, M. S. N., Asyraf, M. R. M., Ishak, M. R., Razman, M. R., Nurazzi, N. M., Norrrahim, M. N. F., Abral, H., & Asrofi, M. (2021). Polylactic acid (Pla) biocomposite: Processing, additive manufacturing and advanced applications. In *Polymers* (Vol. 13, Issue 8). MDPI AG. https://doi.org/10.3390/polym13081326
Ilyas, R. A., Sapuan, S. M., & Ishak, M. R. (2018). Isolation and characterization of nanocrystalline cellulose from sugar palm fibres (Arenga Pinnata). *Carbohydrate Polymers*, *181*, 1038–1051. https://doi.org/10.1016/j.carbpol.2017.11.045
Ishak, M. R., Sapuan, S. M., Leman, Z., Rahman, M. Z. A., Anwar, U. M. K., & Siregar, J. P. (2013). Sugar palm (Arenga pinnata): Its fibres, polymers and composites. In *Carbohydrate Polymers* (Vol. 91, Issue 2, pp. 699–710). https://doi.org/10.1016/j.carbpol.2012.07.073
ISO/ASME International. (2015). *Additive manufacturing-General principles-Terminology COPYRIGHT PROTECTED DOCUMENT*. www.iso.orgwww.astm.orgiTehSTANDARDPREVIEWISO/ASTM52900:2015https://standards.iteh.ai/catalog/standards/sist/d9adc3ce-ca51-4c21-b508-00fbbe01687d/iso-astm-52900-2015
John, M. J., & Thomas, S. (2008). Biofibres and biocomposites. In *Carbohydrate Polymers* (Vol. 71, Issue 3, pp. 343–364). https://doi.org/10.1016/j.carbpol.2007.05.040
Kaynak, C., & Varsavas, S. D. (2019). Performance comparison of the 3D-printed and injection-molded PLA and its elastomer blend and fiber composites. *Journal of Thermoplastic Composite Materials*, *32*(4), 501–520. https://doi.org/10.1177/0892705718772867
Kazmer, D. (2017). Three-Dimensional Printing of Plastics. In *Applied Plastics Engineering Handbook: Processing, Materials, and Applications: Second Edition* (pp. 617–634). Elsevier Inc. https://doi.org/10.1016/B978-0-323-39040-8.00029-8
Kontárová, S., Přikryl, R., Melčová, V., Menčík, P., Horálek, M., Figalla, S., Plavec, R., Feranc, J., Sadílek, J., & Pospíšilová, A. (2020). Printability, mechanical and thermal properties of poly(3-hydroxybutyrate)-poly(lactic acid)-plasticizer blends for three-dimensional (3D) printing. *Materials*, *13*(21), 1–28. https://doi.org/10.3390/ma13214736
Li, N., Li, Y., & Liu, S. (2016). Rapid prototyping of continuous carbon fiber reinforced polylactic acid composites by 3D printing. *Journal of Materials Processing Technology*, *238*, 218–225. https://doi.org/10.1016/j.jmatprotec.2016.07.025
Liu, W., Zhou, J., Ma, Y., Wang, J., & Xu, J. (2018). Fabrication of PLA Filaments and its Printable Performance. *IOP Conference Series: Materials Science and Engineering*, *275*(1). https://doi.org/10.1088/1757-899X/275/1/012033
MARIANNE LAVELLE. (2011, June 25). *A Rain Forest Advocate Taps the Energy of the Sugar Palm*.

Martins, M. A., Kiyohara, P. K., & Joekes, I. (2004). Scanning electron microscopy study of raw and chemically modified sisal fibers. *Journal of Applied Polymer Science*, *94*(6), 2333–2340. https://doi.org/10.1002/app.21203

Mazani, N., Sapuan, S. M., Sanyang, M. L., Atiqah, A., & Ilyas, R. A. (2019). Design and fabrication of a shoe shelf from kenaf fiber reinforced unsaturated polyester composites. In *Lignocellulose for Future Bioeconomy* (pp. 315–332). Elsevier. https://doi.org/10.1016/B978-0-12-816354-2.00017-7

Melchels, F. P. (2012). *Celebrating three decades of stereolithography*.

Melocchi, A., Parietti, F., Maccagnan, S., Ortenzi, M. A., Antenucci, S., Briatico-Vangosa, F., Maroni, A., Gazzaniga, A., & Zema, L. (2018). Industrial Development of a 3D-Printed Nutraceutical Delivery Platform in the Form of a Multicompartment HPC Capsule. *AAPS PharmSciTech*, *19*(8), 3343–3354. https://doi.org/10.1208/s12249-018-1029-9

Migneault, S., Koubaa, A., Erchiqui, F., Chaala, A., Englund, K., Krause, C., & Wolcott, M. (2008). Effect of fiber length on processing and properties of extruded wood-fiber/HDPE composites. *Journal of Applied Polymer Science*, *110*(2), 1085–1092. https://doi.org/10.1002/app.28720

Misri, S., Leman, Z., Sapuan, S. M., & Ishak, M. R. (2010). Mechanical properties and fabrication of small boat using woven glass/sugar palm fibres reinforced unsaturated polyester hybrid composite. *IOP Conference Series: Materials Science and Engineering*, *11*, 012015. https://doi.org/10.1088/1757-899x/11/1/012015

Mukherjee, T., & Kao, N. (2011). PLA Based Biopolymer Reinforced with Natural Fibre: A Review. *Journal of Polymers and the Environment*, *19*(3), 714–725. https://doi.org/10.1007/s10924-011-0320-6

My, D., Laila, A. H. A. M., Nurazzi, M., Khalina, A., Sapuan, S. M., Laila, D., Rahmah, M., & Hanafee, Z. (2017). SCIENCE & TECHNOLOGY A Review: Fibres, Polymer Matrices and Composites. *Pertanika J. Sci. & Technol*, *25*(4), 1085–1102. http://www.pertanika.upm.edu.my/

Najmon, J. C., Raeisi, S., & Tovar, A. (2019). Review of additive manufacturing technologies and applications in the aerospace industry. In *Additive Manufacturing for the Aerospace Industry* (pp. 7–31). Elsevier Inc. https://doi.org/10.1016/B978-0-12-814062-8.00002-9

Nasir, M. H. M., Taha, M. M., Razali, N., Ilyas, R. A., Knight, V. F., & Norrrahim, M. N. F. (2022). Effect of Chemical Treatment of Sugar Palm Fibre on Rheological and Thermal Properties of the PLA Composites Filament for FDM 3D Printing. *Materials*, *15*(22). https://doi.org/10.3390/ma15228082

Netravali, A. N. (2005). Biodegradable natural fiber composites. In *Biodegradable and Sustainable Fibres: A Volume in Woodhead Publishing Series in Textiles* (pp. 271–309). Elsevier Ltd. https://doi.org/10.1533/9781845690991.271

Ngo, T. D., Kashani, A., Imbalzano, G., Nguyen, K. T. Q., & Hui, D. (2018). Additive manufacturing (3D printing): A review of materials, methods, applications and challenges. In *Composites Part B: Engineering* (Vol. 143, pp. 172–196). Elsevier Ltd. https://doi.org/10.1016/j.compositesb.2018.02.012

Norizan, M. N., Abdan, K., Salit, M. S., & Mohamed, R. (2018). The effect of alkaline treatment on the mechanical properties of treated sugar palm yarn fibre reinforced unsaturated polyester composites reinforced with different fibre loadings of sugar palm fibre. *Sains Malaysiana*, *47*(4), 699–705. https://doi.org/10.17576/jsm-2018-4704-07

Nurazzi, N. M., Asyraf, M. R. M., Khalina, A., Abdullah, N., Aisyah, H. A., Rafiqah, S. A., Sabaruddin, F. A., Kamarudin, S. H., Norrrahim, M. N. F., Ilyas, R. A., & Sapuan,

S. M. (2021). A review on natural fiber reinforced polymer composite for bullet proof and ballistic applications. *Polymers*, *13*(4), 1–42. https://doi.org/10.3390/polym13040646
Nurazzi, N. M., Khalina, A., Sapuan, S. M., Ilyas, R. A., Rafiqah, S. A., & Hanafee, Z. M. (2020). Thermal properties of treated sugar palm yarn/glass fiber reinforced unsaturated polyester hybrid composites. *Journal of Materials Research and Technology*, *9*(2), 1606–1618. https://doi.org/10.1016/j.jmrt.2019.11.086
Obada, D. O., Kuburi, L. S., Dauda, M., Umaru, S., Dodoo-Arhin, D., Balogun, M. B., Iliyasu, I., & Iorpenda, M. J. (2020). Effect of variation in frequencies on the viscoelastic properties of coir and coconut husk powder reinforced polymer composites. *Journal of King Saud University - Engineering Sciences*, *32*(2), 148–157. https://doi.org/10.1016/j.jksues.2018.10.001
Oksman, K., Skrifvars, M., & Selin, J. F. (2003). Natural fibres as reinforcement in polylactic acid (PLA) composites. *Composites Science and Technology*, *63*(9), 1317–1324. https://doi.org/10.1016/S0266-3538(03)00103-9
Pérez, B., Nykvist, H., Brøgger, A. F., Larsen, M. B., & Falkeborg, M. F. (2019). Impact of macronutrients printability and 3D-printer parameters on 3D-food printing: A review. *Food Chemistry*, *287*, 249–257. https://doi.org/10.1016/j.foodchem.2019.02.090
Pitjamit, S., Thunsiri, K., Nakkiew, W., Wongwichai, T., Pothacharoen, P., & Wattanutchariya, W. (2020). The possibility of interlocking nail fabrication from FFF 3D printing PLA/PCL/HA composites coated by local silk fibroin for canine bone fracture treatment. *Materials*, *13*(7). https://doi.org/10.3390/ma13071564
Rafiee, M., Abidnejad, R., Ranta, A., Ojha, K., Karakoç, A., & Paltakari, J. (2021). Exploring the Possibilities of Fdm Filaments Comprising Natural Fiber-reinforced Biocomposites for Additive Manufacturing. *AIMS Materials Science*, *8*(4), 524–537. https://doi.org/10.3934/matersci.2021032
Rashid, B., Leman, Z., Jawaid, M., Ghazali, M. J., & Ishak, M. R. (2017). Palm phenolic composites. In *BioResources* (Vol. 12, Issue 2).
Saba, N., Jawaid, M., Alothman, O. Y., & Paridah, M. T. (2016). A review on dynamic mechanical properties of natural fibre reinforced polymer composites. In *Construction and Building Materials* (Vol. 106, pp. 149–159). Elsevier Ltd. https://doi.org/10.1016/j.conbuildmat.2015.12.075
Sabaruddin, F. A., Tahir, P. M., Sapuan, S. M., Ilyas, R. A., Lee, S. H., Abdan, K., Mazlan, N., Roseley, A. S. M., & Khalil Hps, A. (2021). The effects of unbleached and bleached nanocellulose on the thermal and flammability of polypropylene-reinforced kenaf core hybrid polymer bionanocomposites. *Polymers*, *13*(1), 1–19. https://doi.org/10.3390/polym13010116
Sahari, J., & Sapuan, S. M. (2012). *Physical and Chemical Properties of Different Morphological Parts of Sugar Palm Fibres Modeling Technology Transfer View project DEVELOPMENT AND CHARACTERIZATION OF SUGAR PALM NANOCELLULOSE FIBRE REINFORCED SUGAR PALM STARCH BIOPOLYMER COMPOSITE View project*. https://www.researchgate.net/publication/267944415
Sahari, J., Sapuan, S. M., Zainudin, E. S., & Maleque, M. A. (2012). Sugar Palm Tree: A Versatile Plant and Novel Source for Biofibres, Biomatrices, and Biocomposites. In *Polymers from Renewable Resources* (Vol. 3, Issue 2).
Saleh Alghamdi, S., John, S., Roy Choudhury, N., & Dutta, N. K. (2021). *polymers Additive Manufacturing of Polymer Materials: Progress, Promise and Challenges*. https://doi.org/10.3390/polym13

Sanyang, M. L., Sapuan, S. M., Jawaid, M., Ishak, M. R., & Sahari, J. (2016). Recent developments in sugar palm (Arenga pinnata) based biocomposites and their potential industrial applications: A review. In *Renewable and Sustainable Energy Reviews* (Vol. 54, pp. 533–549). Elsevier Ltd. https://doi.org/10.1016/j.rser.2015.10.037

Sapuan, S. M., & Abdan, K. (2020). *REVIEW ON GREEN TECHNOLOGY PYROLYSIS FOR PLASTIC WASTES Seminar on Advanced Bio-and Mineral based Natural Fibre Composites (SBMC2021) View project FEA on Kenaf Polymer Composite for Automotive Engine Rubber Mounting View project*. https://www.researchgate.net/publication/345958932

Sastra, H. Y., Siregar, J. P., Sapuan, S. M., & Hamdan, M. M. (2006a). Tensile properties of Arenga pinnata fiber-reinforced epoxy composites. *Polymer - Plastics Technology and Engineering*, *45*(1), 149–155. https://doi.org/10.1080/03602550500374038

Sastra, H. Y., Siregar, J. P., Sapuan, S. M., & Hamdan, M. M. (2006b). Tensile properties of Arenga pinnata fiber-reinforced epoxy composites. *Polymer - Plastics Technology and Engineering*, *45*(1), 149–155. https://doi.org/10.1080/03602550500374038

S.C Tjong. (2009). *Advances in Biomedical Sciences and Engineering*. Bentham Science Publishers.

Suriani, M. J., Radzi, F. S. M., Ilyas, R. A., Petrů, M., Sapuan, S. M., & Ruzaidi, C. M. (2021). Flammability, tensile, and morphological properties of oil palm empty fruit bunches fiber/pet yarn-reinforced epoxy fire retardant hybrid polymer composites. *Polymers*, *13*(8). https://doi.org/10.3390/polym13081282

Tanase-Opedal, M., Espinosa, E., Rodríguez, A., & Chinga-Carrasco, G. (2019). Lignin: A biopolymer from forestry biomass for biocomposites and 3D printing. *Materials*, *12*(18). https://doi.org/10.3390/ma12183006

Team Xometry. (2022). *PLA (Polylactic Acid): Definition, Applications, and Different Types*.

Tholibon, D., Tharazi, I., Sulong, A. B., Muhamad, N., Ismail, N. F., Md Radzi, M. K. F., Mohd Radzuan, N. A., & Hui, D. (2019). Kenaf Fiber Composites: A Review on Synthetic and Biodegradable Polymer Matrix. *Jurnal Kejuruteraan*, *31*(1), 65–76. https://doi.org/10.17576/jkukm-2019-31(1)-08

Tiersch, T. R., & Monroe, W. T. (2016). Three-dimensional printing with polylactic acid (PLA) thermoplastic offers new opportunities for cryobiology. *Cryobiology*, *73*(3), 396–398. https://doi.org/10.1016/j.cryobiol.2016.10.005

Todd Grim. (2003). *FUSED DEPOSITION MODELLING- A TECHNOLOGY EVALUATION*.

Too, M. H., Leong, K. F., Chua, C. K., Du, Z. H., Yang, S. F., Cheah, C. M., & Ho, S. L. (2002). Investigation of 3D Non-Random Porous Structures by Fused Deposition Modelling. In *Int J Adv Manuf Technol* (Vol. 19). Springer-Verlag London Limited.

Wambua, P., Ivens, J., & Verpoest, I. (2003). Natural fibres: Can they replace glass in fibre reinforced plastics? *Composites Science and Technology*, *63*(9), 1259–1264. https://doi.org/10.1016/S0266-3538(03)00096-4

Wang, L., Gramlich, W. M., & Gardner, D. J. (2017). Improving the impact strength of Poly(lactic acid) (PLA) in fused layer modeling (FLM). *Polymer*, *114*, 242–248. https://doi.org/10.1016/j.polymer.2017.03.011

Wang, M., Favi, P., Cheng, X., Golshan, N. H., Ziemer, K. S., Keidar, M., & Webster, T. J. (2016). Cold atmospheric plasma (CAP) surface nanomodified 3D printed polylactic acid (PLA) scaffolds for bone regeneration. *Acta Biomaterialia*, *46*, 256–265. https://doi.org/10.1016/j.actbio.2016.09.030

Wang, Y., Tan, Q., Pu, F., Boone, D., & Zhang, M. (2020). A Review of the Application of Additive Manufacturing in Prosthetic and Orthotic Clinics from a Biomechanical

Perspective. In *Engineering* (Vol. 6, Issue 11, pp. 1258–1266). Elsevier Ltd. https://doi.org/10.1016/j.eng.2020.07.019

Wang, Y., Zhou, Y., Lin, L., Corker, J., & Fan, M. (2020). Overview of 3D additive manufacturing (AM) and corresponding AM composites. In *Composites Part A: Applied Science and Manufacturing* (Vol. 139). Elsevier Ltd. https://doi.org/10.1016/j.compositesa.2020.106114

Wasti, S., & Adhikari, S. (2020). Use of Biomaterials for 3D Printing by Fused Deposition Modeling Technique: A Review. In *Frontiers in Chemistry* (Vol. 8). Frontiers Media S.A. https://doi.org/10.3389/fchem.2020.00315

Wong, K. V., & Hernandez, A. (2012). A Review of Additive Manufacturing. *ISRN Mechanical Engineering*, *2012*, 1–10. https://doi.org/10.5402/2012/208760

APPENDIX

APPENDIX A

Gantt Chart for PSM 1																
No	**Task Project**	**Plan / Actual**	**Week**													
			1	**2**	**3**	**4**	**5**	**6**	**7**	**8**	**9**	**10**	**11**	**12**	**13**	**14**
1	PSM title registration	Plan														
		Actual														
2	Project briefing with supervisor.	Plan														
		Actual						R								
3	Crushing filament	Plan														
		Actual						A								
4	Filament extrusion	Plan														
		Actual						Y								
5	Printing some samples	Plan														
		Actual						A								
6	Chapter 1: Introduction	Plan														
		Actual														
7	Chapter 2: Literature Review	Plan						B								
		Actual														
8	Chapter 3: Research Methodology	Plan						R								
		Actual						E								
9	Chapter 4: Preliminary result	Plan														
		Actual						A								
10	Checking report draft	Plan														
		Actual						K								
11	Report submission for PSM 1	Plan														
		Actual														
12	PSM 1 presentation	Plan														
		Actual														

Info

Planning	
Actual	

APPENDIX B

Gantt Chart for PSM 2																	
No	**Task Project**	**Plan / Actual**	**Week**														
			1	**2**	**3**	**4**	**5**	**6**	**7**	**8**	**9**	**10**	**11**	**12**	**13**	**14**	**15**
1	Printing samples	Plan								MID SEMESTER BREAK							
		Actual															
2	Measure dimensional accuracy	Plan															
		Actual															
3	Measure surface roughness	Plan															
		Actual															
4	Tensile testing	Plan															
		Actual															
5	Flexural testing	Plan															
		Actual															
6	Impact testing	Plan															
		Actual															
7	Chapter 4: Analysis and Result	Plan															
		Actual															
8	Chapter 5: Conclusion and Recommendation	Plan															
		Actual															
9	Checking report draft	Plan															
		Actual															
10	Report submission for PSM 2	Plan															
		Actual															
11	PSM 2 presentation	Plan															
		Actual															

Info

Planning	
Actual	

APPENDIX C

RAW DATA FLEXURAL TEST

PLA Flexural															
Load				stroke				stress				strain			
s1	s2	s3	avg	s1	s2	s3	avg	s1	s2	s3	avg	s1	s2	s3	avg
-0.05	0.00	0.02	-0.01	0.00	0.00	0.00	0.00	0.00	0.00	0.00	0.00	0.00	0.00	0.00	0.00
12.78	10.79	7.41	10.33	0.41	0.41	0.41	0.41	0.34	0.28	0.19	0.27	0.00	0.00	0.00	0.00
28.45	26.26	24.43	26.38	0.83	0.83	0.83	0.83	0.75	0.69	0.64	0.69	0.01	0.01	0.01	0.01
51.05	48.29	46.08	48.47	1.25	1.25	1.25	1.25	1.34	1.27	1.21	1.27	0.01	0.01	0.01	0.01
74.75	71.92	71.06	72.58	1.66	1.66	1.66	1.66	1.96	1.89	1.87	1.90	0.01	0.01	0.01	0.01
99.79	97.21	93.95	96.98	2.08	2.08	2.08	2.08	2.62	2.55	2.47	2.55	0.02	0.02	0.02	0.02
121.58	123.15	119.00	121.24	2.50	2.50	2.50	2.50	3.19	3.23	3.12	3.18	0.02	0.02	0.02	0.02
143.43	146.36	139.68	143.16	2.91	2.91	2.91	2.91	3.76	3.84	3.67	3.76	0.02	0.02	0.02	0.02
161.23	164.75	156.91	160.96	3.33	3.33	3.33	3.33	4.23	4.32	4.12	4.22	0.03	0.03	0.03	0.03
175.40	177.42	170.80	174.54	3.75	3.75	3.75	3.75	4.60	4.66	4.48	4.58	0.03	0.03	0.03	0.03
184.89	186.40	181.68	184.32	4.16	4.16	4.16	4.16	4.85	4.89	4.77	4.84	0.03	0.03	0.03	0.03
190.53	193.21	188.21	190.65	4.58	4.58	4.58	4.58	5.00	5.07	4.94	5.00	0.04	0.04	0.04	0.04
193.42	195.14	192.85	193.80	5.00	5.00	5.00	5.00	5.08	5.12	5.06	5.09	0.04	0.04	0.04	0.04
193.63	197.97	195.42	195.67	5.41	5.41	5.41	5.41	5.08	5.20	5.13	5.14	0.04	0.04	0.04	0.04
176.22	197.76	198.08	190.69	5.83	5.83	5.83	5.83	4.63	5.19	5.20	5.00	0.05	0.05	0.05	0.05
167.40	155.67	200.21	174.43	6.25	6.25	6.25	6.25	4.39	4.09	5.25	4.58	0.05	0.05	0.05	0.05
147.52	104.57	201.64	151.24	6.66	6.66	6.66	6.66	3.87	2.74	5.29	3.97	0.05	0.05	0.05	0.05
46.63	24.37	201.61	90.87	7.08	7.08	7.08	7.08	1.22	0.64	5.29	2.39	0.06	0.06	0.06	0.06
33.68	21.51	191.29	82.16	7.50	7.50	7.50	7.50	0.88	0.56	5.02	2.16	0.06	0.06	0.06	0.06
26.34	18.64	177.42	74.13	7.91	7.91	7.91	7.91	0.69	0.49	4.66	1.95	0.06	0.06	0.06	0.06
20.92	16.64	156.66	64.74	8.33	8.33	8.33	8.33	0.55	0.44	4.11	1.70	0.07	0.07	0.07	0.07
19.71	14.81	24.51	19.68	8.75	8.75	8.75	8.75	0.52	0.39	0.64	0.52	0.07	0.07	0.07	0.07
15.96	13.49	21.47	16.98	9.16	9.16	9.16	9.16	0.42	0.35	0.56	0.45	0.07	0.07	0.07	0.07
12.29	11.98	18.66	14.31	9.58	9.58	9.58	9.58	0.32	0.31	0.49	0.38	0.08	0.08	0.08	0.08
10.43	10.98	17.10	12.84	10.00	10.00	10.00	10.00	0.27	0.29	0.45	0.34	0.08	0.08	0.08	0.08
9.70	10.36	16.37	12.14	10.20	10.20	10.20	10.20	0.25	0.27	0.43	0.32	0.08	0.08	0.08	0.08

	9.90	15.80	12.85		10.34	10.34	10.34		0.26	0.41	0.34	0.00	0.08	0.08	0.06
		15.64	15.64			10.41	10.41			0.41	0.41	0.00	0.00	0.08	0.03
		14.24	14.24			10.83	10.83			0.37	0.37	0.00	0.00	0.09	0.03
		13.05	13.05			11.25	11.25			0.34	0.34	0.00	0.00	0.09	0.03
		11.81	11.81			11.66	11.66			0.31	0.31	0.00	0.00	0.09	0.03
		10.11	10.11			12.08	12.08			0.27	0.27	0.00	0.00	0.10	0.03
		10.08	10.08			12.09	12.09			0.26	0.26	0.00	0.00	0.10	0.03

SPF Flexural															
Load				stroke				stress				strain			
s1	s2	s3	avg	s1	s2	s3	avg	s1	s2	s3	avg	s1	s2	s3	avg
0.08	-0.08	-0.11	-0.04	0.00	0.00	0.00	0.00	0.00	0.00	0.00	0.00	0.00	0.00	0.00	0.00
7.01	7.61	7.61	7.41	0.41	0.41	0.41	0.41	0.18	0.20	0.20	0.19	0.00	0.00	0.00	0.00
12.06	22.62	24.03	19.57	0.83	0.83	0.83	0.83	0.32	0.59	0.63	0.51	0.01	0.01	0.01	0.01
25.78	44.70	47.97	39.48	1.25	1.25	1.25	1.25	0.68	1.17	1.26	1.04	0.01	0.01	0.01	0.01
40.45	67.36	74.88	60.90	1.66	1.66	1.66	1.66	1.06	1.77	1.97	1.60	0.01	0.01	0.01	0.01
55.27	90.07	101.53	82.29	2.08	2.08	2.08	2.08	1.45	2.36	2.66	2.16	0.02	0.02	0.02	0.02
68.66	111.21	124.03	101.30	2.50	2.50	2.50	2.50	1.80	2.92	3.26	2.66	0.02	0.02	0.02	0.02
80.27	129.86	141.03	117.05	2.91	2.91	2.91	2.91	2.11	3.41	3.70	3.07	0.02	0.02	0.02	0.02
85.70	138.78	-0.72	74.59	3.15	3.15	3.15	3.15	2.25	3.64	-0.02	1.96	0.03	0.03	0.03	0.03
88.83	143.97		116.40	3.33	3.33		3.33	2.33	3.78		3.06	0.03	0.03	0.00	0.02
91.85	154.24		123.05	3.75	3.75		3.75	2.41	4.05		3.23	0.03	0.03	0.00	0.02
83.96	155.04		119.50	4.16	4.16		4.16	2.20	4.07		3.14	0.03	0.03	0.00	0.02
43.54	66.09		54.81	4.58	4.58		4.58	1.14	1.73		1.44	0.04	0.04	0.00	0.02
35.10	40.25		37.67	5.00	5.00		5.00	0.92	1.06		0.99	0.04	0.04	0.00	0.03
23.25	24.27		23.76	5.41	5.41		5.41	0.61	0.64		0.62	0.04	0.04	0.00	0.03
18.90	19.49		19.19	5.83	5.83		5.83	0.50	0.51		0.50	0.05	0.05	0.00	0.03
15.61	17.12		16.36	6.25	6.25		6.25	0.41	0.45		0.43	0.05	0.05	0.00	0.03
13.14	14.85		14.00	6.66	6.66		6.66	0.35	0.39		0.37	0.05	0.05	0.00	0.04

11.75	12.49		12.12	7.08	7.08		7.08	0.31	0.33		0.32	0.06	0.06	0.00	0.04
10.74	10.14		10.44	7.50	7.50		7.50	0.28	0.27		0.27	0.06	0.06	0.00	0.04
9.70	9.39		9.54	7.91	7.91		7.91	0.25	0.25		0.25	0.06	0.06	0.00	0.04
8.54	8.12		8.33	8.33	8.33		8.33	0.22	0.21		0.22	0.07	0.07	0.00	0.04
8.46	7.77		8.11	8.43	8.43		8.43	0.22	0.20		0.21	0.07	0.07	0.00	0.04
7.10			7.10	8.75			8.75	0.19	0.00		0.09	0.07	0.00		0.03
6.42			6.42	9.16			9.16	0.17	0.00		0.08	0.07	0.00		0.04
5.59			5.59	9.58			9.58	0.15	0.00		0.07	0.08	0.00		0.04
4.64			4.64	10.00			10.00	0.12	0.00		0.06	0.08	0.00		0.04
4.56			4.56	10.02			10.02	0.12	0.00		0.06	0.08	0.00		0.04

APPENDIX D

RAW DATA TENSILE TEST

Pla															
Load				stroke				stress				strain			
s1	s2	s3	avg	s1	s2	s3	avg	s1	s2	s3	avg	s1	s2	s3	avg
-0.002	-0.002	-0.002	-0.002	0.000	0.000	0.000	0.000	0	0	0	0.0000	0	0	0	0.0000
0.040	0.031	0.030	0.034	0.039	0.039	0.039	0.039	0.001	0.0008	0.0008	0.0009	0.0007	0.0007	0.0007	0.0007
0.087	0.063	0.067	0.072	0.081	0.081	0.081	0.081	0.0022	0.0016	0.0017	0.0018	0.0014	0.0014	0.0014	0.0014
0.131	0.094	0.100	0.108	0.122	0.122	0.122	0.122	0.0034	0.0024	0.0026	0.0028	0.0021	0.0021	0.0021	0.0021
0.176	0.122	0.129	0.143	0.164	0.164	0.164	0.164	0.0045	0.0031	0.0033	0.0036	0.0029	0.0029	0.0029	0.0029
0.220	0.142	0.153	0.172	0.206	0.206	0.206	0.206	0.0056	0.0036	0.0039	0.0044	0.0036	0.0036	0.0036	0.0036
0.262	0.161	0.176	0.200	0.247	0.247	0.247	0.247	0.0067	0.0041	0.0045	0.0051	0.0043	0.0043	0.0043	0.0043
0.344	0.202	0.224	0.257	0.331	0.331	0.331	0.331	0.0088	0.0052	0.0057	0.0066	0.0058	0.0058	0.0058	0.0058
0.386	0.224	0.248	0.286	0.372	0.372	0.372	0.372	0.0099	0.0058	0.0064	0.0074	0.0065	0.0065	0.0065	0.0065
0.425	0.247	0.272	0.315	0.414	0.414	0.414	0.414	0.0109	0.0063	0.007	0.0081	0.0073	0.0073	0.0073	0.0073
0.464	0.269	0.297	0.343	0.456	0.456	0.456	0.456	0.0119	0.0069	0.0076	0.0088	0.008	0.008	0.008	0.0080
0.502	0.292	0.321	0.372	0.497	0.497	0.497	0.497	0.0129	0.0075	0.0082	0.0095	0.0087	0.0087	0.0087	0.0087
0.540	0.314	0.346	0.400	0.539	0.539	0.539	0.539	0.0138	0.0081	0.0089	0.0103	0.0095	0.0095	0.0095	0.0095
0.576	0.339	0.370	0.428	0.581	0.581	0.581	0.581	0.0148	0.0087	0.0095	0.0110	0.0102	0.0102	0.0102	0.0102
0.612	0.362	0.396	0.456	0.622	0.622	0.622	0.622	0.0157	0.0093	0.0102	0.0117	0.0109	0.0109	0.0109	0.0109
0.647	0.386	0.421	0.485	0.664	0.664	0.664	0.664	0.0166	0.0099	0.0108	0.0124	0.0116	0.0116	0.0116	0.0116
0.681	0.410	0.447	0.513	0.706	0.706	0.706	0.706	0.0175	0.0105	0.0115	0.0132	0.0124	0.0124	0.0124	0.0124
0.713	0.434	0.472	0.540	0.747	0.747	0.747	0.747	0.0183	0.0111	0.0121	0.0138	0.0131	0.0131	0.0131	0.0131
0.748	0.460	0.498	0.569	0.789	0.789	0.789	0.789	0.0192	0.0118	0.0128	0.0146	0.0138	0.0138	0.0138	0.0138
0.780	0.485	0.524	0.596	0.831	0.831	0.831	0.831	0.02	0.0124	0.0134	0.0153	0.0146	0.0146	0.0146	0.0146
0.811	0.511	0.550	0.624	0.872	0.872	0.872	0.872	0.0208	0.0131	0.0141	0.0160	0.0153	0.0153	0.0153	0.0153
0.843	0.536	0.578	0.652	0.914	0.914	0.914	0.914	0.0216	0.0138	0.0148	0.0167	0.016	0.016	0.016	0.0160
0.873	0.562	0.604	0.680	0.956	0.956	0.956	0.956	0.0224	0.0144	0.0155	0.0174	0.0168	0.0168	0.0168	0.0168

0.904	0.589	0.631	0.708	0.997	0.997	0.997	0.997	0.0232	0.0151	0.0162	0.0182	0.0175	0.0175	0.0175	0.0175
0.935	0.615	0.658	0.736	1.039	1.039	1.039	1.039	0.024	0.0158	0.0169	0.0189	0.0182	0.0182	0.0182	0.0182
0.965	0.642	0.686	0.764	1.081	1.081	1.081	1.081	0.0247	0.0165	0.0176	0.0196	0.019	0.019	0.019	0.0190
0.994	0.669	0.714	0.792	1.122	1.122	1.122	1.122	0.0255	0.0171	0.0183	0.0203	0.0197	0.0197	0.0197	0.0197
1.023	0.695	0.741	0.820	1.164	1.164	1.164	1.164	0.0262	0.0178	0.019	0.0210	0.0204	0.0204	0.0204	0.0204
1.053	0.721	0.770	0.848	1.206	1.206	1.206	1.206	0.027	0.0185	0.0197	0.0217	0.0212	0.0211	0.0212	0.0212
1.082	0.749	0.797	0.876	1.247	1.247	1.247	1.247	0.0277	0.0192	0.0204	0.0224	0.0219	0.0219	0.0219	0.0219
1.111	0.776	0.826	0.904	1.289	1.289	1.289	1.289	0.0285	0.0199	0.0212	0.0232	0.0226	0.0226	0.0226	0.0226
1.140	0.803	0.854	0.932	1.331	1.331	1.331	1.331	0.0292	0.0206	0.0219	0.0239	0.0233	0.0233	0.0233	0.0233
1.168	0.831	0.882	0.960	1.372	1.372	1.372	1.372	0.0299	0.0213	0.0226	0.0246	0.0241	0.0241	0.0241	0.0241
1.197	0.860	0.910	0.989	1.414	1.414	1.414	1.414	0.0307	0.0221	0.0233	0.0254	0.0248	0.0248	0.0248	0.0248
1.225	0.887	0.939	1.017	1.456	1.456	1.456	1.456	0.0314	0.0228	0.0241	0.0261	0.0255	0.0255	0.0255	0.0255
1.254	0.915	0.967	1.045	1.497	1.497	1.497	1.497	0.0321	0.0235	0.0248	0.0268	0.0263	0.0263	0.0263	0.0263
1.282	0.943	0.995	1.073	1.539	1.539	1.539	1.539	0.0329	0.0242	0.0255	0.0275	0.027	0.027	0.027	0.0270
1.310	0.971	1.024	1.102	1.581	1.581	1.581	1.581	0.0336	0.0249	0.0263	0.0283	0.0277	0.0277	0.0277	0.0277
1.338	0.999	1.052	1.130	1.622	1.622	1.622	1.622	0.0343	0.0256	0.027	0.0290	0.0285	0.0285	0.0285	0.0285
1.365	1.027	1.081	1.158	1.664	1.664	1.664	1.664	0.035	0.0263	0.0277	0.0297	0.0292	0.0292	0.0292	0.0292
1.392	1.054	1.110	1.185	1.706	1.706	1.706	1.706	0.0357	0.027	0.0285	0.0304	0.0299	0.0299	0.0299	0.0299
1.419	1.083	1.138	1.213	1.747	1.747	1.747	1.747	0.0364	0.0278	0.0292	0.0311	0.0307	0.0307	0.0307	0.0307
1.446	1.111	1.165	1.241	1.789	1.789	1.789	1.789	0.0371	0.0285	0.0299	0.0318	0.0314	0.0314	0.0314	0.0314
1.472	1.140	1.194	1.269	1.831	1.831	1.831	1.831	0.0377	0.0292	0.0306	0.0325	0.0321	0.0321	0.0321	0.0321
1.498	1.166	1.223	1.296	1.872	1.872	1.872	1.872	0.0384	0.0299	0.0314	0.0332	0.0328	0.0328	0.0328	0.0328
1.525	1.195	1.251	1.324	1.914	1.914	1.914	1.914	0.0391	0.0306	0.0321	0.0339	0.0336	0.0336	0.0336	0.0336
1.549	1.224	1.280	1.351	1.956	1.956	1.956	1.956	0.0397	0.0314	0.0328	0.0346	0.0343	0.0343	0.0343	0.0343
1.572	1.252	1.309	1.378	1.997	1.997	1.997	1.997	0.0403	0.0321	0.0336	0.0353	0.035	0.035	0.035	0.0350
1.593	1.279	1.337	1.403	2.039	2.039	2.039	2.039	0.0409	0.0328	0.0343	0.0360	0.0358	0.0358	0.0358	0.0358
1.613	1.308	1.365	1.429	2.081	2.081	2.081	2.081	0.0414	0.0335	0.035	0.0366	0.0365	0.0365	0.0365	0.0365
1.629	1.336	1.393	1.453	2.122	2.122	2.122	2.122	0.0418	0.0343	0.0357	0.0373	0.0372	0.0372	0.0372	0.0372
1.641	1.364	1.421	1.476	2.164	2.164	2.164	2.164	0.0421	0.035	0.0364	0.0378	0.038	0.038	0.038	0.0380

1.637	1.391	1.449	1.492	2.206	2.206	2.206	2.206	0.042	0.0357	0.0371	0.0383	0.0387	0.0387	0.0387	0.0387
-0.418	1.419	1.477	0.826	2.247	2.247	2.247	2.247	-0.0107	0.0364	0.0379	0.0212	0.0394	0.0394	0.0394	0.0394
	1.447	1.504	1.476		2.289	2.289	2.289		0.0371	0.0386	0.0379		0.0402	0.0402	0.0402
	1.475	1.533	1.504		2.331	2.331	2.331		0.0378	0.0393	0.0386		0.0409	0.0409	0.0409
	1.503	1.560	1.532		2.372	2.372	2.372		0.0385	0.04	0.0393		0.0416	0.0416	0.0416
	1.532	1.586	1.559		2.414	2.414	2.414		0.0393	0.0407	0.0400		0.0423	0.0424	0.0424
	1.559	1.613	1.586		2.456	2.456	2.456		0.04	0.0414	0.0407		0.0431	0.0431	0.0431
	1.585	1.640	1.613		2.497	2.497	2.497		0.0406	0.0421	0.0414		0.0438	0.0438	0.0438
	1.612	1.663	1.637		2.539	2.539	2.539		0.0413	0.0426	0.0420		0.0445	0.0445	0.0445
	1.640	1.684	1.662		2.581	2.581	2.581		0.042	0.0432	0.0426		0.0453	0.0453	0.0453
	1.666	-0.245	0.711		2.622	2.600	2.611		0.0427	-0.0063	0.0182		0.046	0.0456	0.0458
	1.692		1.692		2.664		2.664		0.0434		0.0434		0.0467		0.0467
	1.717		1.717		2.706		2.706		0.044		0.0440		0.0475		0.0475
	1.744		1.744		2.747		2.747		0.0447		0.0447		0.0482		0.0482
	1.768		1.768		2.789		2.789		0.0453		0.0453		0.0489		0.0489
	1.792		1.792		2.831		2.831		0.046		0.0460		0.0497		0.0497
	1.815		1.815		2.872		2.872		0.0465		0.0465		0.0504		0.0504
	1.837		1.837		2.914		2.914		0.0471		0.0471		0.0511		0.0511
	1.857		1.857		2.956		2.956		0.0476		0.0476		0.0519		0.0519
	1.873		1.873		2.997		2.997		0.048		0.0480		0.0526		0.0526
	1.886		1.886		3.039		3.039		0.0484		0.0484		0.0533		0.0533
	1.893		1.893		3.081		3.081		0.0485		0.0485		0.054		0.0540
	-0.206		-0.206		3.122		3.122		-0.0053		-0.0053		0.0548		0.0548

SPF															
Load				stroke				stress				strain			
s1	s2	s3	avg	s1	s2	s3	avg	s1	s2	s3	avg	s1	s2	s3	avg
-0.001	-0.001	-0.001	-0.001	0.000	0.000	0.000	0.000	-0.00001	-0.00003	-0.00002	-0.00002	0	0	0	0.00000
0.031	0.031	0.028	0.030	0.039	0.039	0.039	0.039	0.0008	0.00079	0.00072	0.00077	0.00068	0.00068	0.00068	0.00068
0.062	0.063	0.060	0.062	0.081	0.081	0.081	0.081	0.00159	0.0016	0.00154	0.00158	0.00141	0.00141	0.00141	0.00141
0.088	0.094	0.090	0.090	0.122	0.122	0.122	0.122	0.00226	0.0024	0.0023	0.00232	0.00214	0.00214	0.00214	0.00214
0.111	0.123	0.110	0.115	0.164	0.164	0.164	0.164	0.00285	0.00315	0.00282	0.00294	0.00288	0.00287	0.00288	0.00288
0.135	0.147	0.128	0.137	0.206	0.206	0.206	0.206	0.00346	0.00377	0.00327	0.00350	0.00361	0.00361	0.00361	0.00361
0.157	0.167	0.142	0.155	0.247	0.247	0.247	0.247	0.00403	0.00428	0.00364	0.00398	0.00434	0.00434	0.00434	0.00434
0.181	0.186	0.156	0.174	0.289	0.289	0.289	0.289	0.00465	0.00476	0.004	0.00447	0.00507	0.00507	0.00507	0.00507
0.203	0.205	0.170	0.193	0.331	0.331	0.331	0.331	0.00522	0.00525	0.00435	0.00494	0.0058	0.0058	0.0058	0.00580
0.228	0.222	0.183	0.211	0.372	0.372	0.372	0.372	0.00586	0.00569	0.00468	0.00541	0.00653	0.00653	0.00653	0.00653
0.253	0.240	0.197	0.230	0.414	0.414	0.414	0.414	0.00648	0.00615	0.00504	0.00589	0.00726	0.00726	0.00726	0.00726
0.278	0.260	0.212	0.250	0.456	0.456	0.456	0.456	0.00712	0.00666	0.00543	0.00640	0.00799	0.00799	0.00799	0.00799
0.303	0.280	0.227	0.270	0.497	0.497	0.497	0.497	0.00776	0.00718	0.00582	0.00692	0.00872	0.00872	0.00872	0.00872
0.328	0.299	0.243	0.290	0.539	0.539	0.539	0.539	0.00842	0.00766	0.00624	0.00744	0.00945	0.00945	0.00945	0.00945
0.353	0.319	0.260	0.311	0.581	0.581	0.581	0.581	0.00906	0.00818	0.00666	0.00797	0.01018	0.01018	0.01018	0.01018
0.378	0.339	0.275	0.331	0.622	0.622	0.622	0.622	0.0097	0.0087	0.00704	0.00848	0.01092	0.01092	0.01092	0.01092
0.402	0.360	0.291	0.351	0.664	0.664	0.664	0.664	0.01032	0.00922	0.00747	0.00900	0.01165	0.01165	0.01165	0.01165
0.427	0.381	0.307	0.372	0.706	0.706	0.706	0.706	0.01094	0.00976	0.00787	0.00952	0.01238	0.01238	0.01238	0.01238
0.451	0.401	0.323	0.392	0.747	0.747	0.747	0.747	0.01157	0.01028	0.00828	0.01004	0.01311	0.01311	0.01311	0.01311
0.476	0.421	0.338	0.412	0.789	0.789	0.789	0.789	0.01221	0.0108	0.00867	0.01056	0.01384	0.01384	0.01384	0.01384
0.500	0.443	0.351	0.432	0.831	0.831	0.831	0.831	0.01283	0.01137	0.00901	0.01107	0.01457	0.01457	0.01457	0.01457
0.525	0.464	0.368	0.452	0.872	0.872	0.872	0.872	0.01346	0.01189	0.00944	0.01160	0.0153	0.0153	0.0153	0.01530
0.549	0.486	0.383	0.473	0.914	0.914	0.914	0.914	0.01407	0.01247	0.00983	0.01212	0.01603	0.01603	0.01603	0.01603
0.572	0.508	0.399	0.493	0.956	0.956	0.956	0.956	0.01467	0.01302	0.01023	0.01264	0.01676	0.01676	0.01676	0.01676
0.596	0.529	0.416	0.514	0.997	0.997	0.997	0.997	0.01527	0.01358	0.01066	0.01317	0.01749	0.01749	0.01749	0.01749
0.620	0.552	0.433	0.535	1.039	1.039	1.039	1.039	0.01589	0.01414	0.01111	0.01371	0.01823	0.01823	0.01823	0.01823

0.643	0.574	0.450	0.556	1.081	1.081	1.081	1.081	0.0165	0.01471	0.01153	0.01425	0.01896	0.01896	0.01896	0.01896
0.668	0.596	0.467	0.577	1.122	1.122	1.122	1.122	0.01713	0.01529	0.01197	0.01480	0.01969	0.01969	0.01969	0.01969
0.691	0.618	0.486	0.598	1.164	1.164	1.164	1.164	0.01772	0.01584	0.01245	0.01534	0.02042	0.02042	0.02042	0.02042
0.716	0.640	0.502	0.619	1.206	1.206	1.206	1.206	0.01835	0.01641	0.01287	0.01588	0.02115	0.02115	0.02115	0.02115
0.740	0.663	0.522	0.642	1.247	1.247	1.247	1.247	0.01898	0.01701	0.01339	0.01646	0.02188	0.02188	0.02188	0.02188
0.765	0.686	0.540	0.664	1.289	1.289	1.289	1.289	0.01962	0.01758	0.01384	0.01701	0.02261	0.02261	0.02261	0.02261
0.788	0.707	0.557	0.684	1.331	1.331	1.331	1.331	0.02022	0.01813	0.01429	0.01755	0.02334	0.02334	0.02334	0.02334
0.813	0.729	0.576	0.706	1.372	1.372	1.372	1.372	0.02085	0.0187	0.01478	0.01811	0.02407	0.02407	0.02407	0.02407
0.838	0.752	0.593	0.728	1.414	1.414	1.414	1.414	0.02149	0.01928	0.0152	0.01866	0.0248	0.0248	0.0248	0.02480
0.862	0.774	0.611	0.749	1.456	1.456	1.456	1.456	0.0221	0.01986	0.01565	0.01920	0.02554	0.02554	0.02554	0.02554
0.887	0.798	0.629	0.771	1.497	1.497	1.497	1.497	0.02275	0.02045	0.01614	0.01978	0.02627	0.02627	0.02627	0.02627
0.912	0.819	0.647	0.793	1.539	1.539	1.539	1.539	0.02338	0.02099	0.0166	0.02032	0.027	0.027	0.027	0.02700
0.935	0.841	0.666	0.814	1.581	1.581	1.581	1.581	0.02398	0.02157	0.01709	0.02088	0.02773	0.02773	0.02773	0.02773
0.959	0.863	0.685	0.836	1.622	1.622	1.622	1.622	0.0246	0.02214	0.01757	0.02144	0.02846	0.02846	0.02846	0.02846
0.984	0.886	0.705	0.858	1.664	1.664	1.664	1.664	0.02522	0.02271	0.01807	0.02200	0.02919	0.02919	0.02919	0.02919
1.007	0.908	0.724	0.880	1.706	1.706	1.706	1.706	0.02582	0.02329	0.01855	0.02255	0.02992	0.02992	0.02992	0.02992
1.030	0.931	0.744	0.902	1.747	1.747	1.747	1.747	0.02642	0.02388	0.01908	0.02313	0.03065	0.03065	0.03065	0.03065
1.052	0.951	0.763	0.922	1.789	1.789	1.789	1.789	0.02699	0.02439	0.01957	0.02365	0.03138	0.03138	0.03138	0.03138
1.076	0.974	0.783	0.944	1.831	1.831	1.831	1.831	0.02759	0.02497	0.02008	0.02421	0.03211	0.03211	0.03211	0.03211
1.099	0.995	0.802	0.965	1.872	1.872	1.872	1.872	0.02818	0.02552	0.02056	0.02475	0.03285	0.03285	0.03285	0.03285
1.122	1.018	0.822	0.987	1.914	1.914	1.914	1.914	0.02877	0.02611	0.02108	0.02532	0.03358	0.03358	0.03358	0.03358
1.145	1.038	0.841	1.008	1.956	1.956	1.956	1.956	0.02935	0.02662	0.02157	0.02585	0.03431	0.03431	0.03431	0.03431
1.166	1.060	0.861	1.029	1.997	1.997	1.997	1.997	0.0299	0.02717	0.02209	0.02639	0.03504	0.03504	0.03504	0.03504
1.189	1.080	0.880	1.050	2.039	2.039	2.039	2.039	0.03048	0.0277	0.02257	0.02692	0.03577	0.03577	0.03577	0.03577
1.210	1.100	0.899	1.070	2.081	2.081	2.081	2.081	0.03101	0.02821	0.02306	0.02743	0.0365	0.0365	0.0365	0.03650
1.231	1.120	0.918	1.089	2.122	2.122	2.122	2.122	0.03156	0.02871	0.02353	0.02793	0.03723	0.03723	0.03723	0.03723
1.250	1.139	0.938	1.109	2.164	2.164	2.164	2.164	0.03206	0.02921	0.02404	0.02844	0.03796	0.03796	0.03796	0.03796
1.269	1.159	0.956	1.128	2.206	2.206	2.206	2.206	0.03255	0.02972	0.02451	0.02893	0.03869	0.03869	0.03869	0.03869
1.287	1.179	0.974	1.147	2.247	2.247	2.247	2.247	0.03299	0.03022	0.02499	0.02940	0.03942	0.03942	0.03942	0.03942

1.304	1.196	0.993	1.164	2.289	2.289	2.289	2.289	0.03344	0.03067	0.02545	0.02985	0.04016	0.04016	0.04016	0.04016
1.319	1.212	1.009	1.180	2.331	2.331	2.331	2.331	0.03382	0.03109	0.02588	0.03026	0.04089	0.04089	0.04089	0.04089
1.330	1.229	1.026	1.195	2.372	2.372	2.372	2.372	0.0341	0.0315	0.02631	0.03064	0.04162	0.04162	0.04162	0.04162
1.326	1.240	1.043	1.203	2.414	2.414	2.414	2.414	0.03399	0.0318	0.02674	0.03084	0.04235	0.04235	0.04235	0.04235
-0.138	1.241	1.047	0.717	2.421	2.421	2.421	2.421	-0.00353	0.03182	0.02683	0.01837	0.04247	0.04248	0.04248	0.04248
	-0.237	1.054	0.408		2.444	2.444	2.444	0	-0.00608	0.02703	0.00698		0.04287	0.04288	0.04288
		1.059	1.059			2.456	2.456	0		0.02714	0.01357			0.04308	0.04308
		1.072	1.072			2.497	2.497	0		0.0275	0.01375			0.04381	0.04381
		1.079	1.079			2.539	2.539	0		0.02766	0.01383			0.04454	0.04454
		-0.152	-0.152			2.569	2.569	0		-0.0039	-0.00195			0.04508	0.04508